UNIVERSITY OF CYPRUS

DEPARTMENT OF MATHEMATICS AND STATISTICS

EXTENSIONS OF THE SINGULAR FUNCTION BOUNDARY INTEGRAL METHOD TO TWO AND THREE DIMENSIONS

Ph.D. Dissertation

EVGENIA CH. CHRISTODOULOU

JUNE 2011

UNIVERSITY OF CYPRUS

DEPARTMENT OF MATHEMATICS AND STATISTICS

EXTENSIONS OF THE SINGULAR FUNCTION BOUNDARY INTEGRAL METHOD TO TWO AND THREE DIMENSIONS

By

Evgenia Ch. Christodoulou

SUBMITTED IN PARTIAL FULFILLMENT OF THE

REQUIREMENTS FOR THE DEGREE OF

DOCTOR OF PHILOSOPHY

AT

UNIVERSITY OF CYPRUS

NICOSIA, CYPRUS

JUNE 2011

This thesis is dedicated to my parents, Christodoulos and Nafsika, whose love, support and encouragement has been a constant in my life.

Πανεπιστήμιο Κύπρου

Τμήμα Μαθηματικών και Στατιστικής

Η παρούσα Διδακτορική Διατριβή
εκπονήθηκε στα πλαίσια των Σπουδών
για την απόκτηση του

Διδακτορικού Διπλώματος στα Μαθηματικά

που απονέμει το
Τμήμα Μαθηματικών και Στατιστικής
του Πανεπιστημίου Κύπρου
στην **Ευγενία Χριστοδούλου**

Εγκρίθηκε την **23η Μαΐου 2011**
από Εξεταστική Επιτροπή αποτελούμενη από τους:

Ονοματεπώνυμο	**Βαθμίδα**	**Υπογραφή**
Γεωργίου Γιώργος Ερευνητικός Σύμβουλος Πανεπιστήμιο Κύπρου	Καθηγητής	**ΠΡΟΣΩΠΙΚΑ ΔΕΔΟΜΕΝΑ**
Ξενοφώντος Χρίστος Ερευνητικός Σύμβουλος Πανεπιστήμιο Κύπρου	Αναπληρωτής Καθηγητής	**ΠΡΟΣΩΠΙΚΑ ΔΕΔΟΜΕΝΑ**
Σμυρλής Γιώργος Πρόεδρος Εξεταστικής Επιτροπής Πανεπιστήμιο Κύπρου	Καθηγητής	**ΠΡΟΣΩΠΙΚΑ ΔΕΔΟΜΕΝΑ**
Μπουντουβής Ανδρέας Μέλος Εξεταστικής Επιτροπής Εθνικό Μετσόβιο Πολυτεχνείο, Ελλάδα	Καθηγητής	**ΠΡΟΣΩΠΙΚΑ ΔΕΔΟΜΕΝΑ**
Yosibash Zohar Μέλος Εξεταστικής Επιτροπής Ben Gurion University, Israel	Καθηγητής	**ΠΡΟΣΩΠΙΚΑ ΔΕΔΟΜΕΝΑ**

\EK

Περίληψη

Η *Μέθοδος Συνοριακού Ολοκληρώματος με Ιδιάζουσες Συναρτήσεις* (*Singular Function Boundary Integral Method,* SFBIM) αναπτύχθηκε από τους Georgiou et. al. (1996) για την αριθμητική επίλυση διδιάστατων προβλημάτων Laplace με συνοριακές ιδιομορφίες. Στη μέθοδο αυτή, η λύση προσεγγίζεται με τους αρχικούς όρους του τοπικού αναπτύγματος της λύσης κοντά στο σημείο της ιδιομορφίας. Σταθμίζοντας τη διαφορική εξίσωση με τις συναρτήσεις βάσης κατά Galerkin και εφαρμόζοντας τη δεύτερη ταυτότητα του Green, το διακριτοποιημένο πρόβλημα ανάγεται σε ένα σύστημα ολοκληρωτικών εξισώσεων πάνω στο σύνορο του χωρίου και μάλιστα μακριά από το ιδιάζον σημείο. Έτσι η διάσταση του προβλήματος μειώνεται κατά ένα με σημαντική μείωση του υπολογιστικού κόστους. Οι συνοριακές συνθήκες τύπου Dirichlet επιβάλλονται μέσω συναρτήσεων πολλαπλασιαστών Lagrange, οι οποίες εμφανίζονται σαν επιπρόσθετοι άγνωστοι στο τελικό γραμμικό σύστημα και προσεγγίζονται τοπικά με πολυωνυμικές συναρτήσεις βάσης. Οι άγνωστοι στην μέθοδο SFBIM είναι οι ιδιάζοντες συντελεστές της προσέγγισης της λύσης, γνωστοί και ως γενικευμένοι συντελεστές συγκέντρωσης τάσεων, και οι διακριτές τιμές των πολλαπλασιαστών Lagrange. Το γεγονός ότι οι ιδιάζοντες συντελεστές υπολογίζονται απευθείας και όχι με μετεπεξεργασία της αριθμητικής λύσης αποτελεί άλλο πλεονέκτημα της μεθόδου. Η μέθοδος μελετήθηκε και εφαρμόστηκε σε Λαπλασιανά και Διαρμονικά προβλήματα στις δύο διαστάσεις, δίνοντας ταχεία σύγκλιση με το πλήθος των ιδιοσυναρτήσεων και το πλήθος των συντελεστών Lagrange. Η σύγκλιση της μεθόδου αναλύθηκε θεωρητικά στην περίπτωση διδιάστατων προβλημάτων Laplace.

Οι στόχοι της διατριβής αυτής ήταν οι εξής:

(i) Η αριθμητική επαλήθευση κάποιων θεωρητικών αποτελεσμάτων σε πρότυπα προβλήματα Laplace.

(ii) Η απόδειξη της σύγκλισης της μεθόδου για ένα διδιάστατο διαρμονικό πρόβλημα με μια συνοριακή ιδιομορφία.

(iii) Η επέκταση της μεθόδου σε τριδιάστατα προβλήματα Laplace με ιδιομορφίες ακμής.

Για την επίτευξη του πρώτου στόχου μελετήσαμε προβλήματα Laplace πάνω σε κυκλικούς τομείς, με γνωστή αναλυτική λύση. Αυτό επέτρεψε τη μελέτη της σύγκλισης της μεθόδου για διάφορους βαθμούς της πολυωνυμικής προσέγγισης των πολλαπλασιαστών Lagrange

και τον ακριβή υπολογισμό των σφαλμάτων προσέγγισης. Τα αριθμητικά μας αποτελέσματα συμφωνούν με τη θεωρητική ανάλυση των Xenophontos et al. (2006).

Ο δεύτερος στόχος επιτεύχθηκε με την επέκταση της ανάλυσης σύγκλισης των Xenophontos et al. (2006) για ένα πρότυπο διδιάστατο διαρμονικό πρόβλημα με συνοριακή ιδιομορφία. Αποδείξαμε ότι οι υπολογιζόμενοι ιδιάζοντες συντελεστές συγκλίνουν εκθετικά με το πλήθος των ιδιοσυναρτήσεων. Εκτελέσαμε επίσης αριθμητικά πειράματα για ένα πρόβλημα ροής Stokes για την παρουσίαση των θεωρητικών ευρημάτων.

Για τον τελευταίο στόχο επεκτείναμε τη μέθοδο για την επίλυση ενός τριδιάστατου προβλήματος Laplace με ιδιομορφία ακμής. Η τοπική λύση γύρω από την ακμή μπορεί να εκφρασθεί σαν ένα ασυμπτωτικό ανάπτυγμα που περιλαμβάνει τις ιδιοτιμές και τις ιδιοσυναρτήσεις του αντίστοιχου διδιάστατου προβλήματος σε πολικές συντεταγμένες, οι συντελεστές των οποίων είναι οι λεγόμενες συναρτήσεις ακμαίων συγκεντρώσεων ροής (edge flux intensity functions, EFIFs). Οι παράγωγοι ανώτερης τάξης αυτών των συναρτήσεων της αξονικής συντεταγμένης εμφανίζονται σε μια εσωτερική απειροσειρά στο ανάπτυγμα της λύσης (Yosibash et al., 2002). Προσεγγίζοντας τις συναρτήσεις EFIFs με τμηματικά πολυώνυμα βαθμού k=0, 1 σε ένα πλέγμα πλάτους h απαλείφουμε την εσωτερική απειροσειρά και μπορούμε να επεκτείνουμε τη μέθοδο SFBIM. Όπως και στα διδιάστατα προβλήματα, η λύση προσεγγίζεται από ένα πεπερασμένο πλήθος όρων του τοπικού αναπτύγματος και οι συνοριακές συνθήκες Dirichlet επιβάλλονται μέσω πολλαπλασιαστών Lagrange. Οι αριθμητικοί υπολογισμοί έδειξαν ότι οι υπολογιζόμενες συναρτήσεις EFIFs συγκλίνουν με τάξη $O(h^{k+1})$ ως προς την L^2-νόρμα.

Abstract

The Singular Function Boundary Integral Method (SFBIM) was introduced by Georgiou et al. (1996) for solving numerically two-dimensional Laplacian problems with one boundary singularity. In this method, the solution is approximated by the leading terms of the local asymptotic expansion near the singular point. By weighting the governing equation with the eigenfunctions in the Galerkin sense and applying Green's second identity, the discretized problem is reduced to a system of boundary integral equations far from the singular point. This reduces the dimension of the problem by one and leads to considerable computational savings. Dirichlet boundary conditions are enforced by means of Lagrange multiplier functions, which appear as additional unknowns in the system. These functions are approximated locally by polynomial basis functions. Therefore, the unknowns in the SFBIM are the coefficients of the eigenfunctions, also known as singular coefficients or generalized stress intensity factors, and the discrete Lagrange multiplier values. The fact that the singular coefficients are calculated directly and not by postprocessing the numerical solution is another advantage of the method. The latter has been applied to both Laplacian and biharmonic two-dimensional problems exhibiting fast convergence with the number of singular coefficients and the number of Lagrange multipliers. The convergence of the method has also been analyzed theoretically in the case of two-dimensional Laplacian problems.

The objectives of this thesis were:

(i) the numerical verification of certain theoretical results on model two-dimensional problems.

(ii) the proof of convergence of the method for a two-dimensional biharmonic problem with one boundary singularity.

(iii) the extension of the method to three-dimensional Laplacian problems with straight-edge singularities.

For accomplishing the first objective, we considered a Laplacian problem over a circular sector, with known analytical solution. This allowed us to study the convergence of the method for various orders of the polynomial approximation of the Lagrange multipliers and to calculate the exact approximation errors. The numerical results agree well with the theoretical analysis of Xenophontos et al. (2006).

Objective number two was achieved by extending the convergence analysis from Xenophontos et. al. (2006) to a model two-dimensional biharmonic problem with a boundary singularity. We proved that the calculated singular coefficients converge exponentially with the number of singular functions. To illustrate the theoretical findings, we have carried out numerical experiments on a Stokes flow problem.

Finally, we extended the method for solving a three-dimensional Laplacian problem with a straight-edge singularity. The solution in the neighbourhood of the straight edge can be expressed as an asymptotic expansion involving the eigenpairs of the analogous two-dimensional problem, which have as coefficients the so-called *edge flux stress intensity functions* (EFIFs). The EFIFs are functions of the axial coordinate the higher derivatives of which appear in an infinite series in the expansion (Yosibash et al., 2002). Approximating the EFIFs by piecewise polynomials of degree $k = 0, 1$ defined on a mesh with width h, eliminates the inner infinite series in the local expansion and allows for the straightforward extension of the SFBIM. As in the case of two-dimensional problems the solution was approximated by the leading terms of the local asymptotic solution expansion and the Dirichlet boundary conditions were imposed by means of Lagrange multiplier functions. Our numerical calculations demostrated that the calculated EFIFs converge with order $O(h^{k+1})$, in the L^2 norm.

Acknowledgments

Looking back to these years of PhD studies, I feel very grateful for all I have received. It certainly shaped me as a person and changed my perspective on life.

I would like to express my deep and sincere gratitude to my supervisors, Associate Professor Christos Xenophontos and Professor Georgios Georgiou, Department of Mathematics and Statistics, University of Cyprus, for their detained and constructive comments, and for their important support and guidance throughout this work. Their wide knowledge on the subject and his logical way of thinking has been valuable. Their understanding and encouraging guidance have provided a solid basis for the present thesis.

I also thank Professor Andreas Boudouvis, NUT Athens, Professor Yiorgos-Sokratis Smyrlis, University of Cyprus and Professor Zohar Yosibash, Ben-Gurion University, for being members of my PhD committee and contributing to this thesis.

During this work I have also collaborated with Miltiades Elliotis, Ph.D., for whom I have the utmost respect. His prior experience with the method was beneficial.

Special mention is due to my parents and friends, to Stella Poyiatzi especially, for their support and encouragement.

My gratitude is also extended to the Cyprus Research Promotion Foundation that has partially supported this effort, $\Pi ENEK/ENI\Sigma X/0308/014$.

Evgenia Ch. Christodoulou

Nicosia, May 2011.

Contents

List of Figures

List of Tables

Chapter 1

Introduction

The solutions of elliptic partial differential equations in two-dimensional domains, such as the Laplace and the biharmonic equations, exhibit singularities at boundary corners or at boundary points where there is an abrupt change in the boundary conditions along a smooth boundary. Such problems are extensively covered in the literature (see, for example, Grisvard 1992, Grisvard 1995, Beagles et al. 1991, Rössle 2000, and more recently Dauge et al. 2011). Elliptic boundary value problems with boundary singularities appear in many engineering applications, such as fracture and fluid mechanics. They have also attracted the attention of numerical analysts, since boundary singularities create convergence difficulties to standard numerical methods and cause inaccuracies in the numerical solutions, at least locally. These numerical difficulties are overcome by using special adaptive grid refinement schemes but the resulting efficiency is not always satisfactory and the required computational cost may be very high (see, e.g., Bernal and Kindelan, 2010). One notable exception is the high order p/hp Finite Element Method (FEM) which produces accurate results if the mesh and polynomial degree of the approximating polynomials is chosen appropriately (see, e.g., Szab*ó* and Babuška, 1991).

In the past few decades, several methods for treating elliptic boundary value problems with

boundary singularities have been proposed. Among them one finds the so-called hybrid methods which incorporate, directly or indirectly, the form of the local asymptotic expansion for the solution in the approximation scheme. Knowledge of the leading singular coefficients of the local solution expansion, which in two-dimensional problems are also known as *Generalized Stress Intensity Factors* (GSIFs) (Szab*ó* and Babuška, 1991) or *Flux Intensity Factors* (Arad et al., 1998), is of great importance in many engineering fields, such as fracture mechanics. Many methods have been proposed in the literature for their effective and efficient approximation, including high order p/hp FEMs with post-processing (Szab*ó* and Yosibash, 1996) and Trefftz methods (Li et al., 2007). In the former, the solution is first approximated on a refined grid designed especially to capture the singularity and the singular coefficients are obtained by an extraction formula which uses the computed solution. Methods that do not require any postprocessing and/or include information about the exact solution in the approximation scheme, such as Trefftz methods, are more attractive if the approximation of the coefficients is the main objective.

Trefftz methods have been reviewed by Li and co-workers (Li et al., 2007) who have also made comparisons with collocation and other boundary methods. Other recent reviews of methods used for elliptic boundary value problems with boundary singularities can be found in the articles of Bernal et al. (2009, 2010), who considered both global and local meshless collocation methods with multiquadrics as basis functions, and Dosiyev and Buranay (2008) who employed the block method which was proposed for the solution of Laplace problems on arbitrary polygons.

Singularities in three dimensional Laplace problems have received less attention, mainly due to their complexity. Different forms of singularity may appear depending on the boundary geometry and conditions. Both edge and vertex singularities are of interest in applications (Kondratiev, 1967. Stephan and Whiteman, 1988. Zaltzman and Yosibash, 2009). Yosibash et al. (2002) discuss the case of the singularity at the intersection of an edge and a vertex.

Edge singularities appear, for example, in V-notched solids loaded by static loads, in which the assumption of plane stress or plane strain condition is not valid. For the solution of such problems, few methods have been proposed, such as the J-integral method (Huber et al., 1993), the B- and H-integral methods (Meda et al., 1998), and, more recently, the methods of Costabel et al. (2004) and Yosibash et al. (2002) in which the quantities of interest are computed by means of a post-processing procedure in a p-version finite element scheme. Yosibash et al. (2002) presented the solution to the Laplace operator in three-dimensional domains in the vicinity of straight edges in the form of an asymptotic expansion involving eigenpairs and having as coefficients the so-called *Edge Flux Intensity Functions* (EFIFs). It turns out that the eigenpairs are those of the two-dimensional problem over a plane perpendicular to the edge.

Vertex singularities appear in electromagnetic fields, in magnetic recording, heat transfer, elasticity, and fluid mechanics problems, as well as in multimaterial problems (Zaltzman and Yosibash, 2009). Among the earliest analyses of Laplacian solutions in the neighbourhood of a vertex are those of Stephan and Whiteman (1988) and Beagles and Whiteman (1989) who used finite elements for the computation of the eigenvalues. Schmitz et al. (1993) also used a method employing the Boundary Element Method (BEM) instead. Recently, Zaltzman and Yosibash (2009) derived explicit analytical expressions for the local solution of the Laplace equation in the neighbourhood of a vertex. They also considered vertices at the intersection of a crack front and a free surface and provided numerical estimates of the eigenpairs obtained by extending a modified Steklov method.

In the sections that follow we will give an overview of the various types of singularities found in two- and three-dimensional Laplacian problems, in order to give the reader a feeling for what one is faced with when it comes time to approximate the solution to such problems. Also, this material will serve as the cornerstone of what is to follow in subsequent chapters.

1.1 Preliminaries

Throughout this dissertation $\Omega \subset \mathbb{R}^n,\ n = 2, 3$ will be used to denote an open, bounded domain with boundary $\partial\Omega$. The space of square integrable functions defined on Ω will be denoted as usual by $L^2(\Omega)$. The notation $H^k(\Omega)$ will be used to denote the Sobolev spaces containing functions on Ω, having k generalized derivatives in $L^2(\Omega)$. For instance,

$$H^1(\Omega) = \{u \in L^2(\Omega) : \nabla u \in L^2(\Omega)\}. \tag{1.1}$$

The norm and seminorm on $H^k(\Omega)$ will be denoted by $\|\cdot\|_{k,\Omega}$ and $|\cdot|_{k,\Omega}$, respectively.

Let the *trace space* of functions in $H^1(\Omega)$ be denoted by

$$H^{1/2}(\partial\Omega) = \left\{u \in H^1(\Omega) : u|_{\partial\Omega} \in L^2(\partial\Omega)\right\}. \tag{1.2}$$

With $T : H^1(\Omega) \to H^{1/2}(\partial\Omega)$ denoting the trace operator, the norm of $H^{1/2}(\partial\Omega)$ is defined as

$$\|\psi\|_{1/2,\partial\Omega} = \inf_{u \in H^1(\Omega)} \left\{\|u\|_{1,\Omega} : Tu = \psi\right\}. \tag{1.3}$$

Then, we define $H^{-1/2}(\partial\Omega)$ as the *closure* of $H^0(\partial\Omega) \equiv L^2(\partial\Omega)$ with respect to the norm

$$\|\varphi\|_{-1/2,\partial\Omega} = \sup_{\psi \in H^{1/2}(\partial\Omega)} \frac{\int_{\partial\Omega} \varphi\psi}{\|\psi\|_{1/2,\partial\Omega}}. \tag{1.4}$$

For other non-integer and/or negative values of k, we will adopt the notations and definitions found in Lions et al. (1972).

Finally, the letters C and c (with or without subscripts) will be used to denote generic positive constants independent of any discretization parameters and possibly having different values in each occurrence.

1.2 Corner Singularities in Planar Laplacian Problems

For Laplace problems with corner singularities, the singular functions can be obtained analytically. To demonstrate this for a two dimensional Laplace problem posed on a domain with a corner, we consider the domain Ω shown in Fig. 1.1 with either Dirichlet or Neumann boundary conditions on each of the sides S_1 and S_2.

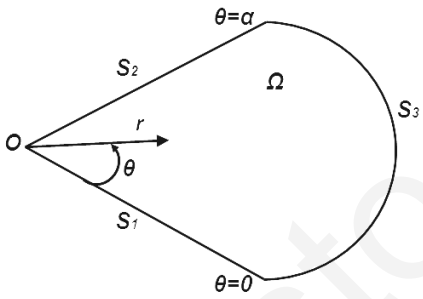

Figure 1.1: A two-dimensional domain Ω with a corner.

The Laplace equation in polar coordinates is:

$$\frac{\partial^2 u}{\partial r^2} + \frac{1}{r}\frac{\partial u}{\partial r} + \frac{1}{r^2}\frac{\partial^2 u}{\partial \theta^2} = 0. \tag{1.5}$$

Assuming that $u(r,\theta) = R(r)\Theta(\theta)$ in the above equation and separating variables, we end up with

$$\frac{r^2 R'' + rR'}{R} = -\frac{\Theta''}{\Theta}. \tag{1.6}$$

Since the right hand side of the last equation is a function of θ and the left hand side a function of r, then they both have to be equal to a constant, say μ^2, where the constant μ is chosen to be positive in order to obtain periodic solutions in θ. We therefore have two second order, linear, homogeneous ordinary differential equations:

$$r^2 R'' + rR' - \mu^2 R = 0 \tag{1.7}$$

and

$$\Theta'' + \mu^2 \Theta = 0. \tag{1.8}$$

Now, Eq. (1.8) has solutions of the form

$$\Theta(\theta) = A\cos(\mu\theta) + B\sin(\mu\theta), \tag{1.9}$$

where A and B are general constants. Equation (1.7) is an Euler differential equation and using the transformation $r = e^t$ we get the simpler equation

$$w''(t) - \mu w(t) = 0, \tag{1.10}$$

which in turn gives solutions for R, of the form

$$R(r) = Cr^{\mu} + Dr^{-\mu}, \tag{1.11}$$

where $C, D \in \mathbb{R}$. Note that solutions of the form $R(r) = Dr^{-\mu}$ are rejected if the solution is bounded near O. Therefore, our problem has solutions of the form

$$u(r,\theta) = \sum_{j=1}^{\infty} r^{\mu_j} \left(A_j \cos(\mu_j \theta) + B_j \sin(\mu_j \theta)\right), \tag{1.12}$$

where the singular coefficients A_j, B_j and the eigenvalues μ_j are uniquely determined by the geometry and the boundary conditions. For instance, see also Fig. 1.2, if we have homogeneous Dirichlet boundary conditions on S_1 and S_2, then $A_j = 0$ and $\mu_j = j\pi/\alpha$; if instead we have homogeneous Neumann boundary conditions on both sides of the corner then $B_j = 0$ and $\mu_j = \frac{(2j+1)\pi}{2\alpha}$. The case when we have a homogeneous Dirichlet boundary condition on S_1 and homogeneous Neumann boundary condition on S_2, is of interest as it would be part of our model problem in Chapter 3 (see Fig. 3.1). In this case $A_j = 0$ and $\mu_j = \frac{(2j-1)\pi}{2\alpha}$. More specifically, if in addition $\alpha = 3\pi/4$, then we have the the L-shaped domain discussed in Chapter 2 (see Fig. 2.3). Changing the boundary conditions to Neumann on S_1 and Dirichlet on S_2 and taking $\alpha = \pi$ we get the local solution of the celebrated Motz

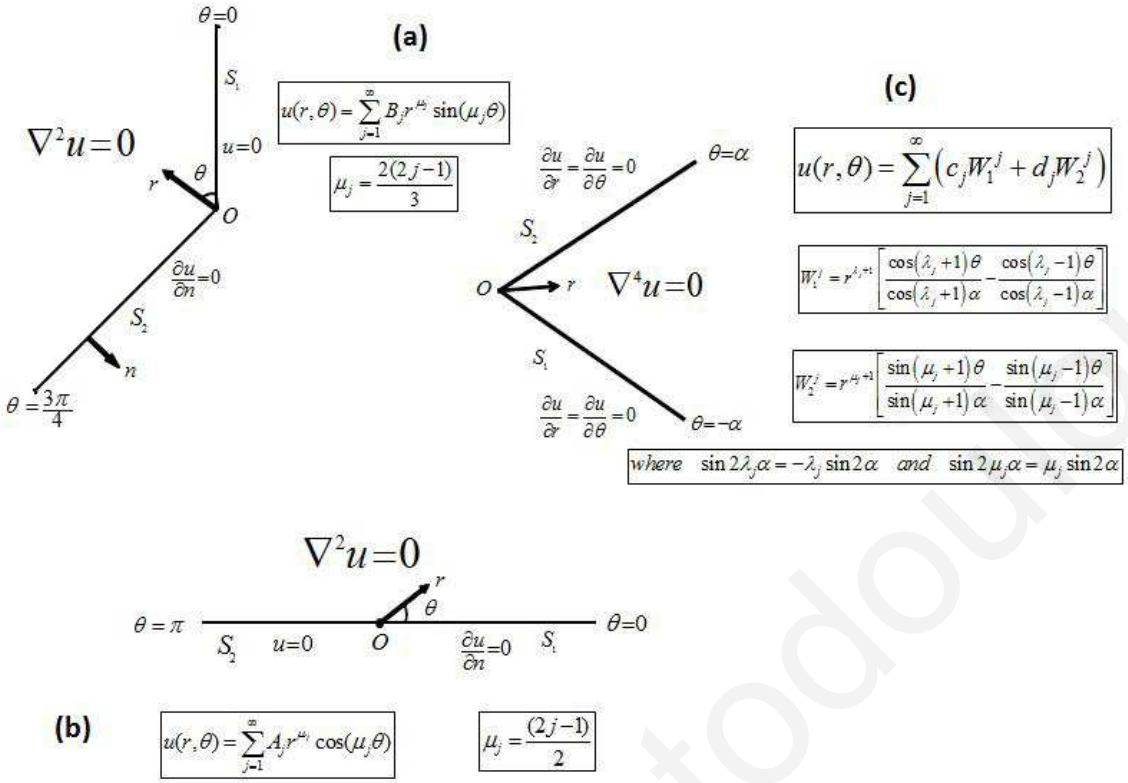

Figure 1.2: Various BVPs with singularities and their local solutions.

problem that is often used for testing various methods proposed in the literature: $B_j = 0$ and $\mu_j = \frac{(2j-1)}{2}$.

The singular coefficients, on the other hand, depend on the boundary conditions on the rest of the boundary of the problem domain.

1.3 Edge Singularities in Three-Dimensional Laplacian Problems

In this section we consider the Laplace equation and discuss the form of the local solution near straight edge singularities as shown in Yosibash et al. (2002). In the cylindrical domain Ω shown in Fig. 1.3, AB is a straight edge and S_1 and S_2 are rectangles. This domain can be a subdomain of any domain with a straight edge. We consider the following boundary value

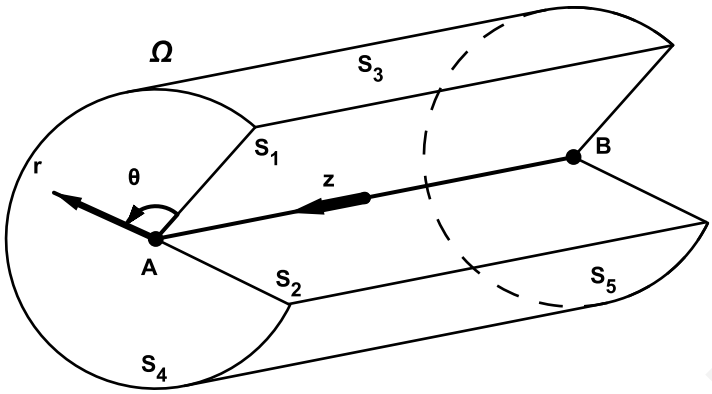

Figure 1.3: A three-dimensional domain Ω with an edge

problem on Ω: Find u such that

$$\nabla^2 u = 0 \text{ in } \Omega, \tag{1.13}$$

with boundary conditions

$$\left.\begin{array}{r} u = g_1 \text{ on } S_1 \\ \frac{\partial u}{\partial z} = g_2 \text{ on } S_2 \end{array}\right\}. \tag{1.14}$$

As shown in Yosibash et al. (2002), the local solution near the edge is of the form

$$u(r,\theta,z) = \sum_{k=1}^{K}\sum_{\ell=0}^{L} a_{k\ell}(z) r^{\mu_k} (lnr)^{\ell} s_{k\ell}(\theta) + \upsilon(r,\theta,z), \tag{1.15}$$

with $a_{k\ell}(z)$ the unknown EFIFs, which are analytic functions of z away of the vertices. The functions $s_{k\ell}(\theta)$ are known as edge eigenfunctions and they are analytic in θ. The function $\upsilon(r,\theta,z)$ belongs in $H^q(\Omega)$ where q depents on K and can be as large as required. The numbers $\mu_{k+1} \geq \mu_k$ are known as edge eigenvalues. If μ_k is not an integer, then $L = 0$. In what follows we assume that μ_k for $k \leq K$ are not integers and that no "crossing point" occurs (cf. Costabel et al.,1993). Under these assumptions Eq. (1.15) becomes

$$u(r,\theta,z) = \sum_{k=1}^{K} a_k(z) r^{\mu_k} s_k(\theta) + \upsilon(r,\theta,z). \tag{1.16}$$

Note that $r^{\mu_n} s_n(\theta)$ satisfies the Laplace equation on the (r, θ) plane (2-D problem), i.e.

$$\nabla^2_{2D}[r^{\mu_n} s_n(\theta)] = 0. \tag{1.17}$$

However, $S_n(r, \theta, z) = a_n(z) r^{\mu_n} s_n(\theta)$ does not satisfy the Laplace equation in Ω, i.e.

$$\nabla^2_{3D}[a_n(z) r^{\mu_n} s_n(\theta)] = (\nabla^2_{2D} + \frac{\partial^2}{\partial z^2})[a_n(z) r^{\mu_n} s_n(\theta)] = \frac{\partial^2}{\partial z^2}[a_n(z) r^{\mu_n} s_n(\theta)] \neq 0, \tag{1.18}$$

Nevertheless, taking into account that $a_n(z)$ is an analytic function and augmenting S_n by $r^{\mu_n} s_n(\theta) \sum_{i=1}^{\infty} \frac{\partial^{2i}}{\partial z^{2i}} a_n(z) r^{2i} \frac{\left(-\frac{1}{4}\right)^i}{\prod_{j=1}^{i} j(\mu_n + j)}$, as demonstrated in Yosibash et al. (2002), the function

$$S_n(r, \theta, z) = r^{\mu_n} s_n(\theta) \sum_{i=0}^{\infty} \frac{\partial^{2i}}{\partial z^{2i}} a_n(z) r^{2i} \frac{\left(-\frac{1}{4}\right)^i}{\prod_{j=1}^{i} j(\mu_n + j)} \tag{1.19}$$

satisfies identically the 3-D Laplace equation (see Appendix B).

1.4 Vertex Singularities in Three-Dimensional Laplacian Problems

The extension of the SFBIM for three-dimensional Laplacian problems with conical vertex singularities will be the subject of a future project. Nevertheless, in this section we discuss the local solution near a vertex singularity. We consider the Laplace problem that was proposed and solved by Zaltzman et al. (2009). In the three-dimensional domain Ω depicted in Fig. 1.4. This domain has a conical vertex on its boundary and $\omega/2 \in [0, \pi]$. The problem is solved in the vicinity of the conical point, with either homogeneous Dirichlet or Neumann boundary conditions, i.e.

$$\nabla^2 u = 0 \quad \text{in} \quad \Omega, \tag{1.20}$$

with

$$u_{\theta=\omega/2} = 0 \quad \text{in} \quad \partial\Omega_C, \tag{1.21}$$

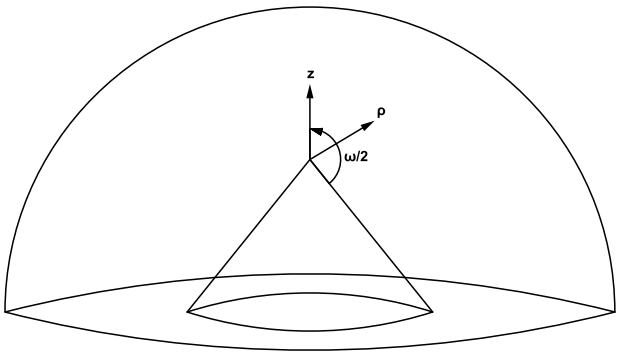

Figure 1.4: A three-dimensional domain with a rotationally symmetric conical vertex.

where $\partial\Omega_C = \Gamma_C$ is the surface of the cone insert. Equation (1.21) may be written as

$$\left.\frac{\partial u}{\partial n}\right|_{\theta=\omega/2} = \left.\frac{1}{\rho}\frac{\partial u}{\partial \theta}\right|_{\theta=\omega/2} = 0 \quad \text{in} \quad \partial\Omega_C. \tag{1.22}$$

Writing u as

$$u(\rho, \theta, \varphi) = R(\rho)\Theta(\theta)\Phi(\varphi), \tag{1.23}$$

and separating variables leads to the following ODEs:

$$\rho^2 R'' + 2\rho R' - \nu(\nu+1)R = 0, \tag{1.24}$$

$$\Phi'' + \mu^2 \Phi = 0, \tag{1.25}$$

$$-\sin^2(\theta)\Theta'' - \sin(\theta)\cos(\theta)\Theta' - \left[\nu(\nu+1)\sin^2(\theta) - \mu^2\right]\Theta = 0, \tag{1.26}$$

where ν and μ^2 are separation constants. The solution to Eq. (1.24) is of the form

$$R(\rho) = A\rho^{\nu}, \tag{1.27}$$

where A is a constant. Note that in order to have $u \in H^1(\Omega)$, then there should hold $\nu \geq 0$. The solution to Eq. (1.25) is

$$\Phi = B\sin(\mu\varphi) + C\cos(\mu\varphi), \tag{1.28}$$

where A and C are constants. Because of conical reentrant corners, a periodic solution is sought in φ , witch leads to the conclusion that μ has to be a positive integer. The case

$\mu = 0$ is associated with axisymmetric solutions, independent of φ. For the solution of Eq. (1.26) one has to change variables using $z = \cos(\theta)$, [see Zaltzman and Yosibash(2011) and the references therein]. Taking into account the axis of symmetry of the domain and that the solution has to be bounded at $\theta = 0$, the latter authors concluded that the solution to Eq. (1.26) is of the form

$$\Theta(\cos\theta) = DP_\nu^\mu(\cos\theta), \tag{1.29}$$

where D is a constant and P_ν^μ is the associated Legendre function of the first kind, of degree ν and order μ. Now, because the BCs give an infinite number of ν's, which are the roots of the Legendre function $P_{\nu_\ell}^\mu$, they are denoted by two indices $\nu_\ell^{(\mu)}$. Hence, the solution can be represented by

$$u(\rho,\theta,\varphi) = \sum_{\mu=0}^{\infty}\sum_{\ell=1}^{\infty} \rho^{\nu_\ell^{(\mu)}} \left[A_{\mu,\ell}\sin(\mu\varphi) + B_{\mu,\ell}\cos(\mu\varphi)\right] P_{\nu_\ell}^\mu(\cos\theta). \tag{1.30}$$

The expression (1.30) may be used to construct an approximation to the solution, but this is outside the scope of the present work.

1.5 The SFBIM

The Singular Function Boundary Integral Method (SFBIM), developed by Georgiou et al. (1996) for (two-dimensional) Laplacian problems with a boundary singularity, belongs to the class of Trefftz methods. To give a brief overview of the SFBIM (a detailed one is provided in Chapter 2), we consider Laplace's equation in a domain Ω with boundary $\partial\Omega = S_1 \cup S_2 \cup S_3$. We assume appropriate boundary conditions so that the solution u has a singularity at a point O, shared by boundary parts S_1 and S_2. The local expansion for u near O is given by

$$u = \sum_{n=1}^{\infty} \alpha_n r^{\mu_n} f_n(\theta), \tag{1.31}$$

with $\mu_n, f_n(\theta)$ known. The coefficients α_n are the unknowns of interest.

In the SFBIM, the solution is approximated by the leading terms of the asymptotic expansion,

$$u_N = \sum_{n=1}^{N_\alpha} \alpha_n^N r^{\mu_n} f_n(\theta), \tag{1.32}$$

and the so-called singular functions $r^{\mu_n} f_n(\theta)$ are used to weight the governing differential equation in the Galerkin sense:

$$\iint_\Omega r^{\mu_i} f_i(\theta)\, \nabla^2 u_N \, dV = 0, \;\; i = 1,\, 2,\, \ldots,\, N_\alpha. \tag{1.33}$$

The discretized equations are then reduced to boundary integrals by means of Green's theorem, reducing the dimension of the problem by one. Since the singular functions exactly satisfy the boundary conditions on the boundary parts S_1 and S_2 that share the singularity we only have to integrate away of the singular point. Hence,

$$\int_{S_3} \left(\frac{\partial u_N}{\partial n}\, r^{\mu_i} f_i(\theta) - u_N \, \frac{\partial (r^{\mu_i} f_i(\theta))}{\partial n} \right) dS = 0, \quad i = 1,\, 2,\, \ldots,\, N_\alpha. \tag{1.34}$$

A particular feature of the SFBIM is that Dirichlet conditions are weakly enforced in the Galerkin sense by means of Lagrange multipliers,

$$\lambda \approx \lambda_h = \sum_{j=1}^{N_\lambda} \lambda_j M^j, \tag{1.35}$$

the discrete values of which are additional unknowns.

It has been demonstrated both numerically and theoretically that the method converges exponentially with the number of singular functions used in the approximation of the solution and the number of Lagrange multipliers (Xenophontos et al. 2006, Christodoulou et al. 2010). The method has also been extended to biharmonic problems in two-dimensions arising from solid and fluid mechanics (Elliotis et al. 2005b, 2006). The main advantages of the SFBIM are that the dimension of the problem is reduced by one, leading to considerable computational savings and that the singular coefficients are calculated directly, hence avoiding the need for post-processing.

Although the error analysis of the method for two dimensional Laplace problems was discussed in Xenophontos et al. (2006), there were no numerical results to demonstrate all that was proven therein. The method was also tested on various two dimensional biharmonic problems, in Elliotis et al. (2005, 2006, 2007) but there was a lack of theoretical results proving the rate of convergence that was demonstrated numerically.

1.6 Objectives and Outline of the Thesis

In the present dissertation we extend the SFBIM in a number of ways, leading up to the extension of the method to three-dimensions. In particular:

- We numerically verify the theoretical results from Xenophontos et al. (2006) by considering two model Laplace problems over circular sectors with known exact solutions. Piecewise constant, linear, quadratic and cubic approximations of the Lagrange multiplier function are used. For linear, quadratic and cubic approximations it is verified that the approximate solution and the approximations of the singular coefficients converge exponentially, whilst the convergence of the approximate Lagrange multipliers is algebraic of order equal to the degree of the approximations used. All these results are in accordance to the theoretical results found in Xenophontos et al. (2006). The case of piecewise constant approximations is also of interest as it is not covered by the theory. We observe that for this case the convergence is algebraic of order 3 for the singular coefficients, of order 2 for the approximate solution and of order 3/4 for the Lagrange multipliers.

- We provide the proof of convergence of the method for a two-dimensional biharmonic problem, as a model for the well-known *Newtonian stick-slip problem* from fluid mechanics and establish the exponential convergence rates observed in the calculations by Elliotis et al. (2005b).

- The method is extended to a three-dimensional Laplacian problem with a straight edge singularity. The SFBIM is formulated and applied to two test problems with a straight-edge singularity caused by two intersecting flat planes, using piecewise polynomials of degree $k = 0, 1$ defined on a mesh with width h, for the approximation of the EFIFs. Our numerical results show that the convergence is, as expected, of $O(h^k)$.

The rest of this dissertation is organized as follows. In Chapter 2 we review the formulation of the SFBIM for a two-dimensional model Laplacian problem and present the error analysis results from Xenophontos et al. (2006). We also describe the application of the method on a model two-dimensional biharmonic problem taken from Elliotis et al. (2006). In Chapter 3 we apply the method on two Laplacian problems over circular sectors and we give numerical evidence in order to verify the theoretical results from Xenophontos et al. (2006). In Chapter 4 we provide the error analysis of the method on a model two-dimensional biharmonic problem with a boundary singularity, and in Chapter 5 we extend the SFBIM to a three-dimensional Laplacian problem with an edge singularity and we present numerical results that demonstrate the approximation of the EFIFs. Finally, in Chapter 6 we summarize our results and provide ideas for future work.

The reader should be warned that an effort was made for each chapter to be independent, in order to make the study of a single chapter easier. In addition, as indicated, certain chapters constitute journal articles that have been published by us. As a result there is some repetition, mainly in the introductions and the method description.

Chapter 2

Review of the Singular Function Boundary Integral Method

In this chapter we present an overview of the Singular Function Boundary Integral Method (SFBIM) for a model Laplacian as well as a model Biharmonic problem in two-dimensions. Our goal is to provide the reader with a feel for the formulation of the method, its implementation, as well as review the existing theoretical and numerical results. The material presented in the present chapter may also be found in Elliotis et al. (2005 a, b), Xenophontos et al. (2006) and Christodoulou et al. (2009).

2.1 Introduction

Planar elliptic boundary value problems with boundary singularities have been extensively studied in the last few decades. Many different methods have been proposed for the solution of such problems, ranging from special mesh-refinement schemes to sophisticated techniques that incorporate, directly or indirectly, the form of the local asymptotic expansion, which is known in many occasions. These methods aim to improve the accuracy and resolve the

convergence difficulties that are known to appear in the neighborhood of such singular points. The local solution, centered at the singular point, in polar coordinates (r, θ) is of the general form:

$$u(r,\theta) = \sum_{i=1}^{\infty} \alpha_i \, r^{\mu_i} f_i(\theta) \tag{2.1}$$

where μ_i are the eigenvalues and f_i are the eigenfunctions of the problem, which are uniquely determined by the geometry and the boundary conditions along the boundaries sharing the singular point. The singular coefficients α_i, also known as generalized stress intensity factors (Szab*ó* and Babuška, 1991) or flux intensity factors (Arad et al., 1998), are determined by the boundary conditions in the rest of the boundary. Knowledge of the singular coefficients is of importance in many engineering applications, especially in fracture mechanics.

In the past few years, Georgiou and co-workers (Georgiou et al., 1996, 1997; Elliotis et al., 2002, 2005a, 2005b, 2006, 2007; Li et al., 2006; Xenophontos et al., 2006) developed the SFBIM, in which the unknown singular coefficients are calculated directly. The solution is approximated by the leading terms of the local asymptotic solution expansion and the Dirichlet boundary conditions are weakly enforced by means of Lagrange multipliers. The method has been tested on standard Laplacian and biharmonic problems, yielding extremely accurate estimates of the leading singular coefficients, and exhibiting exponential convergence with respect to the number of singular functions.

In this chapter, the SFBIM is reviewed and its convergence is discussed. The method is presented in section 2.2. In section 2.3, some convergence results for Laplacian problems are provided. Numerical results for Laplacian and biharmonic problems are presented and discussed in sections 2.4 and 2.5, respectively. Finally, section 2.6 contains the conclusions and briefly discusses our current efforts for extending the method to three dimensional Laplacian problems with edge sngularities.

2.2 The SFBIM for a planar Laplacian Problem

We consider the Laplacian problem with a boundary singularity, as depicted in Fig. 2.1: Find u such that

$$\nabla^2 u = 0 \text{ in } \Omega, \tag{2.2}$$

with boundary conditions

$$\left.\begin{array}{c} \frac{\partial u}{\partial n} = 0 \text{ on } S_1 \\ u = 0 \text{ on } S_2 \\ u = f(r,\theta) \text{ on } S_3 \\ \frac{\partial u}{\partial n} = g(r,\theta) \text{ on } S_4 \end{array}\right\}, \tag{2.3}$$

where Ω has a smooth boundary, $\partial\Omega = S_1 \cup S_2 \cup S_3 \cup S_4$, with the exception of a boundary singularity at the corner O, formed by the straight boundary segments S_1 and S_2. In the remaining parts of the boundary, either Dirichlet or Neumann boundary conditions apply and the given functions f and g are such that no other boundary singularity is present.

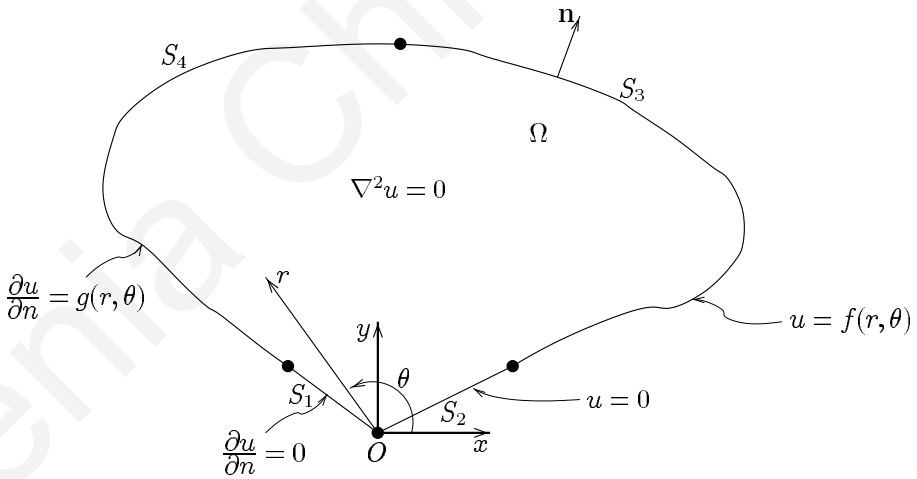

Figure 2.1: A two-dimensional Laplace equation problem with a boundary singularity.

The asymptotic expansion of the solution in polar co-ordinates (r,θ) centered at the singular point, is given by (see, e.g., Grisvard, 1995)

$$u(r,\theta) = \sum_{i=1}^{\infty} \alpha_i \, r^{\mu_i} f_i(\theta), \tag{2.4}$$

where α_i are the unknown singular coefficients or *Generalized Stress Intensity Factors* (GSIFs), μ_i are the singularity powers arranged in ascending order, and the functions $f_i(\theta)$ represent the θ-dependence of the eigensolution. Knowledge of the GSIFs is of great importance in applications (Georgiou et al., 1996; Arad et al., 1998), and their reliable and efficient extraction is the main focus of the SFBIM.

The SFBIM is based on the approximation of the solution by the leading terms of the local solution expansion, viz.

$$u_N = \sum_{i=1}^{N_\alpha} \alpha_i^N W^i, \tag{2.5}$$

where α_i^N are the approximate GSIFs and N_α is the number of singular functions used, which are defined by

$$W^i \equiv r^{\mu_i} f_i(\theta). \tag{2.6}$$

Note that the approximation (2.5) is valid only if Ω is a subset of the convergence domain of expansion (2.4).

By applying Galerkin's principle, we obtain

$$\iint_\Omega W^i \, \nabla^2 u_N \, dV = 0, \quad i = 1,\, 2,\, \ldots,\, N_\alpha. \tag{2.7}$$

By double application of Green's second identity, the above volume integral becomes

$$\int_{\partial\Omega} W^i \, \frac{\partial u_N}{\partial n} \, dS - \int_{\partial\Omega} u_N \, \frac{\partial W^i}{\partial n} \, dS + \iint_\Omega \bar{u} \, \nabla^2 W^i \, dV, \quad i = 1,\, 2,\, \ldots,\, N_\alpha \tag{2.8}$$

and, since the singular functions, W^i, are harmonic, the above volume integral is reduced to a boundary one, as follows:

$$\int_{\partial\Omega} \left(\frac{\partial u_N}{\partial n} \, W^i - u_N \, \frac{\partial W^i}{\partial n} \right) dS = 0, \quad i = 1,\, 2,\, \ldots,\, N_\alpha. \tag{2.9}$$

It is clear that the dimension of the problem is reduced by one, leading to a considerable reduction of the computational cost. Since, now W^i exactly satisfy the boundary conditions

along S_1 and S_2, the above integral along these boundary segments is identically zero, yielding

$$\int_{S_3} \left(\frac{\partial u_N}{\partial n} W^i - u_N \frac{\partial W^i}{\partial n} \right) dS + \int_{S_4} \left(\frac{\partial u_N}{\partial n} W^i - u_N \frac{\partial W^i}{\partial n} \right) dS = 0, \quad i = 1,\ 2,\ \ldots,\ N_\alpha. \tag{2.10}$$

It should be noted that the integrands in Eq. (2.10) are non-singular and all integrations are carried out far from the boundaries causing the singularity.

To impose the Neumann condition along S_4, we simply substitute the normal derivative by the known function g (see Eq. (2.3)). The Dirichlet condition along S_3 is imposed by means of a Lagrange multiplier function λ, replacing the normal derivative. The function λ is expanded in terms of standard, polynomial basis functions M^j of degree p, as

$$\lambda \approx \lambda_h = \sum_{j=1}^{N_\lambda} \lambda_j M^j, \tag{2.11}$$

where N_λ represents the total number of the unknown discrete Lagrange multipliers (or, equivalently, the total number of Lagrange-multiplier nodes) along S_4. The basis functions M^j are used to weight the Dirichlet condition along the corresponding boundary segment S_3. We thus obtain the following linear system of $N_\alpha + N_\lambda$ discretized equations:

$$\int_{S_3} \left(\lambda_h W^i - u_N \frac{\partial W^i}{\partial n} \right) dS - \int_{S_4} u_N \frac{\partial W^i}{\partial n}\, dS = - \int_{S_4} W^i\, g(r,\theta)\, dS, \quad i = 1,\ 2,\ \ldots,\ N_\alpha, \tag{2.12}$$

$$\int_{S_3} u_N\, M^j\, dS = \int_{S_3} f(r,\theta)\, M^j\, dS, \quad j = 1,\ 2,\ \ldots,\ N_\lambda. \tag{2.13}$$

The above system can be written in the following block form:

$$\begin{bmatrix} K_1 & K_2 \\ K_2^T & O \end{bmatrix} \begin{bmatrix} A \\ \Lambda \end{bmatrix} = \begin{bmatrix} F_1 \\ F_2 \end{bmatrix}, \tag{2.14}$$

where $A = [\alpha_1^N, ..., \alpha_{N_\alpha}^N]$ is the vector of the approximate singular coefficients, $\Lambda = [\lambda_1, ..., \lambda_{N_\lambda}]$ is the vector of the unknown Lagrange multipliers, submatrices K_1 and K_2 contain the coefficients of the unknowns (obviously, K_1 is symmetric), and vectors F_1 and F_2 contain the right hand side contributions of Eqs. (2.12) and (2.13), respectively. It is easily shown

that the system (2.14) is symmetric and nonsingular, provided $N_\alpha > N_\lambda$. The "optimal" relationship between these two parameters will be discussed in the next section.

2.3 Convergence Results

In this section we briefly present results from Xenophontos et al. (2006) which show that the method converges at an exponential rate. To this end let

$$H^1(\Omega) = \{u \in L^2(\Omega) : \nabla u \in L^2(\Omega)\}, \tag{2.15}$$

denote the usual Sobolev space, with $\|\cdot\|_{1,\Omega}$ denoting its norm, set

$$H^1_*(\Omega) = \{u \in H^1(\Omega) : u|_{S_2} = 0\}, \tag{2.16}$$

and note that $u \in H^1_*(\Omega)$. The space

$$H^{1/2}(\partial\Omega) = \{u \in H^1(\Omega) : u|_{\partial\Omega} \in L^2(\partial\Omega)\}, \tag{2.17}$$

is referred to as the trace space of functions in $H^1(\partial\Omega)$ and its norm will be denoted by $\|\cdot\|_{1/2,\Omega}$. Finally, the dual space of $H^{1/2}(\partial\Omega)$, denoted by $H^{-1/2}(\partial\Omega)$, with norm $\|\cdot\|_{-1/2,\Omega}$, will also be used (see Xenophontos et al., 2006 for more details). The approximate solution u_N, will be chosen from the finite dimensional space $V_\alpha \subset H^1_*(\Omega)$, defined by

$$V_\alpha = span\{W^i\}_{i=1}^{N_\alpha}. \tag{2.18}$$

The Lagrange multiplier function λ belongs to $H^{-1/2}(S_3)$ and its approximation will be chosen from the finite dimensional space V_λ which is defined as follows. Let S_3 be divided into quasiuniform sections Γ_i, $i = 1, 2, \ldots, n$ such that $S_3 = \cup_{i=1}^n \Gamma_i$. Let $h_i = |\Gamma_i|$ and set $h = \max\limits_{1\le i\le n} h_i$. We assume that for each segment Γ_i there exist an invertible mapping

$F : I \to \Gamma_i$ which maps the interval $I = [-1, 1]$ to Γ_i, and define

$$V_\lambda = \{\lambda_h : \lambda_h|_{\Gamma_i} \circ F_i^{-1} \in P_p(I), i = 1, 2, \ldots, n\}, \tag{2.19}$$

where $P_p(I)$ is the set of polynomials of degree $\leq p$ on $I = [-1, 1]$. In other words, the Lagrange multiplier function λ is a linear combination of piecewise polynomials of degree p, defined on a quasiuniform partition of S_3 characterized by the meshwidth h. Note that the number of Lagrange multipliers N_λ satisfies $N_\lambda = O(p/h)$.

In Xenophontos et al. (2006) it was shown that if u and $\lambda = \partial u/\partial n$ are approximated by u_N and λ_h, given by Eqs. (2.5) and (2.11), respectively, then there exists a positive constant C, independent of N_α and N_λ, such that

$$\|u - u_N\|_{1,\Omega} + \|\lambda - \lambda_h\|_{-1/2,S_3} \leq C \left\{ \inf_{v \in V_\alpha} \|u - v\|_{1,\Omega} + \inf_{\eta \in V_\lambda} \|\lambda - \eta\|_{-1/2,S_3} \right\}. \tag{2.20}$$

Using the above best approximation result it was further shown that if $\lambda \in H^k(S_3)$ for some $k \geq 1$, then there exists positive constants C and $\beta \in (0, 1)$, independent of N_α and N_λ, such that

$$\|u - u_N\|_{1,\Omega} + \|\lambda - \lambda_h\|_{-1/2,S_3} \leq C \left\{ \sqrt{N_\alpha} \beta^{N_\alpha} + h^m p^{-k} \right\}, \tag{2.21}$$

where $m = \min\{k, p + 1\}$. Moreover, since the error between the exact coefficients α_i and approximate coefficients α_i^N satisfies

$$\left|\alpha_i - \alpha_i^N\right| \leq C \|u - u_N\|_{L^2(\Omega)}, \tag{2.22}$$

we have

$$\left|\alpha_i - \alpha_i^N\right| \leq C\beta^{N_\alpha}, \tag{2.23}$$

which shows that the method approximates these coefficients at an exponential rate, as $N_\alpha \to \infty$.

Based on the error estimate (2.21) one may obtain the "optimal" matching between the parameters N_α and h, i.e. the relationship between the number of singular functions and the

number of Lagrange multipliers used in the method, by choosing them in such a way so that the error in (2.22) is balanced. For example in the case when p is kept fixed and $h \to 0$ (or equinalently $N_\lambda \to \infty$) we take $h^{p+1} \approx \sqrt{N_\alpha}\beta^{N_\alpha}$. This leads to the following approximate expression for N_α:

$$N_\alpha \approx (p+1)\left|\frac{\ln \frac{2p}{N_{\lambda-1}}}{\ln \beta}\right|. \tag{2.24}$$

In practice, Eq. (2.24) is used as follows: We pick a value for N_λ and solve the linear system (2.14) for several values of $N_\alpha > N_\lambda$ concentrating only on the calculation of the first approximate α_1^N, which we record. Once we reach a value for N_α which yields an approximate α_1^N with, say, 16 converged significant digits, we then use Eq. (2.24) to calculate the constant β using the values for N_α and N_λ which gave us the converged coefficient α_1^N. With β now known, we can compute subsequent "optimal" pairs of N_α and N_λ.

2.4 Numerical Results for two Laplace Problems

Results for the cracked-beam problem (Georgiou et al., 1997) and a Laplacian problem over an L-shaped domain (Elliotis et al. 2005) are presented in this section. The former problem is defined in Fig. 2.2 . A singularity arises at $x = y = 0$, where the boundary condition suddenly changes from $u = 0$ to $\partial u/\partial y = 0$. The local solution is given by

$$u = \sum_{j=1}^{\infty} \alpha_j r^{\frac{(2j-1)}{2}} \cos\left[\left(\frac{2j-1}{2}\right)\theta\right], \tag{2.25}$$

and its approximation by

$$u_N = \sum_{j=1}^{N_\alpha} \alpha_j^N r^{\frac{(2j-1)}{2}} \cos\left[\left(\frac{2j-1}{2}\right)\theta\right].$$

The system of discretized equations, resulting from the application of the SFBIM, consists of two equation sets as follows:

$$-\int_{S_3} u_N \frac{\partial W^i}{\partial x} dy + \int_{S_4} \left(\lambda W^i - u_N \frac{\partial W^i}{\partial y}\right) dx + \int_{S_5} u_N \frac{\partial W^i}{\partial x} dy = 0, \quad i = 1, 2, \ldots, N_\alpha, \tag{2.26}$$

i	α_i^N
1	0.191118631972
2	−0.118116071967
3	0.000000000000
4	0.000000000000
5	−0.01254698598
6	−0.01903340371

Table 2.1: The coefficients α_i^N calculated with $N_\alpha = 50$ and $N_\lambda = 25$.

$$\int_{S_4} u_N M^j dx = 0.125 \int_{S_4} M^j dx = 0, \quad j = 1, 2, \ldots, N_\lambda. \tag{2.27}$$

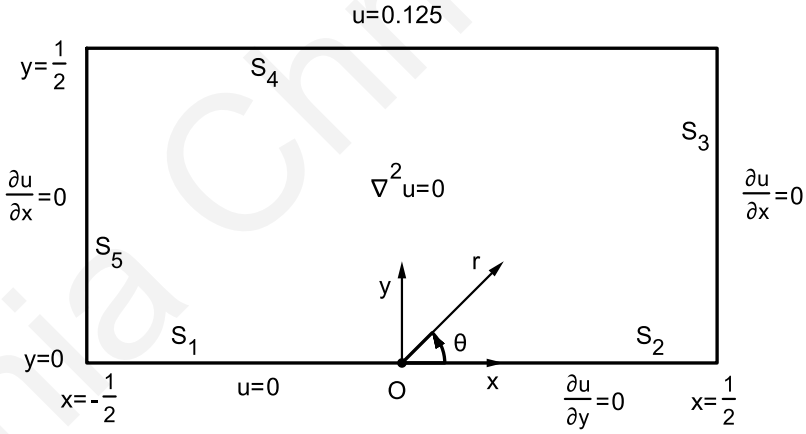

Figure 2.2: The cracked-beam problem.

The interval $[-1/2, 1/2]$, corresponding to the boundary segment S_4, is subdivided unformly into quadratic elements and, thus, the Lagrange multiplier function is approximated locally by quadratic polynomials. All numerical integrations were performed using Gaussian quadrature with 15 nodes on each subinterval. Using Eq. (2.24), we find that the "optimal" values for N_α and N_λ are 50 and 25, respectively, and using them we calculate the first 6 approximate coefficients, as shown in Table 2.1.

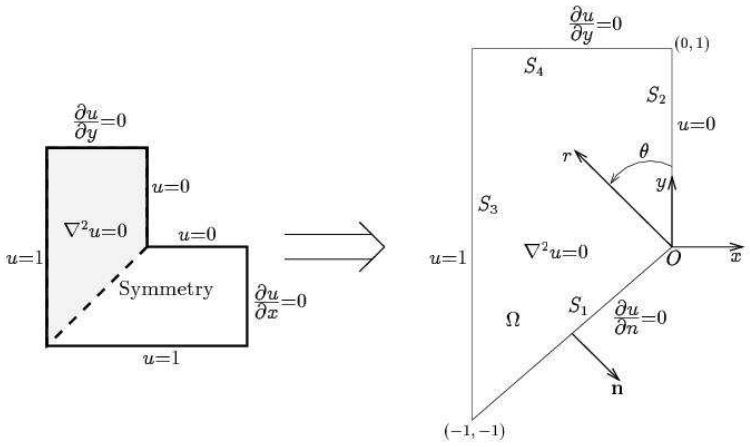

Figure 2.3: A Laplacian problem over an L-shaped domain.

The second Laplacian problem is depicted in Fig. 2.3. This is equivalent to a Poisson equation problem, $\nabla^2 u = -1$, over an L-shaped domain, with homogeneous Dirichlet boundary conditions along the whole boundary. Note that along boundary parts S_2 and S_3 essential boundary conditions are applied. Due to symmetry, only half of the domain is considered. The local solution is given by

$$u = \sum_{j=1}^{\infty} \alpha_j r^{\frac{2(2j-1)}{3}} \sin\left[\frac{2}{3}(2j-1)\theta\right]. \tag{2.28}$$

The quantity $2\alpha_1/3$ is of interest, since it may be considered as the leading "generalized stress intensity factor" (see Arad et al., 1998). It should be noted that two sets of Lagrange multiplier functions, denoted by λ_A and λ_B, are now required. Thus, the Dirichlet boundary conditions along S_2 and S_3 are replaced by:

$$\lambda_A = \frac{\partial u_N}{\partial x} = \sum_{j=1}^{N_{\lambda_A}} \lambda_A^j M^j \text{ and } \lambda_B = \frac{\partial u_N}{\partial y} = \sum_{j=1}^{N_{\lambda_B}} \lambda_B^j M^j, \tag{2.29}$$

where N_{λ_A} and N_{λ_B} are the numbers of nodes along S_2 and S_3, respectively. The following system of $N_\alpha + N_{\lambda_A} + N_{\lambda_B}$ linear equations is thus obtained:

$$-\int_{S_2} \left(\lambda_A W^i - u_N \frac{\partial W^i}{\partial x}\right) dy + \int_{S_3} \left(\lambda_B W^i - u_N \frac{\partial W^i}{\partial y}\right) dx = 0, \quad i = 1, 2, \ldots, N_\alpha, \tag{2.30}$$

$$-\int_{S_2} u_N M^j dy = \int_{S_2} u_p M^j dy, \quad j = 1, 2, \ldots, N_{\lambda_A}, \tag{2.31}$$

$$\int_{S_3} u_N M^k dx = \int_{S_3} u_p M^k dx, \quad k = 1, 2, \ldots, N_{\lambda_B}. \tag{2.32}$$

As before, M^j are chosen as (piecewise) quadratic polynomials and all numerical integrations are performed using Gaussian quadrature with 15 nodes on each subinterval. The "optimal" values for N_α and $N_\lambda = N_{\lambda_A} + N_{\lambda_B}$ are found via Eq. (2.24) to be $N_\alpha = 90$ and $N_\lambda = 38$. The computed leading singular coefficients are listed in Table 2.2.

i	α_i^N		i	α_i^N
1	0.40193103		9	-0.000719
2	0.09364829		10	-0.000565
3	−0.0093830		11	-0.000395
4	−0.0298851		12	-0.000296
5	−0.0083588		13	-0.000219
6	−0.0047302		14	-0.000173
7	−0.0015451		15	-0.000138
8	−0.001098			

Table 2.2: Converged values of the leading singular coefficients with $N_\alpha = 90$ and $N_\lambda = 38$.

2.5 The SFBIM for a Planar Biharmonic Problem

In this section we describe the extension of the SFBIM to biharmonic problems arising in fracture mechanics. Even though no convergence analysis was available before this work, the method was tested on various biharmonic problems (Elliotis et al., 2005a, 2005b, 2006, 2007) and was found to converge (again exponentially) with respect to the number of singular functions. The convergence analysis for a model biharmonic problem with one boundary singularity is presented in Chapter 4. Here we consider a two-dimensional solid elastic plate

containing a single edge crack subjected to a uniform inplane load normal to the two edges parallel to the crack, while the remaining edges are stress free. The resulting boundary value problem is to find u such that:

$$\nabla^4 u = 0 \text{ in } \Omega = (-1,1) \times (0,1), \tag{2.33}$$

with

$$\left.\begin{aligned} u = 0, \quad \frac{\partial u}{\partial y} = 0, \quad \text{on } S_A \\ \frac{\partial u}{\partial y} = 0, \quad \frac{\partial^3 u}{\partial y^3} = 0, \quad \text{on } S_B \\ u = 2, \quad \frac{\partial u}{\partial x} = 2, \quad \text{on } S_C \\ u = \tfrac{1}{2}(x+1)^2, \quad \frac{\partial u}{\partial y} = 0, \quad \text{on } S_D \\ u = 0, \quad \frac{\partial u}{\partial x} = 0, \quad \text{on } S_E \end{aligned}\right\} \tag{2.34}$$

where $\partial\Omega = S_A \cup S_B \cup S_C \cup S_D \cup S_E$.

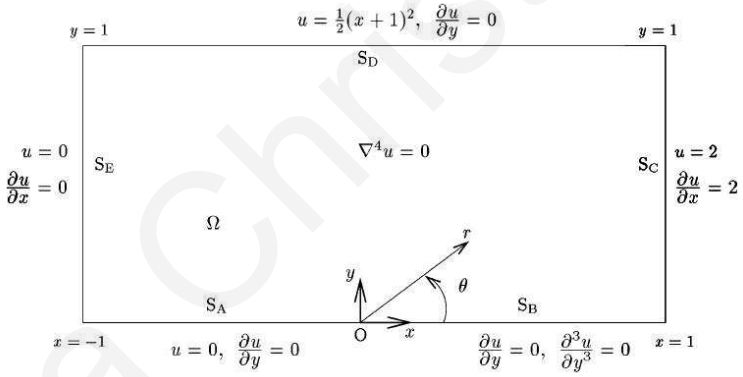

Figure 2.4: Model biharmonic problem.

The asymptotic expansion for u in the neighborhood of the singular point O is given by

$$u(r,\theta) = \sum_{j=1}^{\infty} \left[c_j W_1^j(r,\theta) + d_j W_2^j(r,\theta) \right], \tag{2.35}$$

where (r,θ) are the polar coordinates centered at O, and c_j. d_j correspond to the even and odd coefficients, respectively (see also Schiff 1979). The two sets of singular functions W_k^j, $j = 1, 2, \ldots, N_\alpha$, $k = 1, 2$, are given by

$$W_k^j \equiv^{\mu_j + 1} f_k(\theta, \mu_j), \tag{2.36}$$

where

$$f_1(\theta, \mu_j) = \cos(\mu_j - 1)\theta - \cos(\mu_j + 1)\theta, \quad \mu_j = j \tag{2.37}$$

and

$$f_2(\theta, \mu_j) = \cos(\mu_j - 1)\theta - \frac{\mu_j - 1}{\mu_j + 1}\cos(\mu_j + 1)\theta, \quad \mu_j = j - 1/2. \tag{2.38}$$

Note that the singular functions W_k^j satisfy the PDE (2.33) and the boundary conditions on S_A and S_B.

As in the Laplacian case, the solution will be approximated by the leading terms of the asymptotic expansion, viz:

$$u_N = \sum_{i=1}^{N_\alpha} c_i^N W_1^i + \sum_{i=1}^{N_\alpha} d_i^N W_2^i, \tag{2.39}$$

where c_i^N and d_i^N are the approximations to the coefficients. Applying Galerkin's principle, the governing equation is weighted by the singular functions, which gives the following set of discretized equations:

$$\iint_\Omega W_k^i \nabla^4 u_N dV = 0, \quad i = 1, 2, \ldots, N_\alpha, \;\; k = 1, 2. \tag{2.40}$$

Next, applying Green's theorem twice and since the singular functions satisfy the governing biharmonic equation (2.33), the above integrals are reduced to

$$\int_{\partial\Omega} \left(\frac{\partial u_N}{\partial n} \nabla^2 W_k^i - u_N \frac{\partial(\nabla^2 W_k^i)}{\partial n} \right) dS + \int_{\partial\Omega} \left(\frac{\partial(\nabla^2 u_N)}{\partial n} W_k^i - \nabla^2 u_N \frac{\partial W_k^i}{\partial n} \right) dS = 0, \tag{2.41}$$

for $i = 1, 2, \ldots, N_\alpha$, $k = 1, 2$. Now, since W_k^j satisfy exactly the boundary conditions along S_A and S_B, the above integral along these boundary segments is identically zero. Therefore, we have

$$\int_{S} \left(\frac{\partial u_N}{\partial n} \nabla^2 W_k^i - u_N \frac{\partial(\nabla^2 W_k^i)}{\partial n} \right) dS + \int_{S} \left(\frac{\partial(\nabla^2 u_N)}{\partial n} W_k^i - \nabla^2 u_N \frac{\partial W_k^i}{\partial n} \right) dS = 0, \tag{2.42}$$

where $i = 1, 2, \ldots, N_\alpha$, $k = 1, 2$ and $S = S_C \cup S_D \cup S_E$. As before, the Dirichlet boundary conditions are imposed by means of Lagrange multipliers. In the case of Laplacian problems, the Lagrange multipliers replace the normal derivative $\partial u_N / \partial n$. In the case of biharmonic

problems, another option for the Lagrange multipliers is to replace $\partial\nabla^2 u_N/\partial n$, which is the choice made here. In the present problem, Dirichlet boundary conditions appear along the three boundary parts of interest, i.e. S_C, S_D and S_E, where the normal derivative of the solution is also specified. Therefore, Lagrange multipliers have been chosen to replace $\partial\nabla^2 u_N/\partial n$ on boundary parts S_C, S_D and S_E. These are partitioned into three-node elements and the corresponding Lagrange multipliers, denoted respectively by λ_C, λ_D and λ_E, are expanded in terms of quadratic basis functions M^j as:

$$\lambda_C = \frac{\partial(\nabla^2 u_N)}{\partial x} = \sum_{j=1}^{N_{\lambda_C}} \lambda_C^j M^j \text{ on } S_C, \tag{2.43}$$

$$\lambda_D = \frac{\partial(\nabla^2 u_N)}{\partial y} = \sum_{j=1}^{N_{\lambda_D}} \lambda_D^j M^j \text{ on } S_D, \tag{2.44}$$

and

$$\lambda_E = \frac{\partial(\nabla^2 u_N)}{\partial x} = \sum_{j=1}^{N_{\lambda_E}} \lambda_E^j M^j \text{ on } S_E, \tag{2.45}$$

where N_{λ_C}, N_{λ_D} and N_{λ_E} are the numbers of the discrete Lagrange multipliers λ_C^j, λ_D^j and λ_E^j along the corresponding boundaries. The discrete Lagrange multipliers appear as additional unknowns in the problem. The required $N_{\lambda_C} + N_{\lambda_D} + N_{\lambda_E}$ additional equations are obtained by weighting the Dirichlet boundary conditions along S_C, S_D and S_E by the quadratic basis functions M^j in the Galerkin sense. The following system of $2N_\alpha + N_{\lambda_C} + N_{\lambda_D} + N_{\lambda_E}$ discretized equations is thus obtained:

$$\begin{aligned}
&\int_{S_C} \left(\lambda_C W_k^i - u_N \tfrac{\partial(\nabla^2 W_k^i)}{\partial x} - \nabla^2 u_N \tfrac{\partial W_k^i}{\partial x}\right) dy + \\
&\int_{S_D} \left(\lambda_D W_k^i - u_N \tfrac{\partial(\nabla^2 W_k^i)}{\partial y} - \nabla^2 u_N \tfrac{\partial W_k^i}{\partial y}\right) dx + \\
&\int_{S_E} \left(-\lambda_E W_k^i + u_N \tfrac{\partial(\nabla^2 W_k^i)}{\partial x} + \nabla^2 u_N \tfrac{\partial W_k^i}{\partial x}\right) dy + \\
&= -\int_{S_C} 2\nabla^2 W_k^i dy \quad i = 1, 2, \ldots, N_\alpha \;\; k = 1, 2,
\end{aligned} \tag{2.46}$$

$$\int_{S_C} u_N M^j dy = \int_{S_C} 2M^j dy, \quad j = 1, 2, \ldots, N_{\lambda_C}, \tag{2.47}$$

$$\int_{S_D} u_N M^j dy = \int_{S_D} \left[\frac{1}{2}(x+1)^2\right] M^j dx, \quad j = 1, 2, \ldots, N_{\lambda_D}, \tag{2.48}$$

$$-\int_{S_E} u_N M^j dy = 0, \quad j = 1, 2, \ldots, N_{\lambda_E}. \tag{2.49}$$

As in the case of Laplacian problems, the integrands in Eqs. (2.46)–(2.49) are non-singular and all integrations are carried out far from the boundaries causing the singularity. Also, the stiffness matrix is symmetric and becomes singular if $N_\lambda > 2N_\alpha$ where $N_\lambda = N_{\lambda_C} + N_{\lambda_D} + N_{\lambda_E}$. Since there was no theory available for the biharmonic problems, what was done in Elliotis et al. (2006) was to find the "optimal" values of N_α and N_λ by systematic runs. It was found that the choice $N_\alpha = 47$, $N_\lambda = 39 (= 7 + 25 + 7)$ produces very accurate results. These are converged in the sense that they are not affected by moderate changes of N_α and N_λ (see Elliotis et al. 2006 for more details). Table 2.5 shows the approximate coefficients c_i^N, d_i^N, $i = 1, 2, \ldots, 10$ obtained with this choice of parameters, along with the results from (Li et al. 2004) for comparison. It appears that the SFBIM can be effective for biharmonic problems as well, and this will be mathematically established in Chapter 4.

2.6 Conclusions

The SFBIM for planar Laplacian and biharmonic problems with boundary singularities has been reviewed. The convergence of the method has been demostrated theoretically for Laplacian problems and numerical applications have been presented for two Laplacian and a biharmonic elasticity test problems.

Approx. coeffs	Collocation Trefftz	SFBIM
d_1	2.12751351	2.1275134
d_2	-1.0366925	-1.036692
d_3	0.0371711	0.037170
d_4	0.117749	0.11775
d_5	-0.122728	-0.12273
d_6	-0.109909	-0.10991
d_7	-0.002255	-0.00226
d_8	0.006863	0.00686
d_9	-0.005936	-0.00594
d_{10}	-0.011032	-0.01103
c_1	0.1667621	0.166762
c_2	0.0624433	0.062444
c_3	-0.1324738	-0.132474
c_4	-0.010221	-0.01022
c_5	0.105846	0.10585
c_6	0.031153	0.03115
c_7	-0.007149	-0.00714
c_8	-0.001684	-0.00169
c_9	0.009484	0.00950
c_{10}	0.004281	0.00426

Table 2.3: Comparison of converged values of the coefficients with those reported by Li et al. (2004) using the Collocation Trefftz method.

Chapter 3

The SFBIM for Laplacian Problems Over Circular Sectors

In this chapter we consider two model Laplacian problems over a circular sector, with an exact solution, in order to verify the theoretical convergence of the SFBIM.

All the results discussed in this chapter are also found in Christodoulou et al. (2010).

3.1 Introduction

In the last few decades there has been an extensive study of planar elliptic boundary value problems with boundary singularities. The methods that have been proposed for the solution of such problems range from special mesh-refinement schemes to sophisticated techniques that incorporate, directly or indirectly, the form of the local asymptotic expansion, which is known in many occasions. These methods aim to improve the accuracy and resolve the convergence difficulties that are known to appear in the neighborhood of singular points.

The local solution, centered at the singular point, in polar coordinates (r, θ) is of the general

form

$$u(r,\theta) = \sum_{j=1}^{\infty} \alpha_j r^{\mu_j} f_j(\theta), \tag{3.1}$$

where μ_j, f_j are, respectively, the eigenvalues and eigenfunctions of the problem, which are uniquely determined by the geometry and the boundary conditions along the boundaries sharing the singular point. The singular coefficients α_j also known as generalized stress intensity factors or flux intensity factors (Arad et al., 1998), are determined by the boundary conditions in the rest of the boundary. Knowledge of the singular coefficients is of importance in many engineering applications, especially in fracture mechanics.

In the past few years, Georgiou and co-workers (Georgiou 1996, 1997; Elliotis 2002, 2005a, 2005b, 2006, 2007; Li 2006; Xenophontos 2006) developed the Singular Function Boundary Integral Method (SFBIM), in which the unknown singular coefficients are calculated directly. The solution is approximated by the leading terms of the local asymptotic solution expansion and the Dirichlet boundary conditions are weakly enforced by means of Lagrange multipliers. The method has been tested on standard Laplacian and biharmonic problems, yielding extremely accurate estimates for the leading singular coefficients, and exhibiting exponential convergence with respect to the number of singular functions. Theoretical results on the convergence of the method in the case of Laplacian problems where given by Xenophontos et al. (2006).

The SFBIM belongs to the class of boundary approximation methods (BAMs) or Trefftz methods (TM), which have been recently reviewed by Li and co-workers Li et al. (2004) and compared to collocation and other boundary methods. Other recent reviews of methods used for elliptic boundary value problems with boundary singularities can be found in the articles of Bernal et al. (2009) who considered both global and local meshless collocation methods with multiquadrics as basis functions, and of Dosiyev and Buranay (2008) who employed the block method which was proposed for the solution of Laplace problems on arbitrary polygons. The objective of this chapter is to apply the SFBIM to two model Laplacian problems over

circular sections in order to investigate the effect of the order of the Lagrange multiplier approximation in connection with the theoretical error estimates.

In section 3.2, two Laplacian problems over circular sections are presented. One problem has Dirichlet and the other Neumann boundary conditions along the arc. The formulation of the method for both cases is given in section 3.3. In section 3.4, numerical results are presented for piecewise constant, linear, quadratic and cubic basis functions, used for the approximation of the Lagrange multipliers. These results are compared with the theoretical error estimates. Finally, section 3.5 summarizes the conclusions.

3.2 The Model Problems

We consider two Laplacian test problems over circular sectors of angle $\alpha\pi$ and radius R, as depicted in Fig. 3.1. A boundary singularity occurs at the origin which is due, not only to the geometry (i.e. the presence of an angle in the boundary) but also to the fact that different boundary conditions are imposed on the boundary parts S_1 ($\theta = 0$) and S_2 ($\theta = \alpha\pi$). The two test problems differ only in the boundary condition along the circular arc S_3, where Dirichlet and Neumann boundary conditions are respectively prescribed. For both problems the local solution is

$$u = \sum_{j=1}^{\infty} \alpha_j r^{\mu_j} \sin(\mu_j \theta). \tag{3.2}$$

In problem 1 (Fig. 3.1a), the Dirichlet boundary condition along S_3 is given by

$$u = f(\theta) = \theta - \frac{\theta^2}{2\alpha\pi}. \tag{3.3}$$

In problem 2 (Fig. 3.1b), the Neumann boundary condition along S_3 is given by

$$\frac{\partial u}{\partial r} = g(\theta) = \frac{\theta}{\alpha\pi}. \tag{3.4}$$

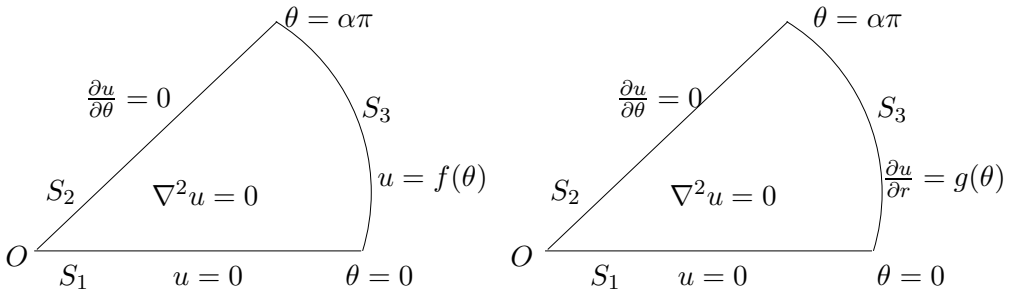

(a) **(b)**

Figure 3.1: Test Laplacian problems over circular sectors. (a) Problem 1 (b) Problem 2.

For both problems, we have

$$\mu_j = \frac{2j-1}{2\alpha}. \tag{3.5}$$

The singular coefficients for problem 1 are given by

$$\alpha_j = \frac{16\alpha}{\pi^2 R^{\mu_j}(2j-1)^3}, \tag{3.6}$$

and for problem 2 by

$$\alpha_j = \frac{(-1)^{j+1}16\alpha}{\pi^2 R^{\mu_j - 1}(2j-1)^3}. \tag{3.7}$$

3.3 Formulation of the SFBIM

The SFBIM is based on the approximation of the solution by the leading terms of the local solution expansion:

$$u_N = \sum_{j=1}^{N_\alpha} \alpha_j^N W_j, \tag{3.8}$$

where N_α is the number of singular functions $W_j = r^{\mu_j}\sin(\mu_j\theta)$. By applying Galerkin's principle, we obtain

$$\iint_\Omega W_j \nabla^2 u_N dV = 0, \quad j = 1, 2, ..., N_\alpha. \tag{3.9}$$

By double application of Green's second identity, and keeping in mind that the singular functions W_j are harmonic, the above volume integral becomes

$$\int_{\partial\Omega} W_j \frac{\partial u_N}{\partial n} dS - \int_{\partial\Omega} u_N \frac{\partial W_j}{\partial n} dS = 0, \quad j = 1, 2, ..., N_\alpha. \tag{3.10}$$

Now, since the W_j's satisfy the boundary conditions along S_1 and S_2, the above integral along these boundaries is zero. Therefore, we get

$$\int_{S_3} \left(W_j \frac{\partial u_N}{\partial n} - u_N \frac{\partial W_j}{\partial n} \right) dS = 0, \quad j = 1, 2, ..., N_\alpha. \tag{3.11}$$

It should be noted that integration is needed only along S_3, i.e. far from the singularity and not along the boundary parts causing the singularity.

3.3.1 Formulation of Problem 1

The Dirichlet condition along S_3 is imposed by means of a Lagrange multiplier function λ, which replaces the normal derivative. The function λ is expanded in terms of standard polynomial basis functions M_i of order p:

$$\lambda = \frac{\partial u_N}{\partial n} = \sum_{i=1}^{N_\lambda} \lambda_i M_i, \tag{3.12}$$

where N_λ represents the total number of unknown discrete Lagrange multipliers λ_i (or, equivalently, the total number of Lagrange multiplier nodes) along S_3. The basis functions M_i are used to weigh the Dirichlet condition along the corresponding boundary segment S_3. Hence, we obtain the following symmetric system of $N_\alpha + N_\lambda$ discretized equations:

$$\int_{S_3} \left(\lambda W_j - u_N \frac{\partial W_j}{\partial n} \right) dS = 0, \quad j = 1, 2, ..., N_\alpha, \tag{3.13}$$

$$\int_{S_3} u_N M_i dS = \int_{S_3} f(r, \theta) M_i dS, \quad i = 1, 2, ..., N_\lambda. \tag{3.14}$$

The above system can be written in (block) matrix form as

$$\begin{bmatrix} D_{N_\alpha \times N_\alpha} & K_{N_\alpha \times N_\lambda} \\ K^T_{N_\lambda \times N_\alpha} & O_{N_\lambda \times N_\lambda} \end{bmatrix} \begin{bmatrix} A \\ \Lambda \end{bmatrix} = \begin{bmatrix} O \\ F \end{bmatrix}, \tag{3.15}$$

where A and Λ are, respectively, the vectors of unknown singular coefficients and Lagrange multipliers. It turns out that for this simple geometry the submatrix D is always diagonal with

$$D_{ii} = -\mu_i R^{2\mu_i} \frac{\alpha\pi}{2}. \tag{3.16}$$

The submatrix K and the forcing vector F are given by

$$K_{ij} = R^{\mu_i+1} \int_0^{\alpha\pi} M_j \sin \mu_i \theta d\theta, \tag{3.17}$$

$$F_i = R \int_0^{\alpha\pi} f(\theta) M_i d\theta, \tag{3.18}$$

and can be calculated analytically for various orders p of the approximation of the Lagrange multiplier function. The entries in K and F for $p = 0, 1, 2$ and 3 are given in the Appendix A.

According to the analysis in Xenophontos et al. (2006), if $\lambda \in H^k(S_3)$ for some $k \geq 1$ and λ_h is the approximation to the Lagrange multiplier function with h being the meshwidth, then there exist positive constants C and $\beta \in (0, 1)$, independent of N_α and h such that

$$\|u - u_N\|_{1,\Omega} + \|\lambda - \lambda_h\|_{-1/2,S_3} \leq C\{\sqrt{N_\alpha}\beta^{N_\alpha} + h^m p^{-k}\}, \tag{3.19}$$

where $m = \min\{k, p+1\}$. Here, $H^k(\Omega), k \in \mathbb{N}$ is the usual Sobolev space which contains functions that have k generalized derivatives in the space of squared integrable functions $L^2(\Omega)$. The norm $\|\cdot\|_{1,\Omega}$ is defined, as usual, by

$$\|f\|_{1,\Omega} := \left[\int_\Omega \{f^2 + f_x^2 + f_y^2\} dxdy\right]^{1/2}. \tag{3.20}$$

The norm $\|\cdot\|_{-1/2,S_3}$ that appears in (3.19) is defined as follows: Let $H^{1/2}(S_3)$ denote the space of functions in $H^1(\Omega)$ whose (trace) values on S_3 belong to $L^2(S_3)$, let $T : H^1(\Omega) \to H^{1/2}(S_3)$ denote the trace operator, and define the norm

$$\|\psi\|_{1/2,S_3} = \inf_{u \in H^1(\Omega)} \{\|u\|_{1,\Omega} : Tu = \psi\}. \tag{3.21}$$

Then,

$$\|\phi\|_{-1/2,S_3} = \sup_{\psi \in H^{1/2}(S_3)} \frac{\int_{S_3} \phi\psi}{\|\psi\|_{1/2,S_3}}. \tag{3.22}$$

For more details see Xenophontos et al. (2006).

From (3.19) it is clear that the approximate solution converges exponentially with respect to the number of singular functions, N_α. Moreover, if we choose the two errors in (3.19) to be balanced, we obtain the following relationship between the number of singular functions and the number of basis functions used to approximate the Lagrange multiplier:

$$h^p \approx \sqrt{N_\alpha}\beta^{N_\alpha} \Longleftrightarrow \left(\frac{\alpha\pi}{N_\lambda - 1}\right)^p \approx \sqrt{N_\alpha}\beta^{N_\alpha} \Rightarrow \tag{3.23}$$

$$N_\lambda \approx 1 + \frac{\alpha\pi}{\left(\sqrt{N_\alpha}\beta^{N_\alpha}\right)^{1/p}}. \tag{3.24}$$

It was also shown in Xenophontos et al. (2006) that

$$|\alpha_j - \alpha_j^N| \leq C\beta^{N_\alpha}, \tag{3.25}$$

which shows that the approximate singular coefficients α_j^N converge exponentially with respect to the number of singular functions.

3.3.2 Formulation of Problem 2

To impose the Neumann conditions, the normal derivative in (3.11) is simply substituted by the known function g. It turns out that for this problem all integrations can be performed analytically as this substitution gives

$$\int_{S_3} u_N \frac{\partial W_i}{\partial n} dS = \int_{S_3} g W_i dS \ , \ \ i = 1, 2, ..., N_\alpha. \tag{3.26}$$

The above expression becomes

$$\alpha_i R^{2\mu_i - 1}\mu_i \int_0^{\alpha\pi} \sin^2(\mu_i\theta) d\theta = R^{\mu_i} \int_0^{\alpha\pi} g(\theta)\sin(\mu_i\theta) d\theta, \tag{3.27}$$

from which we find that

$$\alpha_i = \frac{4}{R^{\mu_i - 1}\pi(2i-1)} \int_0^{\alpha\pi} g(\theta)\sin(\mu_i\theta) d\theta = \frac{(-1)^{i+1}16\alpha}{R^{\mu_i - 1}\pi^2(2i-1)^3}, \tag{3.28}$$

and the method is equivalent to the method of separation of variables. In the next section we will present numerical results for the first test problem.

3.4 Numerical Results

We show results for three different values of the constant α defining the angle θ of the circular sector: $\alpha = 1, 1.5, 2$, which correspond to a semi-circle, an L-shaped domain and a domain with a slit, respectively. Our goal is to verify that

$$\|u - u_N\|_{1,\Omega} + \|\lambda - \lambda_h\|_{-1/2,S_3} \leq C\{\sqrt{N_\alpha}\beta^{N_\alpha} + h^m p^{-k}\}, \tag{3.29}$$

where $m = \min\{k, p+1\}$, as well as

$$|\alpha_j - \alpha_j^N| \leq C\beta^{N_\alpha}. \tag{3.30}$$

3.4.1 Semi-Circle ($\alpha = 1$)

First we consider the case $\alpha = 1$ for the angle θ, which corresponds to the domain being a semi-circle. Our first step was to determine the constant β appearing in (3.29), which was done as follows: We choose a value for N_λ, say $N_\lambda = 10$, and solve the linear system (3.11) for various values of $N_\alpha > 10$, using, e.g., $p = 2$. Concentrating on the first singular coefficient, we record the results in Table 3.1. Since the exact value of the first coefficient is $\alpha_1 = 16/\pi^2 \approx 1.621138938277404$, we see from the results of Table 3.1 that α_1^N has "converged" once $N_\alpha = 30$. Hence, using (3.24) and the "optimal" pair $N_\alpha = 30, N_\lambda = 10$ we compute the value for β as $\beta \approx 0.88$.

With β known, we use (3.30) to determine subsequent "optimal" values for N_λ and N_α, for use in our computations. We should note that in general, the exact value of the first coefficient is unknown, hence in practice we choose the "optimal" value of N_α based on the changes that appear in the computed α_1^N, i.e. once the value of α_1^N does not change significantly.

N_α	α_1^N		N_α	α_1^N
12	1.617187500000000		27	1.621138938152942
13	1.621215820312500		28	1.621138938197758
14	1.619140625000000		29	1.621138938231953
15	1.621154785156250		**30**	**1.621138938258757**
16	1.622070312500000		31	1.621138938280287
17	1.621398925781250		32	1.621138938297822
18	1.621582031250000		33	1.621138938312330
19	1.621154785156250		34	1.621138938324523
20	1.621215820312500		35	1.621138938334964
21	1.621138935554673		36	1.621138938344132
22	1.621138937140710		37	1.621138938352468
23	1.621138937635686		38	1.621138938360383
24	1.621138937869855		39	1.621138938368192
25	1.621138938004718		40	1.621138938368413
26	1.621138938092001			

Table 3.1: Approximate singular coefficient a_1^N, computed with $N_\lambda = 10$, $\alpha = 1$.

In Fig. 3.2 we show the convergence of the approximate solution and in particular the percentage relative error in the approximation of u versus N_α, in a semi-log scale for $p = 1, 2, 3$. Since each curve becomes a straight line as N_α is increased, we see that the error decreases at an exponential rate and the convergence as predicted by (3.29) is verified. Comparing the error curves in Fig. 3.2 we observe that the slope for $p = 3$ is smaller than that for $p = 1$ at high N_α, which is, of course unexpected. This effect may be due to the fact that the number of Lagrange multipliers predicted, under certain assumptions, from (3.29) is not optimal.

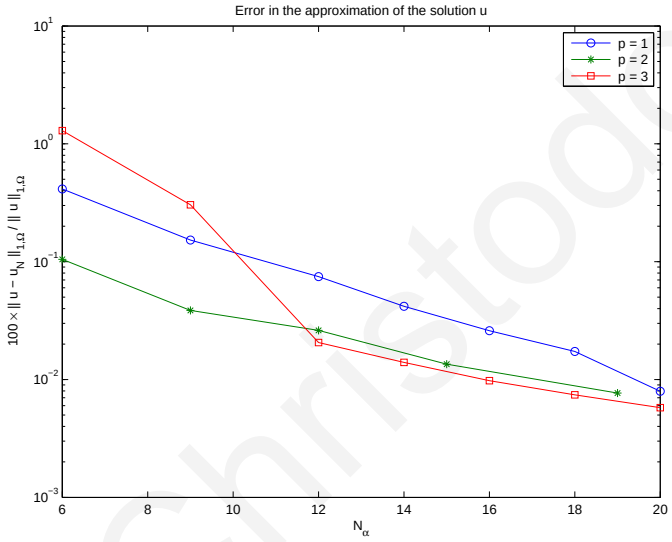

Figure 3.2: Convergence of the approximate solution u_N, $\alpha = 1$.

Figures 3.3–3.5 show the percentage relative error in the first four singular coefficients, versus N_α in a semi-log scale, for $p = 1, 2, 3$, respectively. The exponential convergence as predicted by (3.29) is again readily visible in all three plots.

Next, we would like to compute the error in the approximation of the Lagrange multipliers. Note that for any $v \in H^{-1/2}(S_3)$ we have

$$\|v\|_{-1/2,S_3} \leq C\|v\|_{0,S_3} \leq \hat{C}\|v\|_{\infty,S_3}, \;\; C, \hat{C} \in \mathbb{R}. \tag{3.31}$$

So, instead of $\|\lambda - \lambda_h\|_{-1/2,S_3}$, we use

$$100 \times \max_k \frac{|\lambda(\theta_k) - \lambda_h(\theta_k)|}{|\lambda(\theta_k)|} \tag{3.32}$$

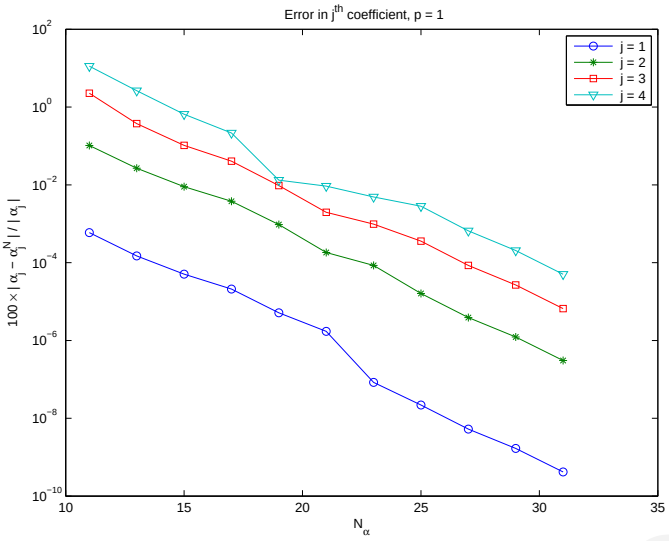

Figure 3.3: Convergence of the singular coefficients α_j^N for $p = 1$, $\alpha = 1$.

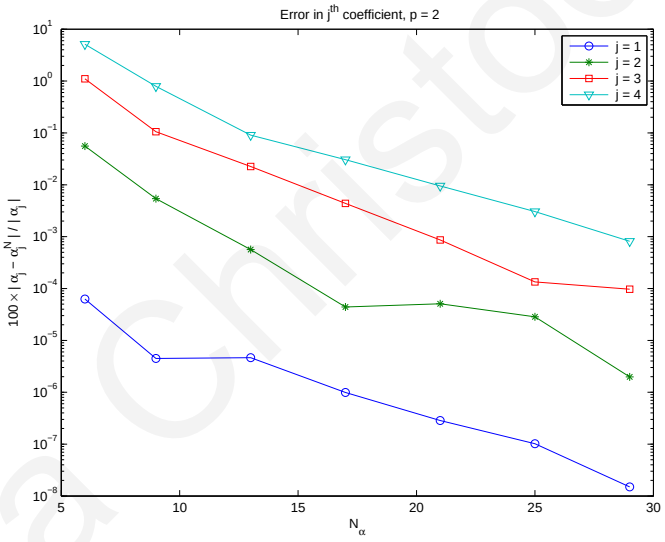

Figure 3.4: Convergence of the singular coefficients α_j^N for $p = 2$, $\alpha = 1$.

where θ_k are the (internal) nodal points along S_3. By construction, $\lambda_h(\theta_k) = \lambda_k$, i.e. $\lambda_h(\theta_k)$ is equal to the k^{th} discrete Lagrange multiplier. Figure 3.6 shows this error versus N_λ (which is directly related to the meshwidth h on S_3) in a log-log scale. The convergence rate indeed appears to be algebraic of order p, i.e. $\lambda_h \to \lambda$ as $N_\lambda \to \infty$ (or, equivalently, as $h \to 0$) at the rate $O(N_\lambda^{-p})$ (or $O(h^p)$). Therefore, from (3.31) we have that $\|\lambda - \lambda_h\|_{-1/2,S_3} = O(h^p)$. Finally, we show numerical results for the case $p = 0$. The error analysis in Xenophontos

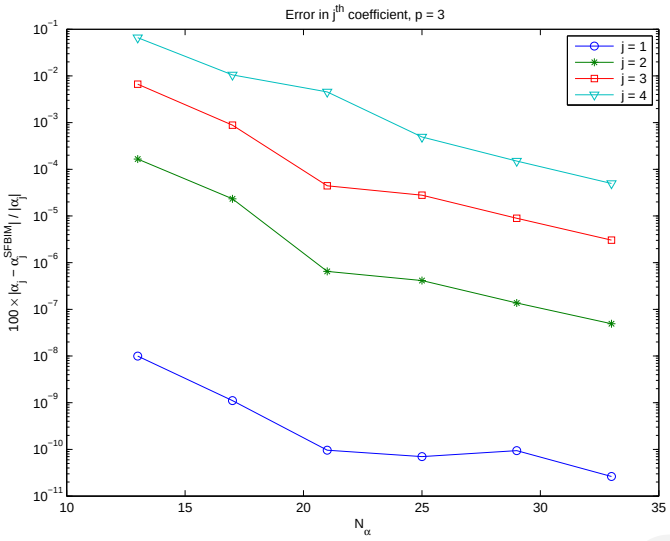

Figure 3.5: Convergence of the singular coefficients α_j^N for $p = 3$, $\alpha = 1$.

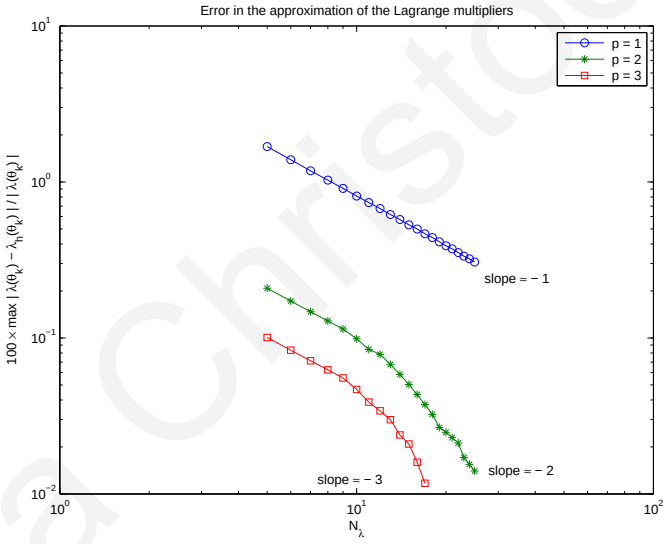

Figure 3.6: Convergence of the Lagrange multipliers, $\alpha = 1$.

et al. (2006) does not cover this case, hence it is not possible to use (3.30) to determine "optimal" values for N_λ and N_α. In what follows we have chosen $N_\alpha = 2N_\lambda$; other choices gave similar results. Figure 3.7 shows the percentage relative error in the first three singular coefficients versus N_α in a log-log scale. We observe that for $p = 0$, the convergence is not exponential, but rather algebraic of order 3.

Figure 3.8 shows the percentage relative error in the approximation of u and of the Lagrange

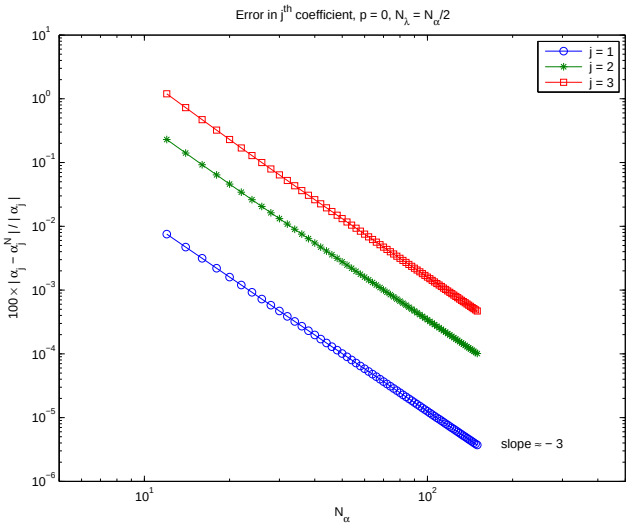

Figure 3.7: Convergence of the singular coefficients α_j^N for $p = 0$, $\alpha = 1$.

multipliers, versus N_α in a log-log scale. Again we have algebraic convergence, with rate 2 for the approximation of u and with rate 3/4 for the approximation of the Lagrange multipliers.

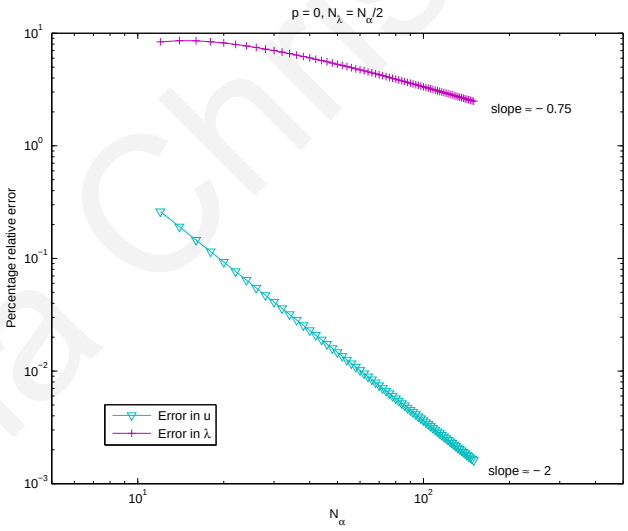

Figure 3.8: Convergence of the approximate solution u_N and Lagrange multiplier λ_h for $p = 0$, $\alpha = 1$.

3.4.2 Domain With a "Slit" ($\alpha = 2$)

We have also repeated the previous computations for the case of $\alpha = 2$, which corresponds to a domain with a "slit". The procedure for determining the constant β in (3.29) was repeated yielding $\beta = 0.92$ for the pair $N_\alpha = 35$ and $N_\lambda = 20$.

Figure 3.9 shows the convergence of the approximate solution and in particular the percentage relative error in the approximation of u versus N_α, in a semi-log scale for $p = 1, 2, 3$. As with α=1, each curve becomes a straight line as N_α is increased, hence the error decreases at an exponential rate as predicted by (3.29).

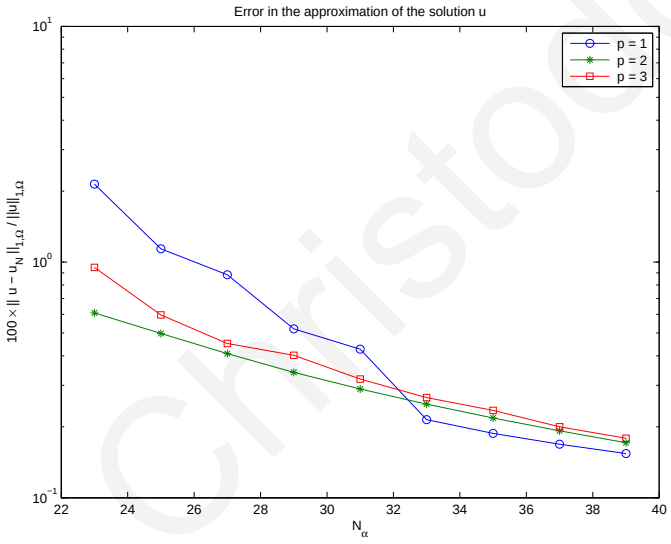

Figure 3.9: Convergence of the approximate solution u_N, $\alpha = 2$.

Figures 3.10 and 3.11 show the percentage relative error in the first four singular coefficients, versus N_α in a semi-log scale, for $p = 1$ and 2, respectively (the case $p = 3$ is almost identical). The exponential convergence is again visible in both plots.

Finally, Fig. 3.12 shows the error in the Lagrange multiplers versus N_λ in a log-log scale. The convergence rate again appears to be algebraic of order p.

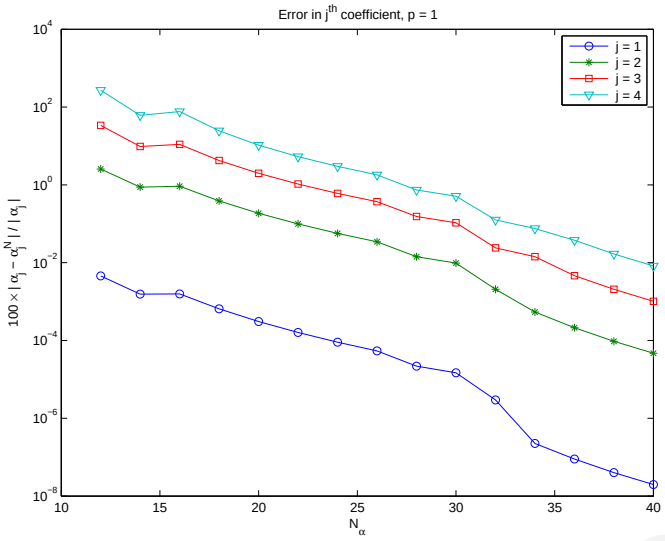

Figure 3.10: Convergence of the singular coefficients α_j^N for $p = 1$, $\alpha = 2$.

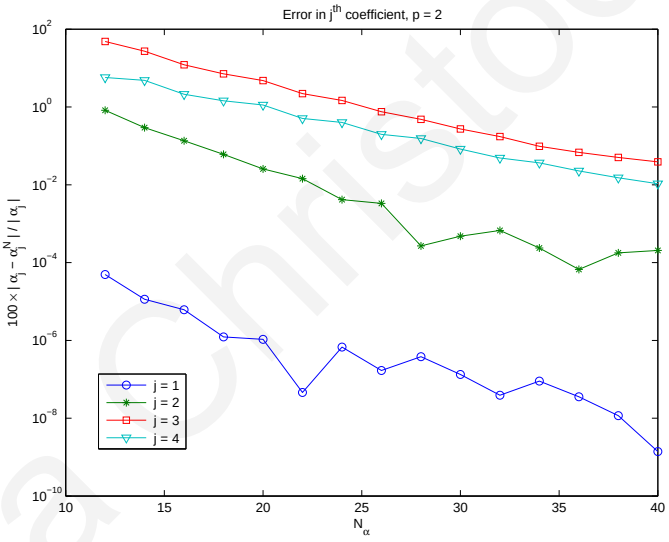

Figure 3.11: Convergence of the singular coefficients α_j^N for $p = 2$, $\alpha = 2$.

3.4.3 L-Shaped Domain ($\alpha = 1.5$)

Similar results have been obtained with $\alpha = 1.5$, which corresponds to an L-shaped domain. The constant β in (3.29) was determined as 0.9 from the pair $N_\alpha = 33, N_\lambda = 15$. Figure 3.13 demonstrates the convergence of the approximate solution, while Figs. 3.14–3.15 show the convergence of the approximate coefficients (for $p = 1$) and of the Lagrange multipliers, respectively. As in Fig. 3.2, the slope for $p = 3$ is smaller than that for $p = 1$. As already

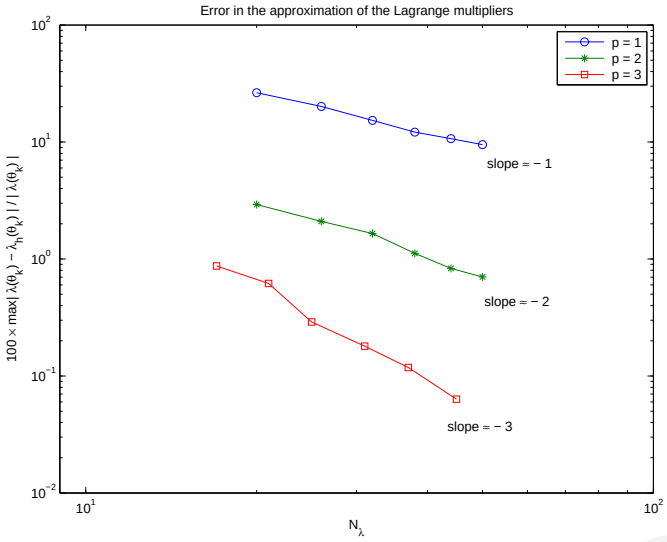

Figure 3.12: Convergence of the Lagrange multipliers, $\alpha = 2$.

pointed out, this unexpected and counterintuititive deceleration of the convergence may be attributed to the fact that the choice of the number of Lagrange multipliers is not optimal.

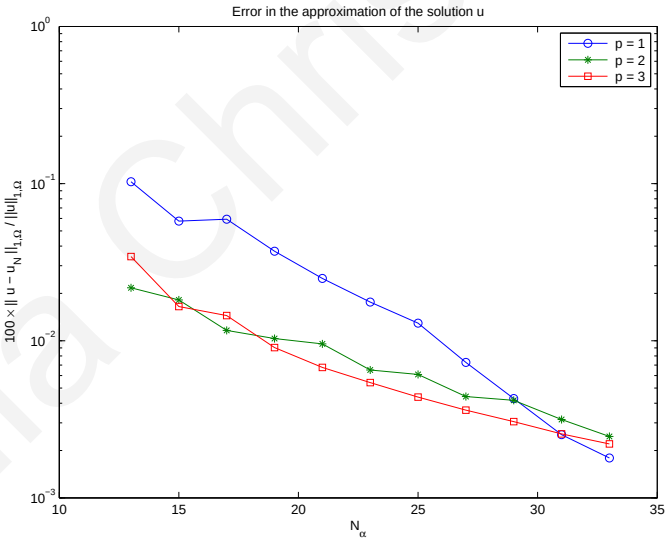

Figure 3.13: Convergence of the approximate solution u_N, $\alpha = 1.5$.

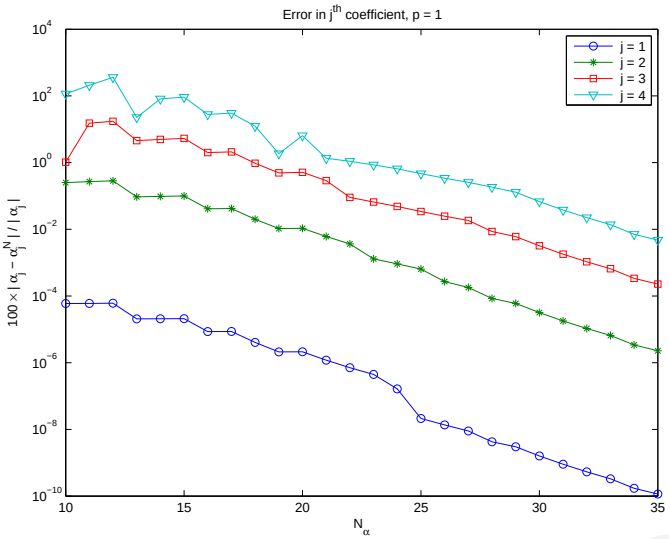

Figure 3.14: Convergence of the singular coefficients α_j^N for $p = 1$, $\alpha = 1.5$.

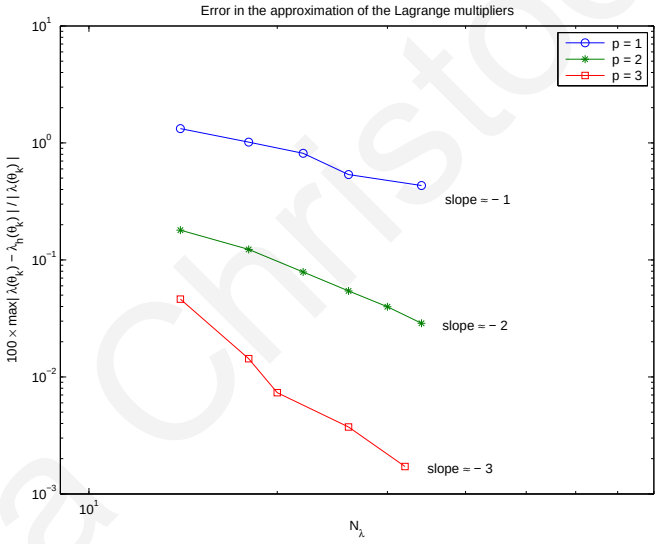

Figure 3.15: Convergence of the Lagrange multipliers, $\alpha = 1.5$.

3.5 Conclusions

In this chapter we revisited the Singular Function Boundary Integral Method (SFBIM) for the solution of two-dimensional elliptic problems with boundary singularities. Our objective was to demonstrate, via numerical examples, the convergence of the method and to show the agreement with the theoretical results provided in the literature. For this purpose the method was applied to a Laplacian test problem over a circular sector with the use of constant, lin-

ear, quadratic and cubic approximations of the Lagrange multipliers. After obtaining the "optimal" values for the number of Lagrange multipliers and the number of singular functions, the exact approximation errors were calculated. In the cases of linear, quadratic and cubic approximations we show that both the singular coefficients and the solution converge exponentially with the number of singular functions and that the convergence of the approximation of the Lagrange multipliers is algebraic of order p with the number of Lagrange multipliers, as predicted by the theory. In the case of constant approximations, which is not covered by the theory, we observed that the convergence is algebraic for both the singular coefficients and the solution.

Chapter 4

Analysis of the SFBIM for a Biharmonic Problem With One Boundary Singularity

The material of this chapter also appears in Christodoulou et al. (2011).

4.1 Introduction

Boundary singularities appear in many problems governed by elliptic partial differential equations. These arise when there is a sudden change in the boundary conditions (e.g. domains with cracks) and/or on the boundary itself (e.g. re-entrant corners). It is well known that ignoring their presence can adversely affect the accuracy and the convergence of standard numerical methods, such as finite element, boundary element, finite difference and spectral methods. One way to deal with singularities is to incorporate their local form into the numerical scheme, something that has been successfully done for two-dimensional Laplacian problems (see, e.g., Georgiou et al., 1996. Li, 1997 and the references therein).

In the case of two-dimensional Laplacian problems with one boundary singularity, and with straight boundary parts sharing the singularity, the local solution expansion is given by

$$u = \sum_{j=1}^{\infty} \alpha_j r^{\mu_j} f_j(\theta), \tag{4.1}$$

where (r, θ) are polar coordinates centered at the singular point, $\alpha_j \in \mathbb{R}$ are the unknown singular coefficients and μ_j, f_j are, respectively, the eigenvalues and eigenfunctions of the problem, which are uniquely determined by the geometry and the boundary conditions along the boundaries sharing the singular point. The α_j's, called singular coefficients (or stress intensity factors if the boundary value problem arises from structural mechanics), are primary unknowns in many applications. With standard numerical schemes, such as the finite element method (FEM), the singular coefficients are calculated via a post-processing procedure (see, e.g.,Babuška and Miller, 1984. Szabó and Yosibash, 1996.). The Singular Function Boundary Integral Method (SFBIM), belongs to the class of Trefftz methods in which the singular coefficients are calculated *directly*. It was originaly developed for two-dimensional Laplacian problems with boundary singularities, by Georgiou and coworkers (Georgiou et al., 1996, 1997), and was recently extended to biharmonic problems by Elliotis et al. (2005b, 2006, 2007). See also Li et al. (2004), Li et al. (2008) and Lu et al. (2009) for reviews of Trefftz methods and recent works with applications to biharmonic problems.

The SFBIM, uses the leading terms of the local asymptotic expansion to approximate the solution. The associated functions $r^{\mu_j} f_j(\theta)$ are used to weight the governing biharmonic equation in the Galerkin sence. This allows for the reduction of the discretized equations to boundary integrals by means of Green's theorem. Any Dirichlet boundary conditions are weakly enforced by means of Lagrange multipliers, which are calculated directly together with the unknown singular coefficients; hence, no post-processing of the numerical solution is performed.

The implementation of the method for the solution of Laplacian and biharmonic problems

with boundary singularities has given highly accurate numerical results, see Elliotis et al. (2002, 2005a, 2005b, 2006, 2007). The convergence of the SFBIM, for Laplacian problems, has been investigated theoretically in Xenophontos et al. (2006), where it was shown that the absolute difference between the true and approximate singular coefficients decreases at an exponential rate as the number N of the terms in the numerical approximation is increased. The main goal of this paper is to extend the analysis to the case of biharmonic problems and establish the (exponential) convergence rates observed in numerical simulations in Elliotis et al. (2005b, 2006, 2007). It should be noted that the Collocation Trefftz method also yields exponential convergence rates, when applied to biharmonic problems, as was shown in Li (1998) and Li et al. (2008).

The rest of this chapter is organized as follows: In Section 4.2 the formulation of the method for a model two-dimensional biharmonic problem with a boundary singularity is presented. In Section 4.3 the convergence analysis is carried out. Finally, in Section 4.4 we discuss the efficient implementation of the method.

4.2 The Model Problem and its Formulation

We consider the following model two-dimensional biharmonic problem (depicted graphically in Fig. 4.2): Find u such that

$$\nabla^4 u = 0 \text{ in } \Omega, \tag{4.2}$$

with

$$\left.\begin{array}{llll} u = 0, & \dfrac{\partial u}{\partial n} = 0 & & \text{on } \mathrm{S}_1 \\ u = 0, & \nabla^2 u = 0 & & \text{on } \mathrm{S}_2 \\ \nabla^2 u = 0, & \dfrac{\partial (\nabla^2 u)}{\partial n} & = 0 & \text{on } \mathrm{S}_3 \\ u = g(r,\theta), & \nabla^2 u = 0 & & \text{on } \mathrm{S}_4 \end{array}\right\}, \tag{4.3}$$

where $\partial\Omega = \cup_{i=1}^{4} S_i$. A boundary singularity arises at the intersection of S_1 and S_2 (point O) due to the sudden changes in the boundary conditions. The function g is assumed to be smooth enough and such that no other boundary singularities arise (at the endpoints of S_4). We also assume that the *only* singularity present is the one at the point O. The above boundary value problem models the so-called Newtonian stick-slip flow problem (see Elliotis et al. (2005b)).

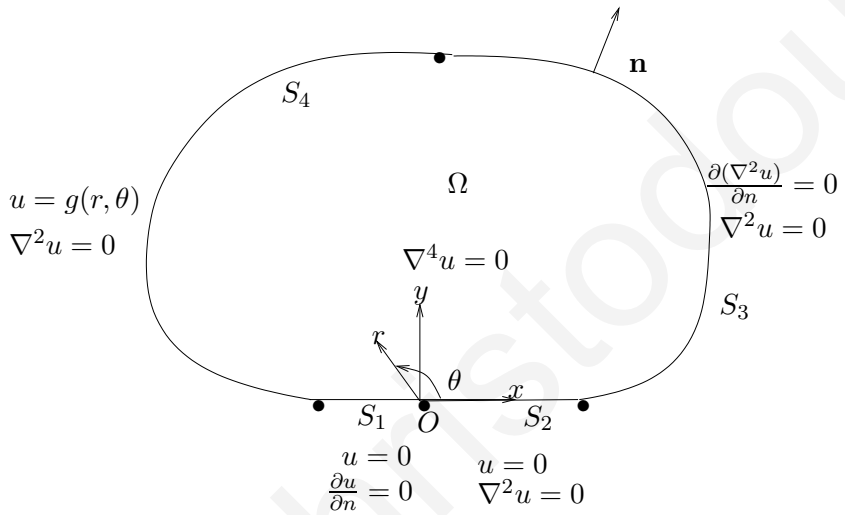

Figure 4.1: The model biharmonic problem with one singular point.

For two-dimensional biharmonic problems, the solution in the neighbourhood of the boundary singularity is given by an asymptotic expansion of the form

$$u(r,\theta) = \sum_{j=1}^{\infty} \alpha_j r^{\mu_j+1} f_1(\theta,\mu_j) + \sum_{j=1}^{\infty} \beta_j r^{\rho_j+1} f_2(\theta,\rho_j), \tag{4.4}$$

where α_j and β_j are the unknown singular coefficients, μ_j and ρ_j are the two sets of singularity powers (i.e., the eigenvalues of the problem) arranged in ascending order, and the functions $f_1(\theta,\mu_j)$ and $f_2(\theta,\rho_j)$ represent the θ-dependence of the eigensolution. The functions $r^{\mu_j+1} f_1(\theta,\mu_j)$ and $r^{\rho_j+1} f_2(\theta,\rho_j)$ are called singular functions. Since we are considering a model for the stick-slip problem where S_1 and S_2 meet at an angle π, the eigenvalues μ_j, ρ_j are real and the functions $f_1(\theta,\mu_j), f_2(\theta,\rho_j)$ are even and odd, respectively (see Michael

(1958) and Papanastasiou et al. (1999)). In fact, in this setting, one finds that

$$f_1(\theta,\mu_j) = \cos(\mu_j+1)\theta - \cos(\mu_j-1)\theta\,,\ \mu_j = j-\frac{1}{2},\ j=1,2,... \tag{4.5}$$

$$f_2(\theta,\rho_j) = (\rho_j-1)\sin(\rho_j+1)\theta - (\rho_j+1)\sin(\rho_j-1)\theta\,,\ \rho_j = j+1,\ j=1,2,... \tag{4.6}$$

Now, suppose v is a function which satisfies

$$\left.\begin{array}{l} \nabla^4 v = 0 \text{ in } \Omega \\ v=0, \dfrac{\partial v}{\partial n} = 0 \text{ on } S_1 \\ v=0, \nabla^2 v = 0 \text{ on } S_2 \end{array}\right\}. \tag{4.7}$$

One choice for v is

$$v = \gamma_j r^{\mu_j+1} f_1(\theta,\mu_j) + \delta_j r^{\rho_j+1} f_2(\theta,\rho_j),$$

for some constants γ_j and δ_j. Multiplying the governing biharmonic equation by v, integrating over Ω and employing Green's formula, we obtain

$$-\iint_\Omega \nabla v\cdot\nabla(\nabla^2 u) + \int_{\partial\Omega} v\frac{\partial(\nabla^2 u)}{\partial n} = 0.$$

Using Green's formula once again, the above expression becomes:

$$\iint_\Omega \nabla^2 v\nabla^2 u - \int_{\partial\Omega}\nabla^2 u\frac{\partial v}{\partial n} + \int_{\partial\Omega} v\frac{\partial(\nabla^2 u)}{\partial n} = 0.$$

Considering the boundary conditions in (4.3) and (4.7), we find that

$$\iint_\Omega \nabla^2 v\nabla^2 u + \int_{S_4} v\frac{\partial(\nabla^2 u)}{\partial n} = 0. \tag{4.8}$$

Now, on S_4 we have $u=g$ and thus

$$\int_{S_4}(u-g)\frac{\partial(\nabla^2 v)}{\partial n} = 0,$$

which added to (4.8) gives

$$\iint_\Omega \nabla^2 v\nabla^2 u + \int_{S_4} v\frac{\partial(\nabla^2 u)}{\partial n} + \int_{S_4} u\frac{\partial(\nabla^2 v)}{\partial n} = \int_{S_4} g\frac{\partial(\nabla^2 v)}{\partial n}.$$

Letting

$$\lambda = \frac{\partial(\nabla^2 u)}{\partial n}|_{S_4}, \mu = \frac{\partial(\nabla^2 v)}{\partial n}|_{S_4}, \tag{4.9}$$

we get

$$\iint_{\Omega} \nabla^2 v \nabla^2 u + \int_{S_4} v\lambda + \int_{S_4} u\mu = \int_{S_4} g\mu, \tag{4.10}$$

which leads to the following variational formulation: Find $(u, \lambda) \in V_1 \times V_2$ such that

$$B(u, v) + b(u, v; \lambda, \mu) = F(v, \mu) \ \forall \ (v, \mu) \in V_1 \times V_2, \tag{4.11}$$

where

$$\left.\begin{array}{l} B(u, v) = \iint_{\Omega} \nabla^2 v \nabla^2 u \\ b(u, v; \lambda, \mu) = \int_{S_4} u\mu + \int_{S_4} v\lambda \\ F(v, \mu) = \int_{S_4} g\mu \end{array}\right\}. \tag{4.12}$$

The spaces V_1 and V_2 are defined as

$$V_1 = H^2_*(\Omega) = \left\{ v \in H^2(\Omega) : v|_{S_1 \cup S_2} = 0, \frac{\partial v}{\partial n}|_{S_1} = 0 \right\}, V_2 = H^{-3/2}(S_4). \tag{4.13}$$

The above formulation will be used in the analysis of the method. It will be shown in Section 4.4 that this formulation is equivalent to the one used for the implementation.

4.3 Discretization and Error Analysis

In order to describe the discrete analog of (4.11), boundary part S_4 is divided into sections Γ_i, with $i = 1, \cdots, n$ such that $S_4 = \cup_{i=1}^{n} \Gamma_i$. Let $h_i = |\Gamma_i|$ and set $h = \max_{1 \le i \le n} h_i$. Now, let

$$v_j^{(1)} = r^{\mu_j + 1} f_1(\theta, \mu_j) \text{ and } v_j^{(2)} = r^{\rho_j + 1} f_2(\theta, \rho_j)$$

denote the singular functions, and define the following finite dimensional space:

$$V_1{}^N = span\left\{ v_j^{(1)} \right\} \cup span\left\{ v_j^{(2)} \right\}, j = 1, 2, \cdots, N. \tag{4.14}$$

We assume that for each segment Γ_i, there exists an invertible mapping $F_i : I = [-1, 1] \to \Gamma_i$ and define the space

$$V_2{}^h = \left\{ \lambda_h : \lambda_h|_{\Gamma_i} \circ F_i^{-1} \in P_k(I), i = 1, \cdots, n \right\}, \tag{4.15}$$

where $P_k(I)$ denotes the set of polynomials of degree $\leq k$ on I. Then the discrete version of (4.11) reads: Find $(u_N,\lambda_h) \in [{V_1}^N \times {V_2}^h] \subset [V_1 \times V_2]$ such that

$$B\left(u_N, v\right) + b\left(u, v; \lambda_h, \mu\right) = F\left(v, \mu\right) \; \forall \left(v, \mu\right) \in {V_1}^N \times {V_2}^h, \tag{4.16}$$

with $B\left(u_N, v\right)$, $b\left(u, v; \lambda_h, \mu\right)$ and $F\left(v, \mu\right)$ given by (4.12).

We have the following result, which is a generalization of Theorem 4.5 from Li et al. (2006).

Theorem 1 *Let (u, λ) and (u_N, λ_h) be the solutions to* (4.11) *and* (4.16)*, respectively. Suppose there exist positive constants c_0, c, β^* and γ, independent of N and h such that the following three conditions hold:*

$$B\left(v_N, v_N\right) \geq c_0 {\|v_N\|}^2_{2,\Omega} \text{ and } \left|B\left(u, v_N\right)\right| \leq c\|u\|_{2,\Omega}\|v_N\|_{2,\Omega} \; \forall \, v_N \in {V_1}^N, \tag{4.17}$$

$$\exists \, 0 \neq w_N \in {V_1}^N s.t. \left|\int_{S_4} \mu_h w_N\right| \geq \beta^* \|\mu_h\|_{-\frac{3}{2},S_4}\|w_N\|_{2,\Omega} \; \forall \, \mu_h \in {V_2}^h, \tag{4.18}$$

$$\left|\int_{S_4} \lambda v_N\right| \leq \gamma \|\lambda\|_{-\frac{3}{2},S_4}\|v_N\|_{2,\Omega} \; \forall \, v_N \in {V_1}^N. \tag{4.19}$$

Then,

$$\|u \, - u_N\|_{2,\Omega} + \|\lambda - \lambda_h\|_{-\frac{3}{2},S_4} \leq C \left\{ \inf_{v_N \in {V_1}^N} \|u - v_N\|_{2,\Omega} + \inf_{\eta_h \in {V_2}^h} \|\lambda - \eta_h\|_{-\frac{3}{2},S_4} \right\}, \tag{4.20}$$

with $C \in \mathbb{R}^+$ independent of N and h.

Proof. Obviously, $\forall \; (v, \mu) \in V_1 \times V_2$ we have

$$B(u - u_N, v) = -b(u - u_N, v; \lambda - \lambda_h, \mu) = -\int_{S_4} (u - u_N)\mu - \int_{S_4} (\lambda - \lambda_h)v.$$

Since $u = g$ on S_4 and $\int_{S_4} \mu_h(u_N - g) = 0 \; \forall \, \mu_h \in V_2^h$, we have

$$\int_{S_4} \mu_h(u_N - u) = 0 \; \forall \, \mu_h \in V_2^h, \tag{4.21}$$

and

$$B(u - u_N, v_N) = -\int_{S_4} (\lambda - \lambda_h)v_N \; \forall \, v_N \in V_1^N. \tag{4.22}$$

Letting $w_N = u_N - v_N \in V_1^N$ we obtain

$$\begin{aligned} B(v_N - u_N, w_N) &= B(u - u_N, w_N) + B(v_N - u, w_N) \\ &= B(v_N - u, w_N) - \int_{S_4} (\lambda - \lambda_h) w_N \\ &= B(v_N - u, w_N) - \int_{S_4} (\lambda - \eta_h) w_N - \int_{S_4} (\eta_h - \lambda_h) w_N, \end{aligned}$$

with $\eta_h \in V_2^h$ arbitrary. Using the definition of w_N and (4.21) with $\mu_h = \lambda_h - w_h \in V_2^h$, we further have

$$\begin{aligned} B(v_N - u_N, w_N) &= B(v_N - u, w_N) - \int_{S_4} (\lambda - \eta_h) w_N - \int_{S_4} (u_N - v_N)(\eta_h - \lambda_h) \\ &= B(v_N - u, w_N) - \int_{S_4} (\lambda - \eta_h) w_N - \int_{S_4} u_N (\eta_h - \lambda_h) + \int_{S_4} v_N (\eta_h - \lambda_h) \\ &= B(v_N - u, w_N) - \int_{S_4} (\lambda - \eta_h) w_N - \int_{S_4} u (\eta_h - \lambda_h) + \int_{S_4} v_N (\eta_h - \lambda_h) \\ &= B(v_N - u, w_N) - \int_{S_4} (\lambda - \eta_h) w_N - \int_{S_4} (u - v_N)(\eta_h - \lambda_h). \end{aligned}$$

This along with Eqs. (4.17) and (4.19) give

$$\begin{aligned} c_0 \|w_N\|_{2,\Omega}^2 &\leq |B(w_N, w_N)| \leq |B(u_N - v_N, w_N)| \\ &\leq |B(v_N - u, w_N)| + \left| \int_{S_4} (\lambda - \eta_h) w_N \right| + \left| \int_{S_4} (\eta_h - \lambda_h)(u - v_N) \right| \\ &\leq c \|v_N - u\|_{2,\Omega} \|w_N\|_{2,\Omega} + \gamma \|\lambda - \eta_h\|_{-\frac{3}{2},S_4} \|w_N\|_{2,\Omega} + \gamma \|\eta_h - \lambda_h\|_{-\frac{3}{2},S_4} \|u - v_N\|_{2,\Omega} \\ &\leq C_1 \left\{ (\|v_N - u\|_{2,\Omega} + \|\lambda - \eta_h\|_{-\frac{3}{2},S_4}) \|w_N\|_{2,\Omega} + \|\eta_h - \lambda_h\|_{-\frac{3}{2},S_4} \|u - v_N\|_{2,\Omega} \right\}, \end{aligned}$$

with $C_1 \in \mathbb{R}$ satisfying $C_1 \geq \max\{c, \gamma\}$. This is an inequality of order 2: $c_0 x^2 \leq bx + d$, where

$$x = \|w_N\|_{2,\Omega}\ ,\ b = C_1 \left\{ \|v_N - u\|_{2,\Omega} + \|\lambda - \eta_h\|_{-\frac{3}{2},S_4} \right\}\ ,\ d = C_1 \|\eta_h - \lambda_h\|_{-\frac{3}{2},S_4} \|u - v_N\|_{2,\Omega}.$$

For any $\epsilon > 0$, we have

$$d \leq \frac{C_1}{2} \left\{ \frac{1}{\epsilon} \|u - v_N\|_{2,\Omega} + \epsilon \|\eta_h - \lambda_h\|_{-\frac{3}{2},S_4} \right\}^2.$$

Therefore, we have the bound

$$x \leq \frac{b + \sqrt{b^2 + 4c_0\, d}}{2c_0},$$

or, equivalently,

$$\|w_N\|_{2,\Omega} \leq C_2 \left\{ \|v_N - u\|_{2,\Omega} + \|\lambda - \eta_h\|_{-\frac{3}{2},S_4} + \frac{1}{\epsilon}\|v_N - u\|_{2,\Omega} \right\} + C_2\epsilon\|\lambda_h - \eta_h\|_{-\frac{3}{2},S_4}, \quad (4.23)$$

with $C_2 \geq \frac{1}{c_0}\max\{C_1, \sqrt{c_0 C_1/2}\}$. Next, using Eq. (4.18) with $\mu_h = \lambda_h - \eta_h$ we have that there exists a nonzero $v_N \in V_1^N$ such that

$$\|\lambda_h - \eta_h\|_{-\frac{3}{2},S_4} \leq \frac{1}{\beta}\frac{\left|\int_{S_4}(\lambda_h - \eta_h)v_N\right|}{\|v_N\|_{2,\Omega}}. \quad (4.24)$$

Also, it follows from (4.22) that

$$\begin{aligned}
\left|\int_{S_4}(\lambda_h - \eta_h)v_N\right| &= \left|\int_{S_4}(\lambda_h - \lambda)v_N + \int_{S_4}(\lambda - \eta_h)v_N\right| \\
&\leq |B(u - u_N, v_N)| + \left|\int_{S_4}(\lambda - \eta_h)v_N\right| \\
&\leq c\|u - u_N\|_{2,\Omega}\|v_N\|_{2,\Omega} + \gamma\|\lambda - \eta_h\|_{-\frac{3}{2},S_4}\|v_N\|_{2,\Omega}.
\end{aligned}$$

Hence, (4.24) becomes

$$\begin{aligned}
\|\lambda_h - \eta_h\|_{-\frac{3}{2},S_4} &\leq C_3\left\{\|u - u_N\|_{2,\Omega} + \|\lambda - \eta_h\|_{-\frac{3}{2},S_4}\right\} \\
&\leq C_3\left\{\|u - v_N\|_{2,\Omega} + \|v_N - u_N\|_{2,\Omega} + \|\lambda - \eta_h\|_{-\frac{3}{2},S_4}\right\},
\end{aligned}$$

with $C_3 \geq \frac{1}{\beta}\max\{c, \gamma\}$. Since $\|v_N - u_N\|_{2,\Omega} = \|w_N\|_{2,\Omega}$, using (4.23) leads to

$$\|\lambda_h - \eta_h\|_{-\frac{3}{2},S_4} \leq C_3(1 + C_2/\epsilon)\|u - v_N\|_{2,\Omega} + C_3(C_2 + 1)\|\lambda - \eta_h\|_{-\frac{3}{2},S_4} + C_3C_2\epsilon\|\lambda - \eta_h\|_{-\frac{3}{2},S_4}.$$

Choosing $\epsilon = 1/(2C_3C_2)$ we get, for some constant $C_4 > \max\{C_2, C_3\}$,

$$\|\lambda_h - \eta_h\|_{-\frac{3}{2},S_4} \leq C_4\left\{\|u - v_N\|_{2,\Omega} + \|\lambda - \eta_h\|_{-\frac{3}{2},S_4}\right\},$$

and using the triangle inequality we have

$$\|\lambda_h - \lambda\|_{-\frac{3}{2},S_4} \leq \|\lambda_h - \eta_h\|_{-\frac{3}{2},S_4} + \|\eta_h - \lambda\|_{-\frac{3}{2},S_4} \leq C\left\{\|u - v\|_{2,\Omega} + \|\lambda - \eta_h\|_{-\frac{3}{2},S_4}\right\}.$$

Similarly, using the above inequality and (4.23), we finally get

$$\begin{aligned}
\|u - u_N\| &\leq \|u - v_N\|_{2,\Omega} + \|v_N - u_N\|_{2,\Omega} \\
&\leq \|u - v_N\|_{2,\Omega} + \|w_N\|_{2,\Omega} \\
&\leq C\left\{\|u - v_N\|_{2,\Omega} + \|\lambda - \eta_h\|_{-\frac{3}{2},S_4}\right\},
\end{aligned}$$

which gives the desired result. ■

Before verifying that (4.17)–(4.19) hold for our problem, consider the following: For any

$$w = \sum_{j=1}^{\infty} \alpha_j v_j^{(1)} + \sum_{j=1}^{\infty} \beta_j v_j^{(2)}$$

we can always write

$$w = w_N + r_N, \tag{4.25}$$

where

$$w_N = \sum_{j=1}^{N} \alpha_j v_j^{(1)} + \sum_{j=1}^{N} \beta_j v_j^{(2)} \in {V_1}^N \,,\; r_N = \sum_{j=N+1}^{\infty} \alpha_j v_j^{(1)} + \sum_{j=N+1}^{\infty} \beta_j v_j^{(2)}, \tag{4.26}$$

with α_j and β_j the true singular coefficients. We will assume that there exists a constant $\alpha \in (0,1)$ such that for $\ell = 0, 1, 2$

$$\left| \frac{\partial^\ell (r_N)}{\partial r^\ell} \right| \leq C N^\ell \alpha^N. \tag{4.27}$$

Note that when $r < 1$, assumption (4.27) can be replaced by the assumption that the singular coefficients are bounded, since then, due to the fact that $f_1(\theta, \mu_j)$ and $f_2(\theta, \rho_j)$ are biharmonic, we have

$$|r_N| \leq \sum_{j=N+1}^{\infty} |\alpha_j| r^{\mu_j + 1} + \sum_{j=N+1}^{\infty} |\beta_j| \, r^{\rho_j + 1} \leq C_1 \frac{r^{\mu_{N+1}+1}}{1-r} + C_2 \frac{r^{\rho_{N+1}+1}}{1-r} \leq C\alpha^N,$$

with $r < \alpha < 1$ and $C \in \mathbb{R}^+$ independent of α and N. Similarly,

$$\begin{aligned}
\left| \frac{\partial r_N}{\partial r} \right| &\leq \sum_{j=N+1}^{\infty} |\alpha_j| \, (\mu_j + 1) r^{\mu_j} + \sum_{j=N+1}^{\infty} |\beta_j| \, (\rho_j + 1) r^{\rho_j} \\
&= \sum_{j=N+1}^{\infty} |\alpha_j| \, (\mu_j + 1) \left\{ \frac{d}{dr} \int_0^r \xi^{\mu_j} d\xi \right\} + \sum_{j=N+1}^{\infty} |\beta_j| \, (\rho_j + 1) \left\{ \frac{d}{dr} \int_0^r \xi^{\rho_j} d\xi \right\} \\
&= \frac{d}{dr} \left(\sum_{j=N+1}^{\infty} |\alpha_j| \, (\mu_j + 1) \left\{ \int_0^r \xi^{\mu_j} d\xi \right\} + \sum_{j=N+1}^{\infty} |\beta_j| \, (\rho_j + 1) \left\{ \int_0^r \xi^{\rho_j} d\xi \right\} \right) \\
&\leq \frac{d}{dr} \left(\sum_{j=N+1}^{\infty} |\alpha_j| \, r^{\mu_j + 1} + \sum_{j=N+1}^{\infty} |\beta_j| \, r^{\rho_j + 1} \right) \\
&\leq C_1 \frac{d}{dr} \left(\frac{r^{\mu_{N+1}+1}}{1-r} \right) + C_2 \frac{d}{dr} \left(\frac{r^{\rho_{N+1}+1}}{1-r} \right) \\
&\leq C N \alpha^N.
\end{aligned}$$

(The case $\ell = 2$ follows in a similar fashion.)

In the case $r \geq 1$ one may partition the domain Ω into subdomains in which separate approximations may be employed, including one (near the singular point O) that is valid for $r < 1$. The solution over the entire domain can then be composed by combining solutions from each subdomain and properly dealing with their interactions across the interfaces separating them (see, e.g., Li et al., 1987, where this idea was applied to a Laplacian problem).

We are now ready to verify that (4.17)–(4.19) hold for the problem (4.16). We have (see, e.g., Johnson, 1987),

$$B(v,v) = \iint_\Omega \nabla^2 v \nabla^2 v = \iint_\Omega \left|\nabla^2 v\right|^2 \geq C_0 \|v\|_{2,\Omega}^2 \; \forall \, v \in V_1$$

and $\exists \, c \in \mathbb{R}^+$ such that

$$|B(u,v)| \leq c\|u\|_{2,\Omega}\|v\|_{2,\Omega} \; \forall \, u, v \in V_1,$$

therefore (4.17) is verified.

In order to verify (4.18) we consider the following auxiliary problem:

$$\nabla^4 w = 0, \text{ in } \Omega, \tag{4.28}$$

with the boundary conditions

$$\left.\begin{array}{lll} w = 0, & \dfrac{\partial w}{\partial n} = 0 & \text{on } S_1 \\ w = 0, & \nabla^2 w = 0 & \text{on } S_2 \\ \dfrac{\partial(\nabla^2 w)}{\partial n} = 0, & \nabla^2 w = 0 & \text{on } S_3 \\ \nabla^2 w = 0, & \dfrac{\partial(\nabla^2 w)}{\partial n} = \mu_h & \text{on } S_4 \end{array}\right\}, \tag{4.29}$$

where $\mu_h \in V_2^h$ in (4.29). By using Green's formula we obtain

$$\begin{aligned} \left|\int_{S_4} w\mu_h\right| &= \left|\int_{S_4} w\frac{\partial(\nabla^2 w)}{\partial n}\right| = \left|\iint_\Omega w\nabla^4 w + \iint_\Omega \nabla w \cdot \nabla(\nabla^2 w)\right| \\ &= \left|-\iint_\Omega \nabla^2 w \nabla^2 w + \int_{\partial\Omega} \nabla^2 w \frac{\partial w}{\partial n}\right| \\ &= \left|\iint_\Omega \nabla^2 w \nabla^2 w\right| = \iint_\Omega \left(\nabla^2 w\right)^2 \\ &\geq C_0 \|w\|_{2,\Omega}^2. \end{aligned} \tag{4.30}$$

Note that (see, e.g., Wloka, 1987)

$$\|\mu_h\|^2_{-3/2,S_4} = \left\| \frac{\partial(\nabla^2 w)}{\partial n} \right\|^2_{-3/2,S_4} \leq C\|w\|^2_{2,\Omega} \leq C \int_{\partial\Omega} \left|\nabla^2 w\right|^2, \;\; C \in \mathbb{R}^+, \tag{4.31}$$

so, by (4.30)

$$\left| \int_{S_4} \mu_h w \right| \geq \beta \|w\|_{2,\Omega} \|\mu_h\|_{-3/2,S_4}, \tag{4.32}$$

with $\beta \in \mathbb{R}^+$ independent of w and h. Now, let $w_N \in V_1^N$ be such that $w = w_N + r_N$, as given by (4.25)–(4.26). We have

$$\left| \int_{S_4} \mu_h w_N \right| = \left| \int_{S_4} \mu_h w - \int_{S_4} \mu_h r_N \right| \geq \left| \int_{S_4} \mu_h w \right| - \left| \int_{S_4} \mu_h r_N \right| \tag{4.33}$$

and

$$\left| \int_{S_4} \mu_h r_N \right| \leq C_1 \|\mu_h\|_{-3/2,S_4} \|r_N\|_{2,\Omega}, \;\; C_1 \in \mathbb{R}^+. \tag{4.34}$$

Now, combining (4.31)–(4.33) we obtain

$$\left| \int_{S_4} \mu_h w_N \right| \geq \beta \|w\|_{2,\Omega} \|\mu_h\|_{-3/2,S_4} - C_1 \|\mu_h\|_{-3/2,S_4} \|r_N\|_{2,\Omega}. \tag{4.35}$$

Also, from the reverse triangle inequality,

$$\|w\|_{2,\Omega} = \|w_N + r_N\|_{2,\Omega} \geq \|w_N\|_{2,\Omega} - \|r_N\|_{2,\Omega},$$

and by (4.34), we get

$$\left| \int_{S_4} \mu_h w_N \right| \geq \beta \left(\|w_N\|_{2,\Omega} - \|r_N\|_{2,\Omega} \right) \|\mu_h\|_{-3/2,S_4} - C_1 \|\mu_h\|_{-3/2,S_4} \|r_N\|_{2,\Omega}. \tag{4.36}$$

Therefore,

$$\left| \int_{S_4} \mu_h w_N \right| \geq \beta \|w_N\|_{2,\Omega} \|\mu_h\|_{-3/2,S_4} - (C_1 + \beta) \|\mu_h\|_{-3/2,S_4} \|r_N\|_{2,\Omega}. \tag{4.37}$$

Since by assumption (4.27), r_N converges to zero exponentially (or, equivalently w_N converges to w exponentially), we have

$$\lim_{N\to\infty} \frac{\|r_N\|_{2,\Omega}}{\|w_N\|_{2,\Omega}} = 0,$$

which means that for any $\varepsilon > 0$ there exists N^* such that $\frac{\|r_N\|_{2,\Omega}}{\|w_N\|_{2,\Omega}} < \varepsilon$ whenever $N > N^*$. Hence, for N sufficiently large we may write

$$\frac{\|r_N\|_{2,\Omega}}{\|w_N\|_{2,\Omega}} \leq \frac{\beta}{2\,(C_1+\beta)}.$$

Combining (4.36) with (4.37) yields

$$\left|\int_{S_4} \mu_h w_N\right| \geq \frac{\beta}{2}\|\mu_h\|_{-3/2,S_4}\|w_N\|_{2,\Omega}.$$

By replacing w_N by v_N and $\frac{\beta}{2}$ by β, inequality (4.18) is obtained. Finally, condition (4.19) follows from (see, e.g., Wloka 1987)

$$\int_{S_4} \lambda v \leq \gamma\|\lambda\|_{-3/2,S_4}\|v\|_{2,\Omega} \;\forall\; v \in V_1^N, \gamma \in \mathbb{R}^+.$$

The above analysis leads to the following theorem.

Theorem 2 *Let* (u,λ) *and* (u_N,λ_h) *be the solutions to* (4.11) *and* (4.16)*, respectively. If* $\lambda \in H^k(S_4)$*, for some* $k \geq 1$*, then there exists a positive constant* C*, independent of* N *and* h*, such that*

$$\|u-u_N\|_{2,\Omega} + \|\lambda-\lambda_h\|_{-3/2,S_4} \leq C\left\{N^2\alpha^N + h^{k+1}\right\},$$

with $\alpha \in (0,1)$*.*

Proof. From Theorem 1 we have

$$||u-u_N||_{2,\Omega} + ||\lambda-\lambda_h||_{-3/2,S_4} \leq C\left\{\inf_{v\in {V_1}^N}||u-v||_{2,\Omega} + \inf_{\eta\in {V_2}^h}||\lambda-\eta||_{-3/2,S_4}\right\}, \quad (4.38)$$

with $C \in \mathbb{R}^+$ independent of N and h. Note that by (4.25) and (4.26)

$$\inf_{v\in {V_1}^N}\|u-v\|_{2,\Omega} \leq \|u-w_N\|_{2,\Omega} = \|r_N\|_{2,\Omega}.$$

Using assumption (4.27) we get

$$\inf_{v\in {V_1}^N}\|u-v\|_{2,\Omega} \leq CN^2\alpha^N, \quad (4.39)$$

where the constant $C > 0$ is independent of N and α. Next let λ_I be the k^{th}-order interpolant of λ. Then, since $\lambda \in H^k(S_4)$ and λ_h is the best approximation, we have

$$\|\lambda - \lambda_h\|_{-3/2,S_4} \leq \|\lambda - \lambda_h\|_{0,S_4} \leq \|\lambda - \lambda_I\|_{0,S_4} \leq h^{k+1}\|\lambda\|_{k,S_4} \leq Ch^{k+1},$$

which, along with (4.38)–(4.39) gives the desired result. ■

The approximation of the singular coefficients is given by the following.

Corollary 1 *Let*

$$u = \sum_{j=1}^{\infty} \alpha_j r^{\mu_j+1} f_1(\theta, \mu_j) + \sum_{j=1}^{\infty} \beta_j r^{\mu_j+1} f_2(\theta, \mu_j) \tag{4.40}$$

and

$$u_N = \sum_{j=1}^{N} \alpha_j^N r^{\mu_j+1} f_1(\theta, \mu) + \sum_{j=1}^{N} \beta_j^N r^{\mu_j+1} f_2(\theta, \mu_j) \tag{4.41}$$

satisfy (4.11) *and* (4.16)*, respectively, with α_j, β_j and α_j^N, β_j^N denoting the true and approximate singular coefficients. Then, there exists a positive constant $C \in \mathbb{R}^+$, independent of N and α, such that*

$$\left|(\alpha_j - \alpha_j^N)\right| + \left|(\beta_j - \beta_j^N)\right| \leq CN^2\alpha^N. \tag{4.42}$$

Proof.

We begin by noting the following (which can be obtained by elementary calculations):

$$\int_0^{2\pi} f_1(\theta, \mu_j) f_1(\theta, \mu_k) d\theta = 2\pi\delta_{j,k} \tag{4.43}$$

$$\int_0^{2\pi} f_1(\theta, \mu_j) f_2(\theta, \rho_k) d\theta = 0 \ \forall j, k = 1, 2, ... \tag{4.44}$$

$$\int_0^{2\pi} f_2(\theta, \rho_j) f_2(\theta, \rho_k) d\theta = 2\pi \frac{4k^2 - 4k + 5}{4k^2 + 4k + 1}\delta_{j,k} \tag{4.45}$$

where f_1, f_2 are given by (4.5)–(4.6) and $\delta_{j,k}$ is the Kronecker delta. Now, in (4.40) take a fixed $r = r_0 < 1$, multiply by $f_1(\theta, \mu_k)$ and integrate from $\theta = 0$ to $\theta = 2\pi$. Using (4.43) and (4.44) we find that

$$\int_0^{2\pi} u(r_0, \theta) f_1(\theta, \mu_k) d\theta = 2\pi r_0^{\mu_k+1} \alpha_k. \tag{4.46}$$

Next, multiply (4.40) by $f_2(\theta, \rho_k)$ and integrate from $\theta = 0$ to $\theta = 2\pi$, to get with the aid of (4.44) and (4.45),

$$\int_0^{2\pi} u(r_0, \theta) f_2(\theta, \rho_k) d\theta = 2\pi r_0^{\rho_k+1} \frac{4k^2 - 4k + 5}{4k^2 + 4k + 1} \beta_k. \tag{4.47}$$

Similarly, one obtains expressions like (4.46), (4.47) corresponding to the approximate coefficients α_k^N, β_k^N, i.e. Eqs. (4.46), (4.47) with u replaced by u_N and α_k, β_k replaced by α_k^N, β_k^N, respectively. Therefore, we have

$$\left|\alpha_k - \alpha_k^N\right| \leq \frac{1}{2\pi r_0^{\mu_k+1}} \int_0^{2\pi} |u - u_N| \, |f_1| \, d\theta \leq \hat{C}_k \|u - u_N\|_{0,\Omega}, \tag{4.48}$$

$$\left|\beta_k - \beta_k^N\right| \leq \frac{4k^2 + 4k + 1}{2\pi r_0^{\rho_k+1}(4k^2 - 4k + 5)} \int_0^{2\pi} |u - u_N| \, |f_2| \, d\theta \leq \tilde{C}_k \|u - u_N\|_{0,\Omega}, \tag{4.49}$$

where the Cauchy-Schwartz inequality and the smoothness of f_1, f_2 were used. The positive constants $\hat{C}_k, \tilde{C}_k$ depend only on k (and r_0). The result then follows from (4.39) and the fact that $\|u - u_N\|_{0,\Omega} \leq \|u - u_N\|_{2,\Omega}$. ■

Note that the above corollary establishes the exponential convergence of the SFBIM, in the case of the biharmonic problems of the type shown in Fig. 4.2; the term N^2 can be absorbed in the exponentially decaying term α^N. This result is analogous to the one obtained in Xenophontos et al. (2006) for 2-D Laplacian problems.

4.4 Implementation

We now give a description of the implementation of the method and show that the two approaches are (mathematically) equivalent. Recall the discrete problem given by (4.16), which may be rewritten in *mixed* form as follows: Find $(u_N, \lambda_h) \in [V_1^N \times V_2^h] \subset [V_1 \times V_2]$ such that

$$\iint_\Omega \nabla^2 v_N \nabla^2 u_N + \int_{S_4} v_N \lambda_h = 0 \ \forall \, v_N \in V_1^N, \tag{4.50}$$

$$\int_{S_4} \mu_h u_N = \int_{S_4} \mu_h g \ \forall \, \mu_h \in V_2^h. \tag{4.51}$$

We may reduce the double integral in (4.50) using Green's second identity and the boundary conditions in (4.3) and (4.7), as follows:

$$\begin{aligned}\iint_{\Omega} \nabla^2 v_N \nabla^2 u_N &= \int_{\partial\Omega} \left(\nabla^2 v_N \frac{\partial u_N}{\partial n} - u_N \frac{\partial(\nabla^2 v_N)}{\partial n} \right) \\ &= \int_{S_3 \cup S_4} \left(\nabla^2 v_N \frac{\partial u_N}{\partial n} - u_N \frac{\partial(\nabla^2 v_N)}{\partial n} \right). \end{aligned} \tag{4.52}$$

Hence, the problem (4.50)–(4.51) becomes: Find $(u_N, \lambda_h) \in [V_1^N \times V_2^h] \subset [V_1 \times V_2]$ such that

$$\int_{S_3 \cup S_4} \left(\nabla^2 v_N \frac{\partial u_N}{\partial n} - u_N \frac{\partial(\nabla^2 v_N)}{\partial n} \right) + \int_{S_4} v_N \lambda_h = 0 \ \ \forall\, v_N \in V_1^N, \tag{4.53}$$

$$\int_{S_4} \mu_h u_N = \int_{S_4} \mu_h g \ \ \forall\, \mu_h \in V_2^h. \tag{4.54}$$

Obviously, if $(u_N, \lambda_h) \in [V_1^N \times V_2^h] \subset [V_1 \times V_2]$ solves (4.50)–(4.51) (or (4.16)), then it also solves (4.53)–(4.54). Now suppose that $(u_N, \lambda_h) \in [V_1^N \times V_2^h] \subset [V_1 \times V_2]$ solves (4.53)–(4.54). We have from (4.52) that

$$\int_{S_3 \cup S_4} \left(\nabla^2 v_N \frac{\partial u_N}{\partial n} - u_N \frac{\partial(\nabla^2 v_N)}{\partial n} \right) = \iint_{\Omega} \nabla^2 v_N \nabla^2 u_N, \tag{4.55}$$

hence, adding Eqs. (4.53)–(4.54) and using the above fact, we find that

$$\iint_{\Omega} \nabla^2 v_N \nabla^2 u_N + \int_{S_4} v_N \lambda_h + \int_{S_4} \mu_h u_N = \int_{S_4} \mu_h g, \tag{4.56}$$

which shows that (u_N, λ_h) solves (4.16).

Equations (4.53)–(4.54) are used in the implementation, since they are posed only on the boundary of the domain away from the singular point. This reduces the dimension of the problem by one and leads to significant computational savings.

Now, to obtain a linear system of equations corresponding to (4.53)–(4.54), we approximate u and λ by means of

$$u_N = \sum_{i=1}^{N} \alpha_i^N v_i^{(1)} + \sum_{i=1}^{N} \beta_i^N v_i^{(2)} \in V_1^N, \tag{4.57}$$

and

$$\lambda_h = \sum_{k=1}^{M} \gamma_k \psi_k \in V_2^h\,(S_4)\,, \tag{4.58}$$

with α_i^N, β_i^N and γ_k the unknowns in the system, and $V_1^N = span\left\{v_i^{(1)}\right\}_{i=1}^N \cup span\left\{v_i^{(2)}\right\}_{i=1}^N$, $V_2^h = span\left\{\psi_k\right\}_{k=1}^M$. Upon inserting (4.57) and (4.58) into (4.53)–(4.54), a $(2N+M)\times(2N+M)$ linear system of the following composite form is obtained:

$$\begin{bmatrix} K_{11} & K_{12} & \Lambda_1 \\ K_{21} & K_{22} & \Lambda_2 \\ \Lambda_1^T & \Lambda_2^T & 0 \end{bmatrix} \begin{bmatrix} \overrightarrow{\alpha} \\ \overrightarrow{\beta} \\ \overrightarrow{\gamma} \end{bmatrix} = \begin{bmatrix} \overrightarrow{0} \\ \overrightarrow{0} \\ \overrightarrow{G} \end{bmatrix}, \tag{4.59}$$

where $\overrightarrow{\alpha} = \left[\alpha_1^N, ..., \alpha_N^N\right]^T$, $\overrightarrow{\beta} = \left[\beta_1^N, ..., \beta_N^N\right]^T$, $\overrightarrow{\gamma} = \left[\gamma_1, ..., \gamma_M\right]^T$, and

$$\begin{aligned}
[K_{11}]_{i,j} &= \int_{S_3\cup S_4} \left\{ \nabla^2 v_j^{(1)} \frac{\partial v_i^{(1)}}{\partial n} - v_i^{(1)} \frac{\partial}{\partial n}\left(\nabla^2 v_j^{(1)}\right) \right\}, \ i,j = 1, ..., N, \\
[K_{12}]_{i,j} &= \int_{S_3\cup S_4} \left\{ \nabla^2 v_j^{(1)} \frac{\partial v_i^{(2)}}{\partial n} - v_i^{(2)} \frac{\partial}{\partial n}\left(\nabla^2 v_j^{(1)}\right) \right\}, \ i,j = 1, ..., N, \\
[K_{21}]_{i,j} &= \int_{S_3\cup S_4} \left\{ \nabla^2 v_j^{(2)} \frac{\partial v_i^{(1)}}{\partial n} - v_i^{(1)} \frac{\partial}{\partial n}\left(\nabla^2 v_j^{(2)}\right) \right\}, \ i,j = 1, ..., N, \\
[K_{22}]_{i,j} &= \int_{S_3\cup S_4} \left\{ \nabla^2 v_j^{(2)} \frac{\partial v_i^{(2)}}{\partial n} - v_i^{(2)} \frac{\partial}{\partial n}\left(\nabla^2 v_j^{(2)}\right) \right\}, \ i,j = 1, ..., N,
\end{aligned}$$

$$\begin{aligned}
[\Lambda_1]_{k,j} &= \int_{S_4} \psi_k \, v_j^{(1)}, \ k = 1, ..., M, \ j = 1, ..., N, \\
[\Lambda_2]_{k,j} &= \int_{S_4} \psi_k \, v_j^{(2)}, \ k = 1, ..., M, \ j = 1, ..., N, \\
\left[\overrightarrow{G}\right]_\ell &= \int_{S_4} g \, \psi_\ell, \ \ell = 1, ..., M.
\end{aligned}$$

It is easily shown that the coefficient matrix in (4.59) is nonsingular provided $N > M$. Hence, N should be chosen larger than M, but not too large since for excessively large values of N the linear system (4.59) becomes ill-conditioned and the results obtained are unreliable. As a final remark we should point out that all integrals involved in the determination of the coefficient matrix (and right hand side) in (4.59), are along the parts of the domain boundaries that *do not contain the singularity*. These are one-dimensional and can be approximated by standard techniques, such as Gaussian quadrature.

4.5 Numerical Results

In this section we illustrate the main theoretical findings through one numerical experiment, as described below. Since the method is designed for the efficient approximation of the singular cofficients, the numerical results shown below correspond to how fast (and accurately) these coefficients are approximated.

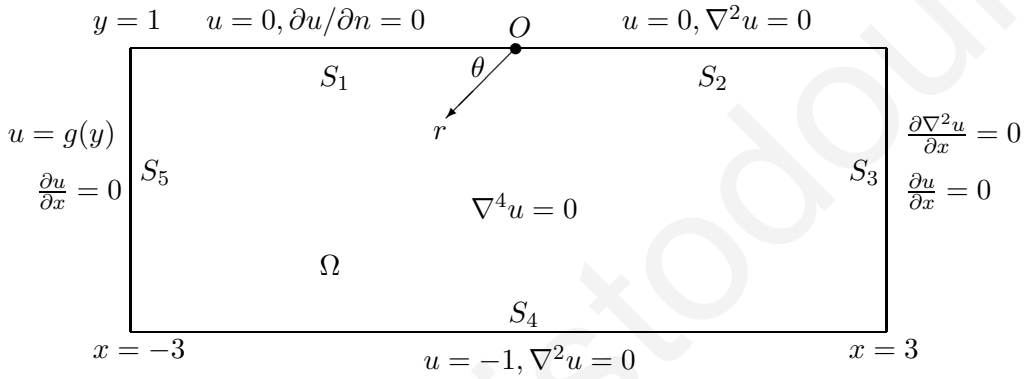

Figure 4.2: Stick-slip problem; $g(y) = \frac{1}{2}y(3 - y^2) - 1$.

We are considering the boundary value problem depicted graphically in Fig. 4.5 which is the classical stick-slip flow problem from fluid mechanics (see, e.g. Elliotis, 2005b). We note that the boundary of the domain consists of five parts, with S_4 and S_5 being the portions of $\partial\Omega$ where Lagrange multipliers will be applied, since Dirichlet boundary conditions are prescribed there.

We implemented our method, as explained in Section 4.4, using piecewise quadratic polynomials for the approximation of the Lagrange multiplier functions, on a subdivision of S_4 and S_5 characterized by a meshwidth h – for simplicity a uniform subdivision of the same meshwidth h was used for both portions of the boundary. All integrals involved were approximated by a 15-point Gaussian quadrature on each element. Systematic runs were performed in order to find the "optimal" combination of N and h (or M), which ultimately was chosen

as the one that gave the "smoothest" approximation to

$$\lambda_4 := \frac{\partial \nabla^2 u}{\partial n}|_{S_4}. \tag{4.60}$$

This is shown in Fig. 4.3 which shows that for $M = 39$ and $N = 45$ the approximation to the Lagrange multipler function on S_4 is free of oscillations (The oscillations observed are due to the ill-conditioning of the stiffness matrix.). Using this pair of values, the constant α in (4.42) is calculated by "balancing" the error estimate of Theorem 2, i.e.

$$N^2 \alpha^N \approx h^{k+1}.$$

We find that $\alpha \approx 0.87$, from which subsequent "optimal" pairs of N and M may be found.

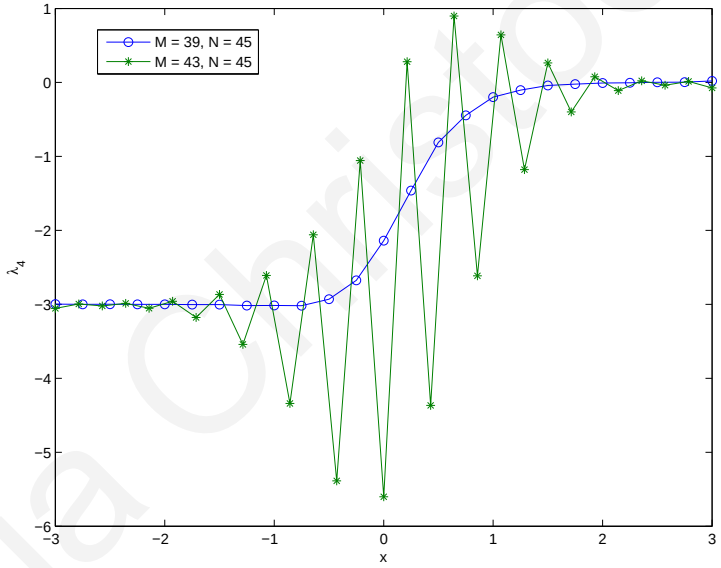

Figure 4.3: Approximation of Lagrange multipler function along S_4.

Figures 4.4 and 4.5 show the (percentage relative) error in the approximation of the first five coefficients $\alpha_j, \beta_j, j = 1, ..., 5$, in a semi-logarithmic scale, as N is increased. The exponential convergence is clearly visible, since the curves are (essentially) straight lines, even for small values of N.

We should mention that for α_1 there is an exact answer while for the rest we used a reference value for the computations.

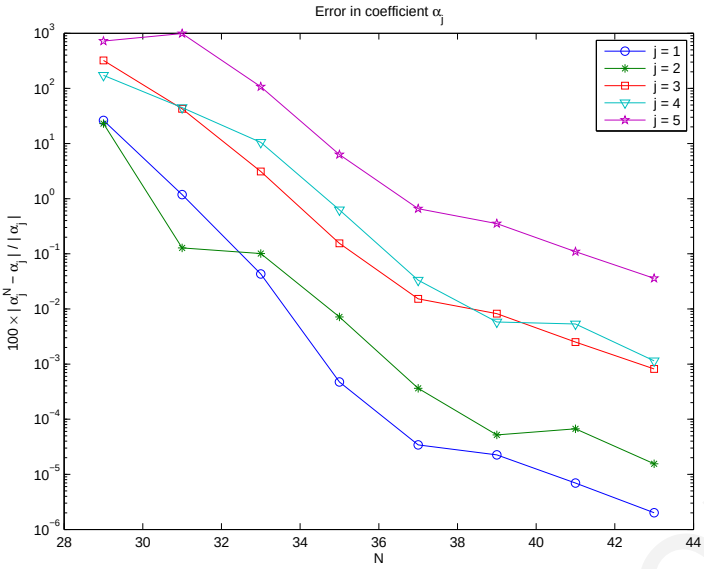

Figure 4.4: Error in coefficient α_j^N.

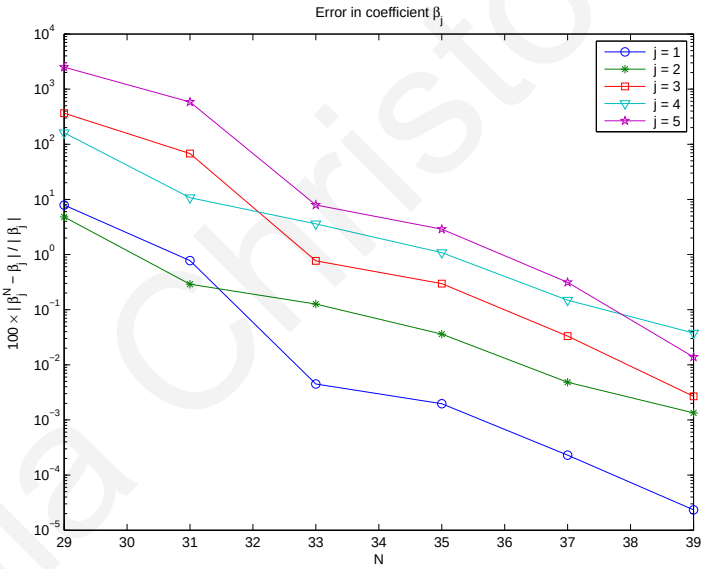

Figure 4.5: Error in coefficient β_j^N.

4.6 Conclusions

In this chapter we analyzed the SFBIM for a two-dimensional biharmonic problem with one boundary singularity, as a model for the Newtonian stick-slip flow problem. We analyzed the convergence of the method and proved that the coefficients in the local asymptotic expansion, also referred to as stress intensity factors, are approximated at an exponential rate as the

number of the employed expansion terms is increased. Our theoretical results were illustrated through a numerical experiment.

Chapter 5

Extensions to Three-Dimensions

5.1 Introduction

5applications both edge and vertex singularities are of interest (see Kondratiev, 1967, Stephan and Whiteman, 1988, and

The objective of this chapter is to extend the SFBIM to three-dimensional Laplacian problems with a boundary straight-edge singularity and calculate directly the Edge Flux Intensity Functions (EFIFs). These are approximated locally by low-degree polynomials the coefficients of which are primary unknowns of the method. To our knowledge, the only methods found in the literature for the calculation of the EFIFs are based on post-processing the numerical solution and/or using extraction formulae (see Omer et al., 2004. Yosibash et al., 2002. Yosibash et al., 2004 and Yosibash et al., 2007)

The rest of the chapter is organized as follows: in Section 5.2 we present a three-dimensional Laplacian problem with an edge singularity and its asymptotic local solution expansion. In Section 5.3 the three-dimensional version of the SFBIM is formulated. Numerical results are given in Section 5.4. Finally, our conclusions are summarized in Section 5.5.

5.2 A Three-Dimensional Problem With a Straight Edge Singularity

We consider a Laplacian problem in the three-dimensional domain $\Omega = [0,1]\times[0,\alpha\pi]\times[-1,1]$, as shown in Fig. 5.1: Find u such that

$$\nabla^2 u = 0 \text{ in } \Omega, \tag{5.1}$$

$$\left.\begin{aligned} u &= 0 \text{ on } S_1 \\ \tfrac{\partial u}{\partial \theta} &= 0 \text{ on } S_2 \\ u &= g(r,\theta,z) \text{ on } S_3 \\ \tfrac{\partial u}{\partial z} &= q_1(r,\theta) \text{ on } S_4 \\ \tfrac{\partial u}{\partial z} &= q_2(r,\theta) \text{ on } S_5 \end{aligned}\right\} \tag{5.2}$$

where $\partial\Omega = \bigcup_{i=1}^{5} S_i$. S_1 and S_2 are quadrilateral surfaces intersecting at a straight edge AB, S_3 is a cylindrical surface of unit radius, and S_4 and S_5 are unit-circular sectors of angle $\alpha\pi$.

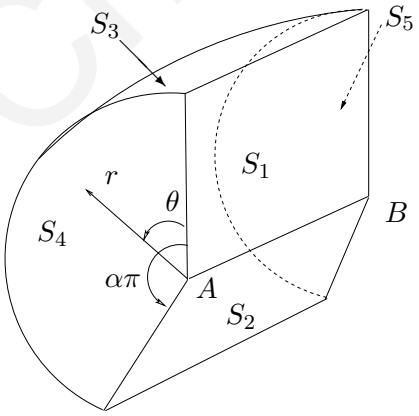

Figure 5.1: A model three-dimensional domain $\Omega = [0,1]\times[0,\alpha\pi]\times[-1,1]$ with a straight edge AB.

To demonstrate the analogy with the two-dimensional case, we consider the Laplace equation over a circular sector, as shown in Fig. 5.2. A boundary singularity arises at the origin O, which is due not only to the presence of a corner in the boundary but also to the fact that

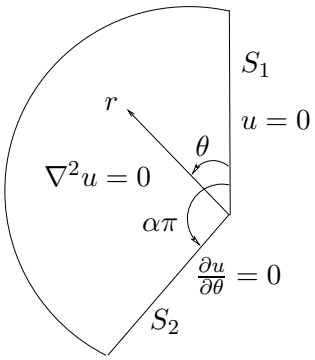

Figure 5.2: A 2-D Laplacian problem with a boundary singularity at point O.

the boundary conditions along boundaries S_1 and S_2 are different: $u = 0$ along $\theta = 0$ and $\partial u/\partial\theta = 0$ along $\theta = \alpha\pi$, where $0 < \alpha < 2$. The local solution in polar coordinates (r, θ), centered at the singular point O, is of the general form

$$u_{2D}(r, \theta) = \sum_{j=1}^{\infty} \alpha_j r^{\mu_j} f_j(\theta), \tag{5.3}$$

where μ_j and f_j are, respectively, the eigenvalues and eigenfunctions of the problem with $\mu_{j+1} > \mu_j$, and α_j are the constant singular coefficients which are unknown. The eigensolution (μ_j, f_j) is uniquely determined by the geometry and the boundary conditions along the boundary parts S_1 and S_2 sharing the singular point. The unknown singular coefficients α_j are determined by the boundary conditions in the remaining parts of the boundary. These coefficients are called (generalized) stress intensity factors (Szabó and Yosibash, 1996) and, in many applications, are the main unknowns. In the case of the boundary conditions depicted in Fig. 5.1, the eigenvalues μ_j and eigenfunctions $f_j(\theta)$ are given by

$$\mu_j = \frac{2j - 1}{2\alpha}, \tag{5.4}$$

and

$$f_j(\theta) = \sin(\mu_j \theta). \tag{5.5}$$

As pointed out by Yosibash et al. (2002), once the eigen-pairs for the 2-D Laplacian problem are obtained, one may construct the full series expansion solution for the 3-D Laplacian

operator in the vicinity of straight edges. In the case of the Laplace equation, the solution can be decomposed as follows:

$$u = \sum_{j=1}^{J} \sum_{\ell=1}^{L} \alpha_{j\ell}(z) r^{\mu_j} (\ln r)^{\ell} f_{j\ell}(\theta) + v(r, \theta, z), \tag{5.6}$$

where μ_j are identical to the eigenvalues of the 2-D problem and are now called edge eigenvalues, $\alpha_{j\ell}$ are the flux intensity functions (EFIFs) which are analytic in z up to the vertices, $f_{j\ell}$ are the edge eigenfunctions which are analytic in θ, and v is a sufficiently smooth function. $L \geq 0$ is an integer which is zero except when μ_j is an integer. In the present work it is assumed that $\mu_j, j \leq J$ are not integers. Therefore, (5.6) is reduced to

$$u = \sum_{j=1}^{J} \alpha_j(z) r^{\mu_j} f_j(\theta) + v(r, \theta, z). \tag{5.7}$$

As demonstrated in Yosibash et al. (2002), a choice for the function v so that u satisfies identically the 3-D Laplace equation is

$$v(r, \theta, z) = r^{\mu_j} f_j(\theta) \sum_{i=1}^{\infty} \frac{d^{2i}}{dz^{2i}} \left(\alpha_j(z)\right) \frac{r^{2i} (-1/4)^i}{\prod_{n=1}^{i} n (\mu_j + n)}. \tag{5.8}$$

Thus, the solution takes the form :

$$u = \sum_{j=1}^{J} r^{\mu_j} f_j(\theta) \left\{ \alpha_j(z) + \sum_{i=1}^{\infty} \frac{d^{2i}}{dz^{2i}} \left(\alpha_j(z)\right) \frac{r^{2i} (-1/4)^i}{\prod_{n=1}^{i} n (\mu_j + n)} \right\}. \tag{5.9}$$

In Appendix B we show that for any $\alpha_j(z) \in C^{\infty}(AB)$, the above function u satisfies the three-dimensional Laplace equation and the boundary conditions on S_1 and S_2. The calculation of the EFIFs $\alpha_j(z), j = 1, 2, ..., J$ is the main objective of the present chapter. It should be noted that Eqs. (5.7)–(5.9) hold only for the special case of the Laplace equation and not for the general elliptic equation considered by Yosibash et al. (2002). More details are provided in Appendix C.

5.3 Formulation of the SFBIM

The basic assumption for the development of the SFBIM for 3-D Laplacian problems with edge singularities is the use of piecewise polynomial approximations for the EFIFs by partitioning the interval $[-1,1]$ into M subintervals and writing

$$\alpha_j^M(z) = \sum_{k=1}^{M_\phi} \alpha_{jk}\phi_k(z)\ ,\ j = 1,2,...,N, \tag{5.10}$$

where α_{jk} are unknown coefficients, $\phi_k(z)$ are (piecewise polynomial) basis functions, and M_ϕ is the number of basis functions (e.g. $M_\phi = M$ for constant, $M_\phi = M+1$ for linear basis functions, etc.). Thus, the solution (5.9) can be approximated as follows:

$$u_N = \sum_{j=1}^{N} \alpha_j^M(z) r^{\mu_j} f_j(\theta), \tag{5.11}$$

or

$$u_N = \sum_{j=1}^{N}\sum_{k=1}^{M_\phi} \alpha_{jk} W_j^k(r,\theta,z), \tag{5.12}$$

where

$$W_j^k(r,\theta,z) = r^{\mu_j} f_j(\theta)\phi_k(z)\ ,\ j = 1,2,...,N,\ k = 1,2,...,M_\phi. \tag{5.13}$$

It is important to note that the functions W_j^k satisfy identically the governing equation and the boundary conditions on boundaries S_1 and S_2 sharing the edge AB. In order to calculate the $N_\alpha = NM_\phi$ unknown coefficients α_{jk}, we discretize the problem by weighting the governing equation over Ω by means of the functions W_j^k. Applying Green's theorem twice one gets:

$$\iint\limits_{S_3\cup S_4\cup S_5} \left(\frac{\partial u_N}{\partial n} W_j^k - \frac{\partial W_j^k}{\partial n} u_N \right) dS = 0\ ,\ j = 1,2,...,N,\ k = 1,2,...,M_\phi. \tag{5.14}$$

The Neumann conditions on boundaries S_4 and S_5 are weakly imposed by simply substituting the functions q_1 and q_2, respectively. The Dirichlet boundary condition on S_3 is imposed by means of a Lagrange multiplier function $\lambda(\theta,z)$ which replaces the normal derivative of the

solution. In this work, λ is approximated by means of locally polynomial (depending on the choice for ϕ_k) basis functions Ψ_i:

$$\lambda(\theta, z) = \left.\frac{\partial u_N}{\partial r}\right|_{r=1} = \sum_{i=1}^{N_\lambda} \lambda_i \Psi_i(\theta, z), \tag{5.15}$$

where $\lambda_i, i = 1, 2, ..., N_\lambda$ are the unknown discrete Lagrange multipliers. To define the basis functions Ψ_i, the two-dimensional domain $[0, \alpha\pi] \times [-1, 1]$ is partitioned into $N_\theta \times M_\phi$ elements, which means that $N_\lambda = M_\phi N_\theta$ or $M_\phi(N_\theta + 1)$ for, respectively, constant or bilinear Lagrange multipliers. The additional required equations are obtained by weighting the Dirichlet condition $u = g(\theta, z)$ on S_3 by means of the basis functions Ψ_i. The following linear system of $N_\alpha + N_\lambda$ discretized equations is obtained:

$$\begin{aligned} &\iint_{S_3} \left(\lambda W_j^k - u_N \frac{\partial W_j^k}{\partial r}\right) dS + \iint_{S_4} u_N \frac{\partial W_j^k}{\partial z} dS - \iint_{S_5} u_N \frac{\partial W_j^k}{\partial z} dS \\ = \; &\iint_{S_4} q_1 W_j^k dS - \iint_{S_4} q_1 W_j^k dS, \text{ for } j = 1, 2, ..., N \;,\; k = 1, 2, ..., M_\phi, \end{aligned} \tag{5.16}$$

and

$$\iint_{S_3} u_N \Psi_i dS = \iint_{S_3} g \Psi_i dS \;,\; i = 1, 2, ..., N_\lambda. \tag{5.17}$$

Equations (5.16) and (5.17) involve two-dimensional integrals, while our problem is three-dimensional, as mentioned before, the dimensional reduction is one of the main advantages of the SFBIM. It should also be noted that the contributions over boundary parts S_4 and S_5 in the RHS of Eq. (5.16) are identically zero if the basis functions ϕ_k are constant. The system of Eqs. (5.16) and (5.17) can be written in block form as follows:

$$\begin{bmatrix} K & L \\ L^T & O \end{bmatrix} \begin{bmatrix} A \\ \Lambda \end{bmatrix} = \begin{bmatrix} B \\ C \end{bmatrix}, \tag{5.18}$$

where A is the vector of the unknown coefficients α_{jk} of the EFIFs and Λ is the vector of the unknown discrete Lagrange coefficients. It is easily observed that the stiffness matrix is symmetric and becomes singular if $N_\alpha < N_\lambda$ or, equivalently, when $N < N_\theta$ for constant ϕ_k and $N < N_\theta + 1$ for linear ϕ_k. In order to assure that the stiffness matrix is non-singular, in all the numerical results of this work we have chosen $N_\theta = \min\{M, N - 2, 20\}$.

5.4 Numerical Results

Following Yosibash et al. (2002), we construct test problems having analytical solutions of the form:

$$u_s(r,\theta,z)=\sum_{i=1}^{J}\left[\left(\alpha_{i1}+a_{i2}z+a_{i3}z^2\right)r^{\mu_i}\sin\left(\mu_i\theta\right)-\frac{\alpha_{i3}}{2\left(\mu_i+1\right)}r^{\mu_i+2}\sin\left(\mu_i\theta\right)\right], \tag{5.19}$$

where $\alpha_{ij}, i=1,...,J, j=1,2,3$ are specified as desired. Any solution of the form (5.19) satisfies the 3D Laplace equation as well as the boundary conditions along S_1 and S_2. Once the solution u_s is specified, it is straightforward to find the functions g, q_1 and q_2 that appear in Eq. (5.2):

$$g(\theta,z)=u_s\left(1,\theta,z\right)=\sum_{i=1}^{J}\left[\alpha_{i1}-\frac{\alpha_{i3}}{2\left(\mu_i+1\right)}+a_{i2}z+a_{i3}z^2\right]\sin\left(\mu_i\theta\right), \tag{5.20}$$

$$q_1(r,\theta)=\frac{\partial u_s}{\partial z}(r,\theta,-1)=\sum_{i=1}^{J}\left(a_{i2}-2a_{i3}\right)r^{\mu_i}\sin\left(\mu_i\theta\right), \tag{5.21}$$

$$q_2(r,\theta)=\frac{\partial u_s}{\partial z}(r,\theta,1)=\sum_{i=1}^{J}\left(a_{i2}+2a_{i3}\right)r^{\mu_i}\sin\left(\mu_i\theta\right). \tag{5.22}$$

In what follows we investigate the implementation of the above method for $\alpha=3\pi/4$. The eigenvalues and eigenfunctions in this case are

$$\mu_j=\frac{2(2j-1)}{3}, \tag{5.23}$$

and

$$f_j(\theta)=\sin\left(\mu_j\theta\right)=\sin\left[\frac{2(2j-1)}{3}\theta\right]. \tag{5.24}$$

We will consider two test problems: In Test Problem 1 we take $J=100$ with

$$\alpha_{i1}=\frac{1}{i^4},\alpha_{i2}=\frac{2}{i^4+i^2},\alpha_{i3}=\frac{3}{i^4}\ ,\ i=1,...,J. \tag{5.25}$$

In Test Problem 2, $J=3$ with $\alpha_{11}=\alpha_{12}=\alpha_{13}=1,\alpha_{21}=\alpha_{22}=0.5,\alpha_{23}=1$, and $\alpha_{31}=\alpha_{32}=\alpha_{33}=0.2$. The entries of K, L, C and B of the system (5.18) for both test problems can be found in Appendix D.

Due to the form of the essential boundary condition (5.2), the SFBIM calculates directly the EFIFs, which are given by

$$\alpha_i(z) = \alpha_{i1} - \frac{\alpha_{i3}}{2\,(\mu_i + 1)} + \alpha_{i2} z + \alpha_{i3} z^2. \tag{5.26}$$

For both test problems we will be interested in the relative errors

$$\varepsilon_i = \frac{\left\| \alpha_i - \alpha_i^M \right\|_{L^2(AB)}}{\|\alpha_i\|_{L^2(AB)}},$$

where,

$$\|f(z)\|_{L^2(AB)} = \left[\int_{-1}^{1} f^2(z) dz \right]^{1/2}. \tag{5.27}$$

Let us first discuss the results of the SFBIM obtained for Test Problem 1 using constant basis functions ϕ_k in the axial direction. In Fig. 5.3, we plot the approximations of the first EFIF, α_1, obtained with three different numbers of elements in the axial direction ($M = 5$, 10 and 100) and $N = 20$, along with the analytical solution. Despite the inherent limitations of the constant basis functions, the approximation is improved considerably as M is increased. The results for the other EFIFs are quite similar. Figure 5.4 illustrates this effect in the case of α_5.

Next, in Fig. 5.5, we plot the calculated relative errors in the leading EFIFs (i.e., ε_1, ε_2 and ε_5) versus M. The slope of the lines is approximately -1, as expected since we are (i) using 0^{th} degree polynomials for the approximation and (ii) the L^2-norm is used as an error measure. We can then conclude that in the, e.g., H^1-norm, the method converges linearly with the number of elements, M, in the axial direction.

Figures 5.6 and 5.7 show the convergence of α_1 and α_5, respectively, with N when the number of elements in the axial direction is fixed at 20. Increasing N from 10 to 25 does not seem to lead to any observable improvement; the accuracy appears to be restricted by the value of M, which is rather low as already illustrated in Figs. 5.3 and 5.4. The errors in α_1, α_2 and α_5 are plotted in Fig. 5.8 versus the number N of the expansion terms. For higher

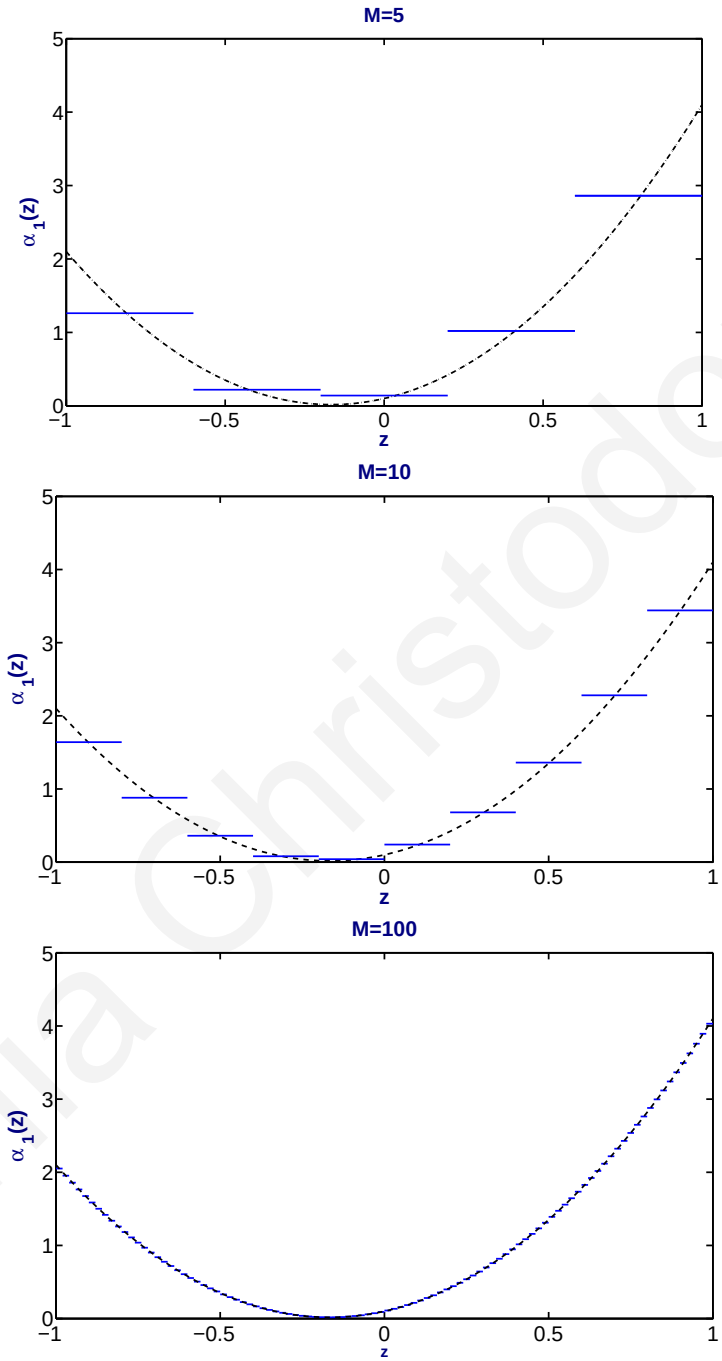

Figure 5.3: Convergence of $\alpha_1(z)$ with M using constant basis functions. $N = 20$.

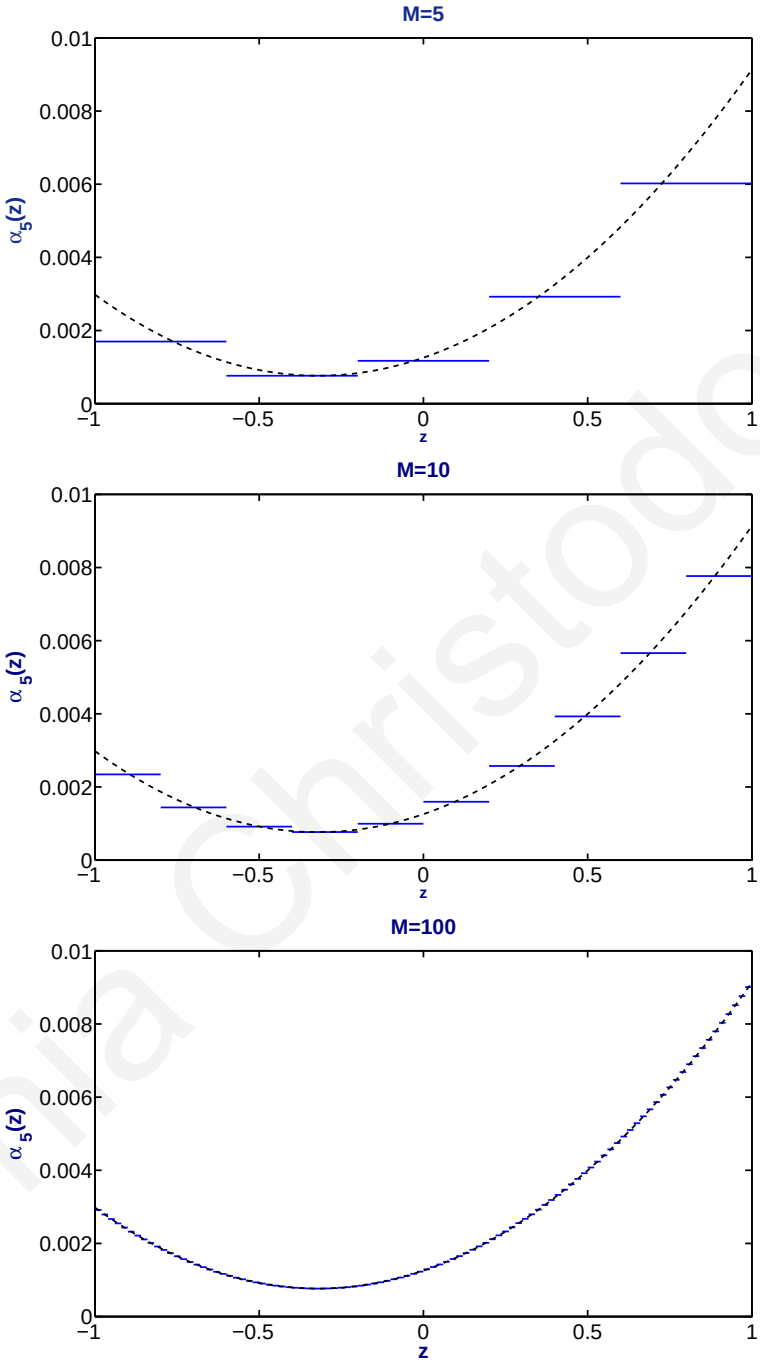

Figure 5.4: Convergence of $\alpha_5(z)$ with M using constant basis functions. $N = 20$.

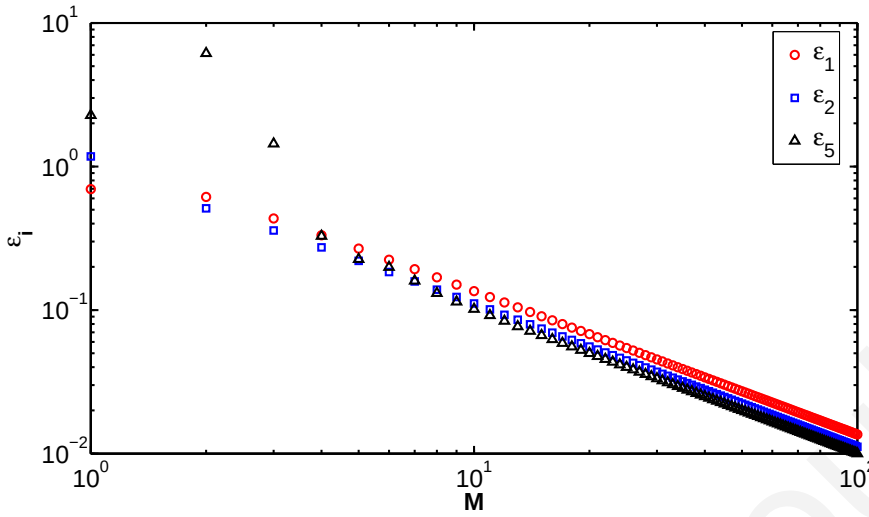

Figure 5.5: The errors ε_1, ε_2 and ε_5 for constant basis functions and $N = 20$ versus M.

values of N, the errors appear to level off very soon. This is simply due to the fact that the optimal approximation for the given value of M has essentially been achieved. This effect is illustrated in Fig. 5.9, where the errors in α_1 for various values of M are plotted.

We now turn our attention to the case when linear basis functions are used for the approximation of the EFIFs. As expected, using linear basis functions ϕ_k leads to more accurate estimated for the EFIFs and faster convergence of the SFBIM. In Figs. 5.10 and 5.11, the approximations of α_1 and α_5 for different values of M and $N = 20$ compare nicely with the analytical solutions for Test Problem 1. The convergence of the method is illustrated in Fig. 5.12, where the errors in the leading coefficients calculated with $N = 40$ are plotted versus M. The (expected) quadratic convergence is illustrated in Fig. 5.16, where we compare the errors in the first EFIF, α_1, obtained with the two sets of basis functions.

Figure 5.12 shows the error in the first, second and fifth EFIF with M. In all cases $N = 60$. Here, $N_\theta = M$ for $M < 30$ and $N_\theta = 30$ for $M \geq 30$.

Figures 5.13 and 5.14 are analogous to Figs. 5.6 and 5.7, for linear basis functions. We have plotted the EFIFs (numerical and analytic) for $M = 20$ and $N = 10$, 20 and 25. Note that

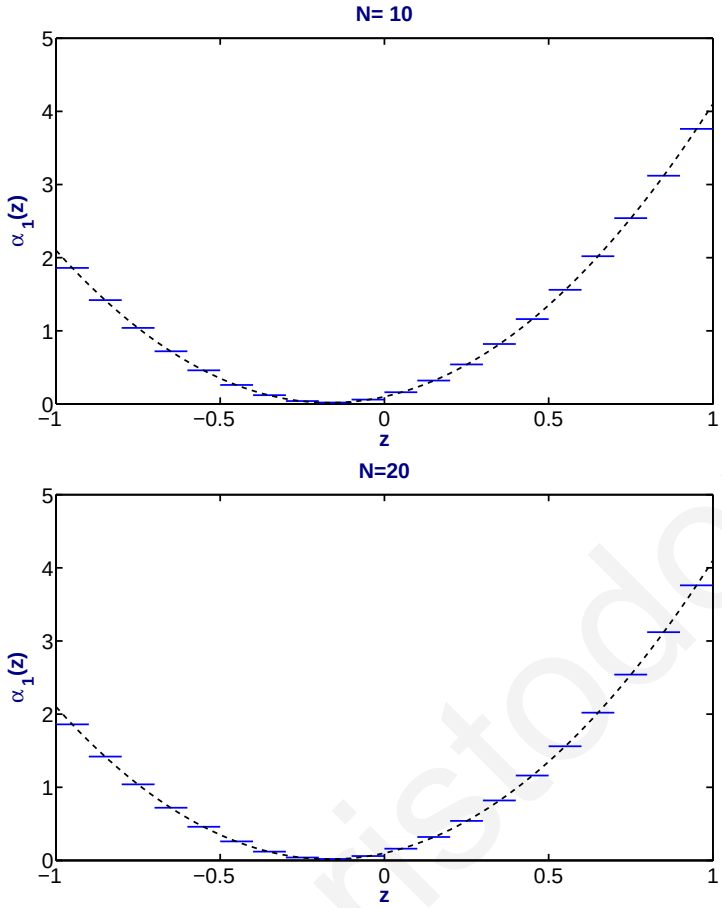

Figure 5.6: Convergence of $\alpha_1(z)$ with the number of singular functions N when using $M = 20$ constant basis functions in the z-direction.

for $N = 10$ and $N = 20$ the stiffness matrix is singular since here $N_\theta = 20$. This singularity is not obvious in α_1 but it can be observed in α_5. For $N = 25$ the matrix is not singular and it can be seen that both EFIFs are very close to the analytic solution.

Figures 5.15 and 5.16 compare the errors obtained with constant and linear basis functions versus the number of singular functions, N, and the number of z-elements, M, respectively. In Fig. 5.15 we have chosen $M = 20$ and $N_\theta = 19$. We have plotted the error in α_1 and α_5 for constant and linear basis functions against N. Note that for $N < 20$ the matrix is singular. Figure 5.16 shows the error in α_1 for constant and linear basis functions against M. Here $N = 70$ and $N_\theta = M$ for $M < 20$ and $N_\theta = 19$ for $M \geq 20$. Note that the slope is -1 for

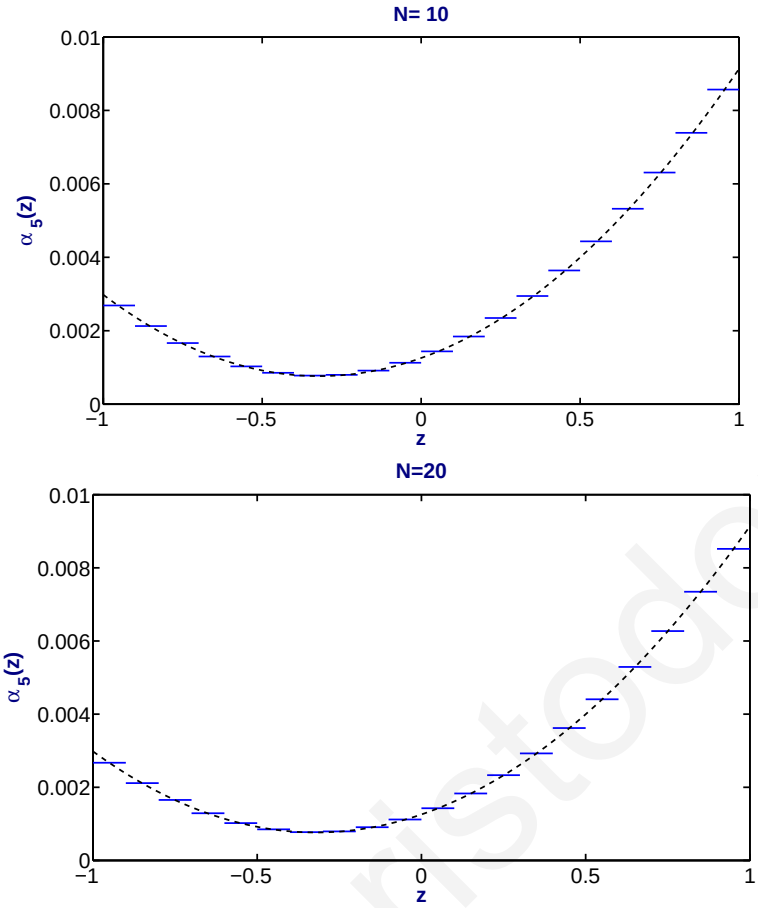

Figure 5.7: Convergence of $\alpha_5(z)$ with the number of singular functions N when using $M = 20$ constant basis functions in the z-direction.

constant approximations and -2 for linear approximations.

Similar results have been obtained for Test Problem 2. The convergence of the SFBIM with the number of z-elements M and the number of singular functions N is illustrated in Figs. 5.17 and 5.18 , respectively, where we plot the errors in α_1 and α_3.

5.5 Conclusions

We have presented an extension of the SFBIM to three-dimensional Laplacian problems with a boundary straight-edge singularity. As in the two-dimensional setting, the SFBIM produced

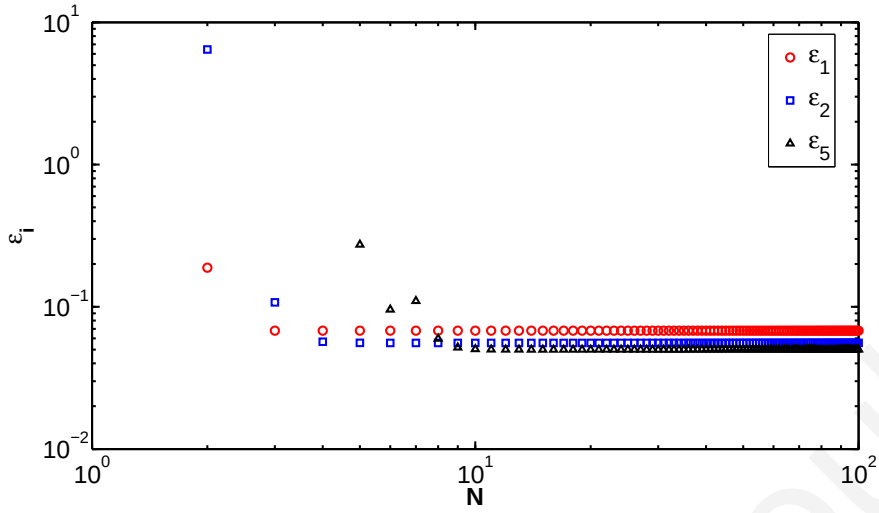

Figure 5.8: The errors ε_1, ε_2 and ε_5 for $M = 20$ constant basis functions versus the number of singular functions N.

accurate results for the coefficients (which in this case are functions of the third dimension). We have observed the following: (i) The approximation of the EFIFs is naturally governed by the choice of basis functions, as expected, hence increasing the number of z-elements M produces more accurate results (for moderately low values of singular functions N). (ii) Increasing N while keeping the number of z-element M fixed does not lead to any advantages.

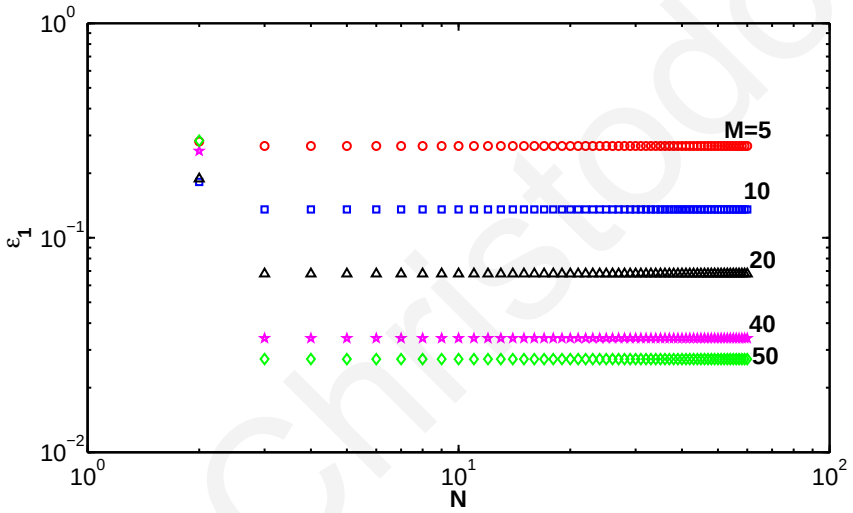

Figure 5.9: The error ε_1 for for various numbers of constant basis functions ($M = 5$, 10, 20, 40 and 80) plotted against N.

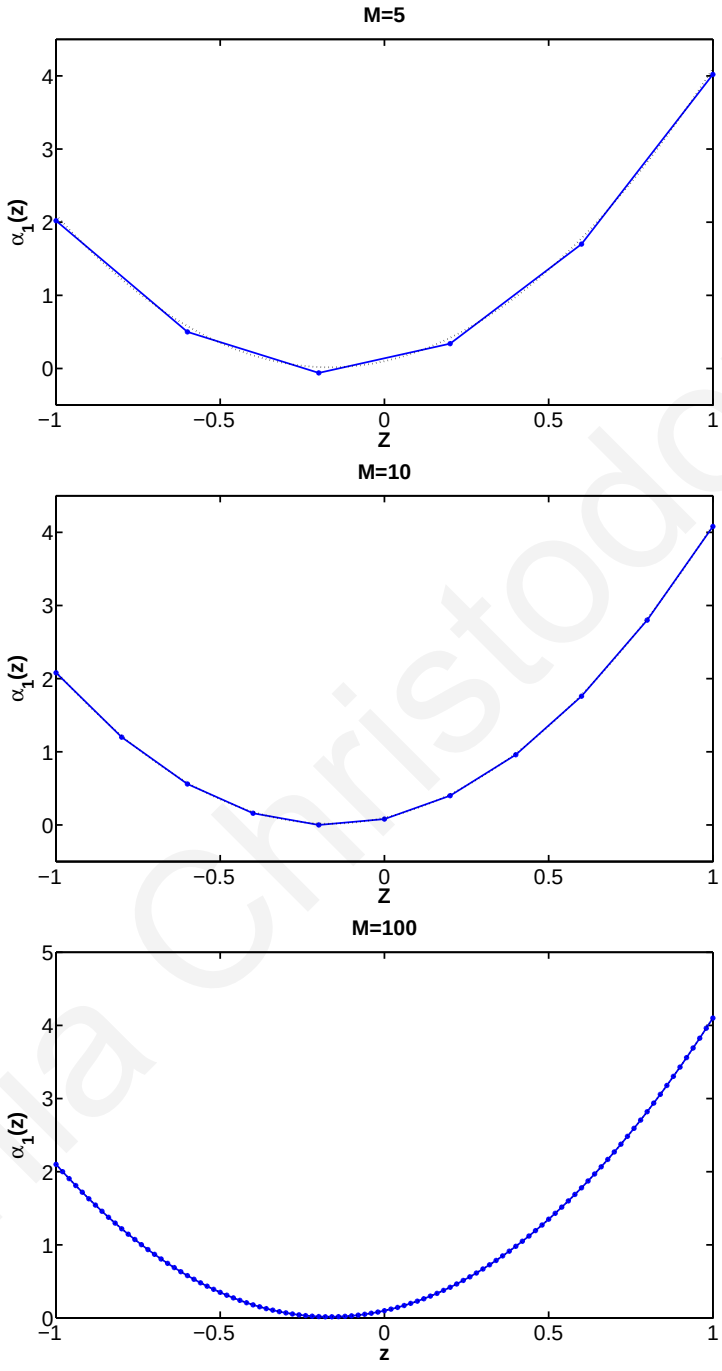

Figure 5.10: Convergence of the fifth EFIF, $\alpha_1(z)$, with M, using linear functions; $N = 20$.

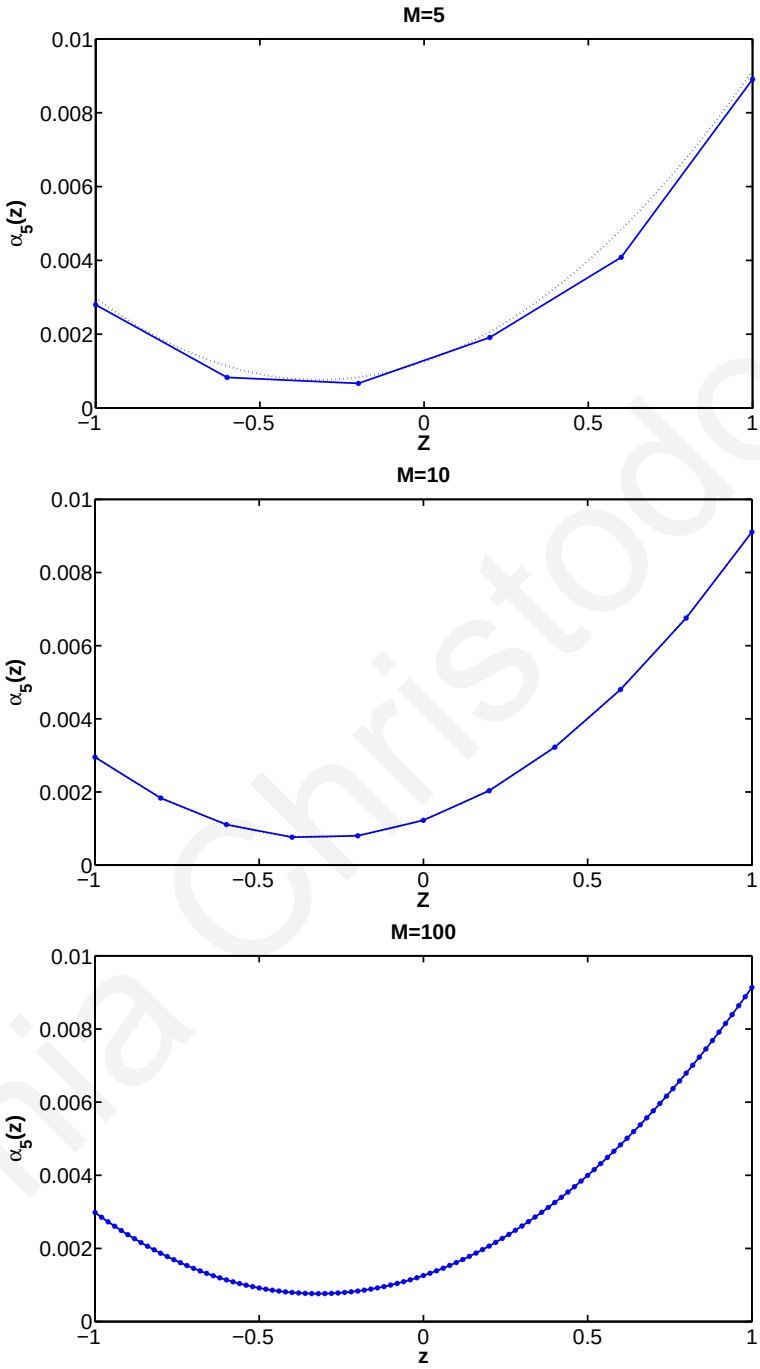

Figure 5.11: Convergence of $\alpha_5(z)$, with M, using linear functions; $N = 20$.

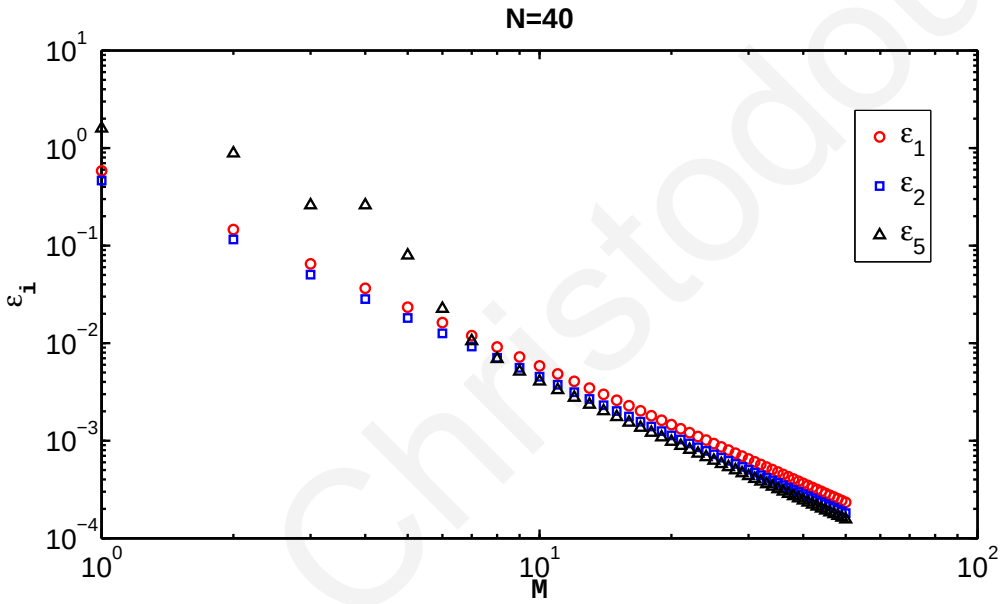

Figure 5.12: The errors ε_1, ε_2 and ε_5 for $N = 60$ linear basis functions versus the number M of the elements in the z-direction.

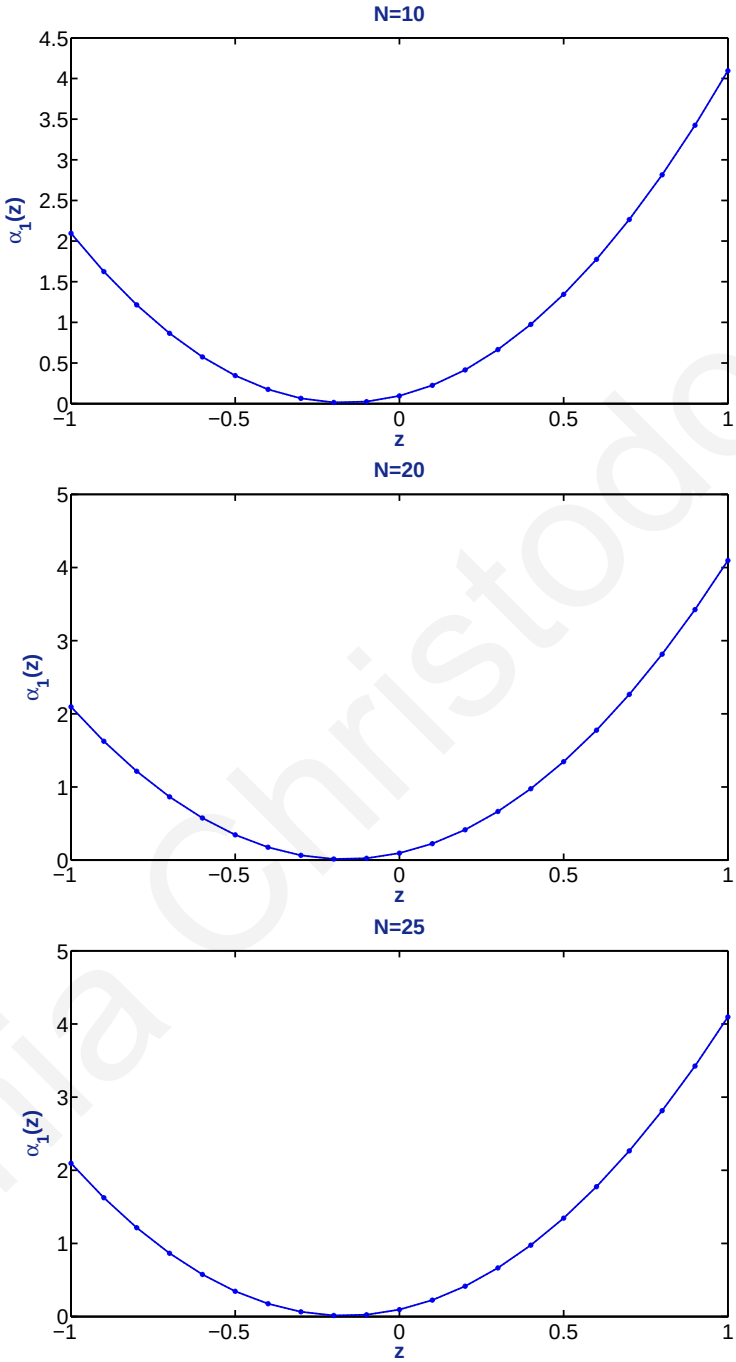

Figure 5.13: Convergence of $\alpha_1(z)$ with N using linear basis functions; $M = 20$.

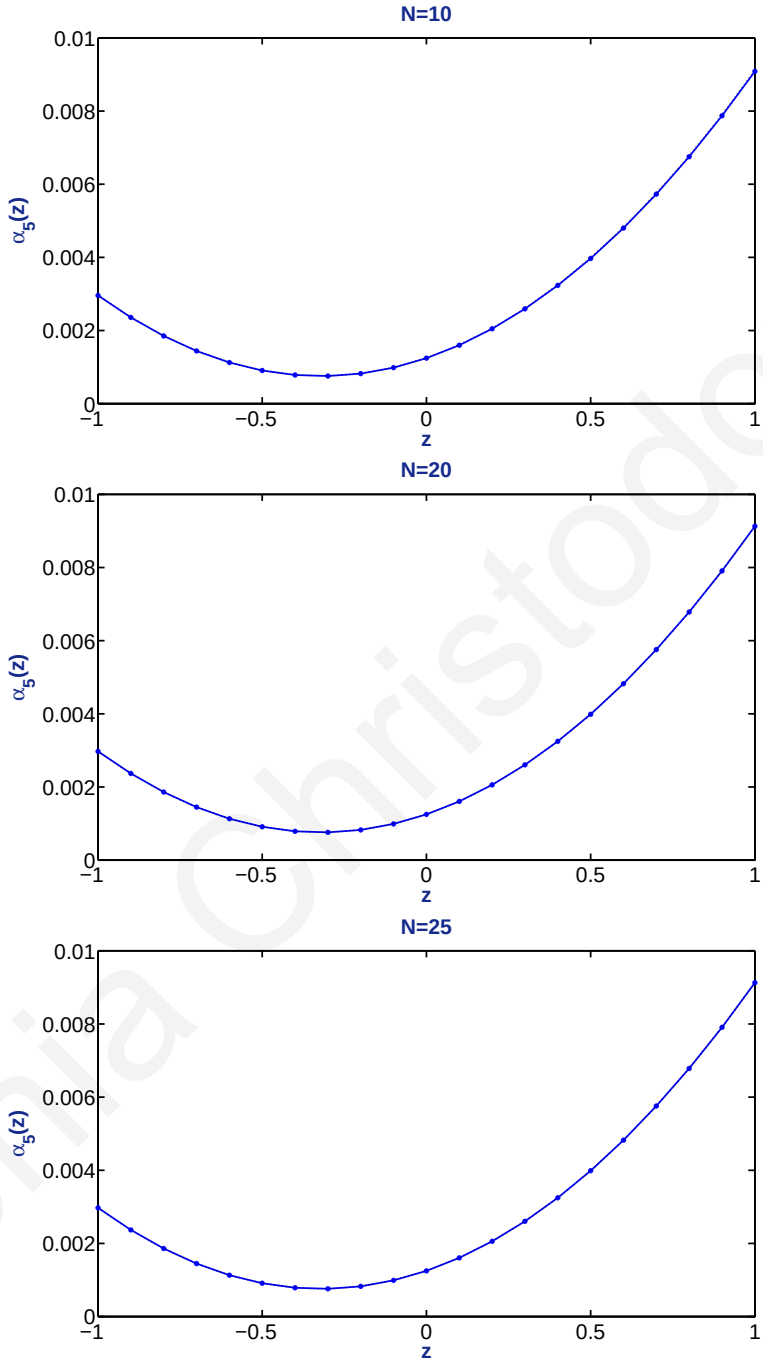

Figure 5.14: Convergence of $\alpha_5(z)$ with N using linear basis functions; $M = 20$.

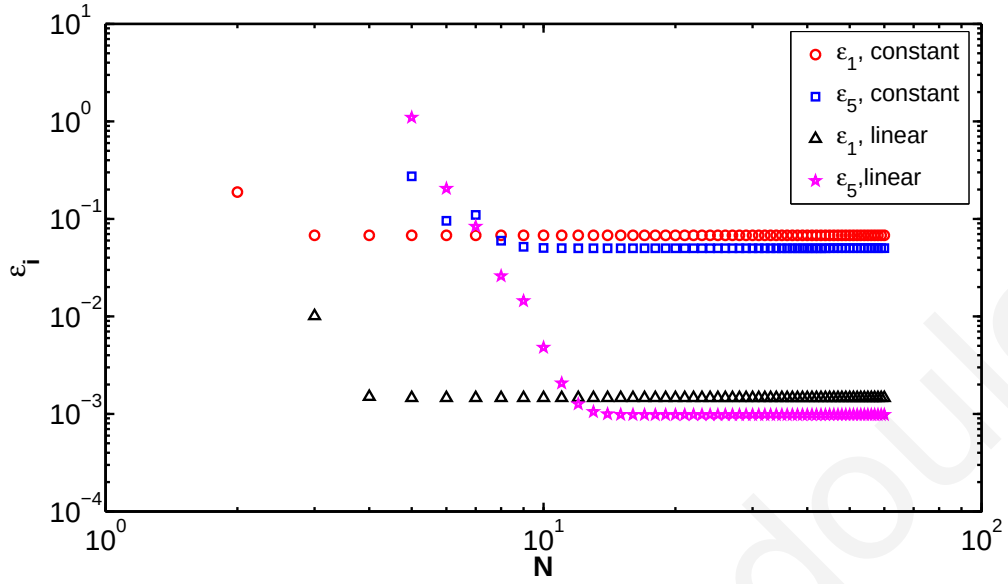

Figure 5.15: The errors ε_1 and ε_5 for constant and linear basis functions, plotted against the number of singular functions N, $M = 20$.

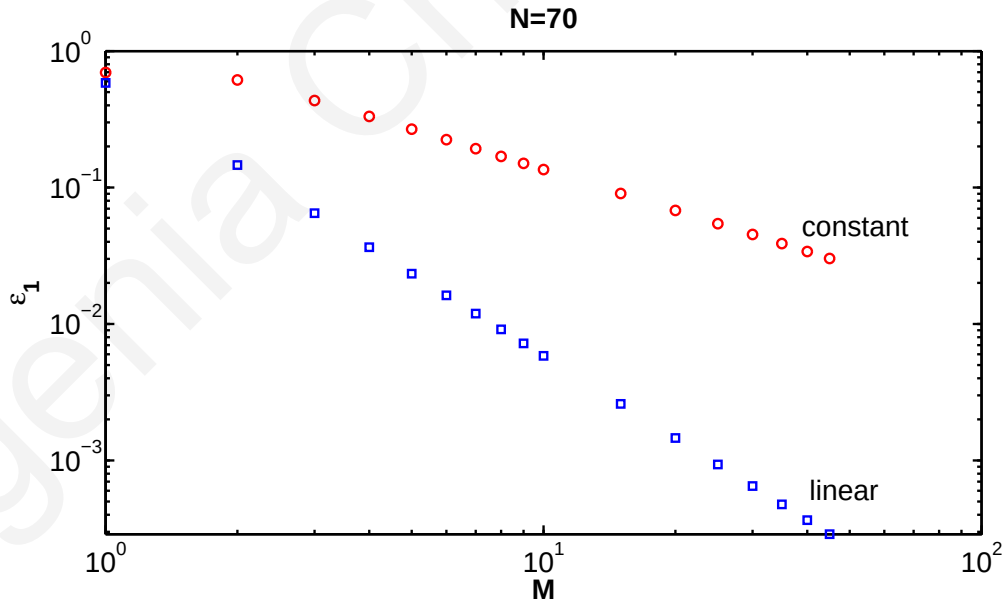

Figure 5.16: The errors ε_1 for constant and linear basis functions, plotted against M; $N = 70$.

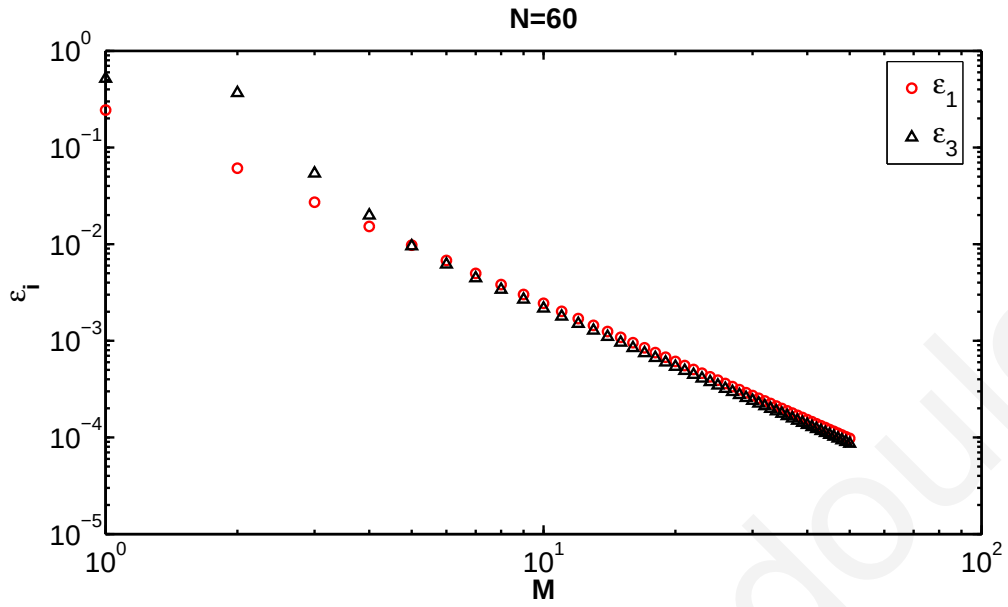

Figure 5.17: ε_1 and ε_3 for linear basis functions, plotted against M; Test Problem 2; $N = 60$.

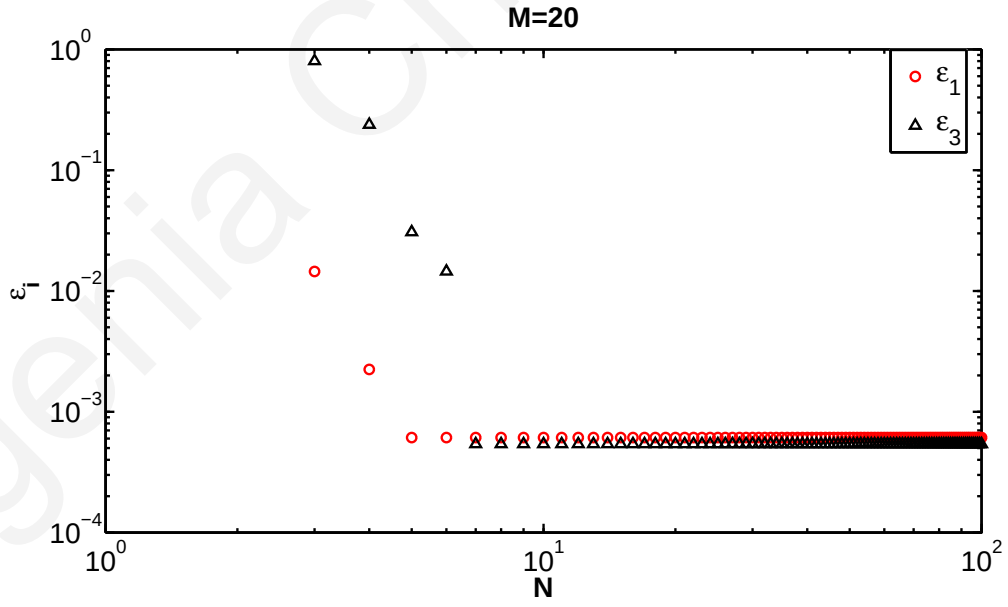

Figure 5.18: ε_1 and ε_3 for linear basis functions, plotted against N; Test Problem 2; $M = 20$.

Chapter 6

Summary and Future Work

In this dissertation we have studied the Singular Function Boundary Integral Method (SFBIM) and investigated some of its extensions to two- and three-dimensions. To begin with, in Chapter 2, we reviewed the method for model Laplacian and biharmonic problems in two-dimensions. We also reviewed the theoretical convergence of the method in the case of a model two-dimensional Laplace problem. In this case, the approximate solution and the approximate values of the singular coefficients converge exponentially with the number of singular functions and the approximate values of the Lagrange multipliers converge algebraically.

Next, in Chapter 3, we have studied systematically the numerical convergence of the method and made comparisons with the theoretical estimates. We considered two model Laplace problems over circular sectors with known exact solutions and we used piecewise constant, linear, quadratic and cubic approximations of the Lagrange multiplier function. The convergence analysis of Xenophontos et al. (2006) does not apply for constant approximations of the Lagrange multiplier function. For this case, that is not covered by the theory, we observed that the convergence was algebraic of order 3 for the singular coefficients, of order 2 for the approximate solution and of order 3/4 for the Lagrange multipliers. The results for the rest of the cases were in accordance with the theory. The approximate solution and the

approximations of the singular coefficients converged exponentially, whilst the convergence of the approximate Lagrange multipliers was algebraic of order equal to the degree of the approximations used.

The theoretical analysis of the SFBIM was then extended to the case of biharmonic problems, in Chapter 4. The convergence of the method was studied for a two-dimensional biharmonic problem, as a model for the well-known *Newtonian stick-slip problem* from fluid mechanics. It was proven that the coefficients in the local asymptotic expansion are approximated at an exponential rate as the number of the employed expansion terms is increased. The theoretical results were then illustrated through a numerical experiment.

Finally, in Chapter 5, the method was extended to three-dimensional Laplace problems with a straight-edge singularity. The asymptotic solution of one such problem was presented and the SFBIM was formulated. The edge flux intensity functions (EFIFs) were approximated locally by low-degree polynomials the coefficients of which were the primary unknowns of the method and were calculated directly. The SFBIM produced accurate results for the coefficients and it was noted that increasing the number of polynomials used produced more accurate results even with just a few singular functions but increasing the number of singular functions while keeping the number of polynomials constant did not lead to any noticeable advantages.

Directions for future work are proposed below:

- The preliminary results suggest that the method can successfully be extended to other three-dimensional elliptic problems. The method should be tested on other problems with edge singularities and with various combinations of boundary conditions in the immediate future. For instance, it would be interesting to solve a Laplacian problem with a boundary straight-edge singularity in the case when more Dirichlet conditions apply and therefore more sets of Lagrange multipliers need to be employed. Also, additional numerical evidence should be obtained, especially to see how the various

parameters in the method affect its accuracy and convergence.

- The next step would be the convergence analysis for a model three-dimensional Laplace problem with a boundary straight-edge singularity. A preliminary analysis to the problem of Chapter 5 is provided in Appendix E.

- Another direction is the extension of the method to three-dimensional problems with conical vertex singularities and the convergence analysis. Such problems have been recently considered by Zaltzman and Yosibash (2009), who derived explicit analytical expressions for the eigen-pairs.

- The method may also be extended for the solution of general corner flows in the Stokes limit. Such flows are governed by the biharmonic equation in terms of the streamfunction and are of interest in fluid dynamics. Such flow problems in a stationary wedge of angle 2α have been recently considered by Hills (2001 b), who used a collocation technique utilizing a basis of eddy functions. It is well known that there exists a critical half-angle (α_{crit}) such that for $\alpha < \alpha_{crit}$ the problem possess complex local solutions (Moffat, 1964). Therefore, the study of this problem for $\alpha < \alpha_{crit}$ will be the extension of the SFBIM to the complex direction. A preliminary formulation for this problem can be found in Appendix F.

Appendix A

In this appendix, the elements of the matrix K and the vector F defined in (3.17) and (3.18) are provided for constant, linear, quadratic and cubic approximations of the Lagrange multiplier function λ defined in (4.35). We note that N is the number of elements:

$$N = \begin{cases} N_\lambda, & p = 0 \\ \frac{N_\lambda - 1}{p}, & p \geq 1 \end{cases}. \tag{A.1}$$

Constant basis functions

For constant basis functions we have for $i = 1, 2, ..., N_\alpha,\ j = 1, 2, ..., N_\lambda$,

$$K_{ij} = \frac{4R^{\mu_i+1}}{(2i-1)} \sin\frac{(2i-1)(2j-1)\pi}{4N} \sin\frac{(2i-1)\pi}{4N}, \tag{A.2}$$

and for $i = 1, 2, ..., N_\lambda$,

$$F_i = \frac{R\alpha^2\pi^2}{2N^2}\left[2i - 1 - \frac{3i^2 - 3i + 1}{3N}\right]. \tag{A.3}$$

Linear basis functions

For linear basis functions we have, for $i = 1, 2, ..., N_\alpha$,

$$K_{i,1} = \frac{2\alpha R^{\mu_i+1}}{(2i-1)}\left[1 - \frac{2N}{(2i-1)\pi}\sin\frac{(2i-1)\pi}{2N}\right], \tag{A.4}$$

$$K_{i,N_\lambda} = \frac{8\alpha N R^{\mu_i+1}}{\pi(2i-1)^2}\sin\frac{(2i-1)\pi}{4N}\cos\frac{(2i-1)(2N-1)\pi}{4N}, \tag{A.5}$$

and for $i = 1, 2, ..., N_\alpha,\ j = 2, ..., N_\lambda - 1$,

$$K_{ij} = \frac{16\alpha N R^{\mu_i+1}}{\pi(2i-1)^2} \sin^2 \frac{(2i-1)\pi}{4N} \sin \frac{(2i-1)(j-1)\pi}{2N}. \tag{A.6}$$

Similarly,

$$F_1 = \frac{R\alpha^2\pi^2}{6N^2}\left(1 - \frac{1}{4N}\right), \tag{A.7}$$

$$F_{N_\lambda} = \frac{R\alpha^2\pi^2}{24N^3}\left(6N^2 - 1\right), \tag{A.8}$$

and for $j = 2, ..., N_\lambda - 1$,

$$F_i = -\frac{R\left(12N(1-i) + 6i^2 - 12i + 7\right)}{12N^3}. \tag{A.9}$$

Quadratic basis functions

For quadratic basis functions we have for $i = 1, 2, ..., N_\alpha$,

$$K_{i,1} = \frac{R^{\mu_i+1}}{2h^2{\mu_i}^3}\left\{2\cos(2h\mu_i) + h\mu_i \sin(2h\mu_i) - 2 + 2h^2{\mu_i}^2\right\}, \tag{A.10}$$

$$K_{i,2N+1} = -\frac{R^{\mu_i+1}}{2h^2\mu_i^3}\left[-3h\mu_i \sin(2hN\mu_i) + (2h^2\mu_i^2 - 2)\cos(2hN\mu_i) + \right.$$
$$\left. + 2\cos(2h(N-1)\mu_i) - h\mu_i \sin(2h(N-1)\mu_i)\right], \tag{A.11}$$

$$K_{i,2k} = -\frac{2R^{\mu_i+1}}{h^2\mu_i^3}\left[\cos(2hk\mu_i) + h\mu_i \sin(2hk\mu_i) - \cos(2h(k-1)\mu_i) + \right.$$
$$\left. + h\mu_i \sin(2h(k-1)\mu_i)\right],\ k = 1, ..., N, \tag{A.12}$$

$$K_{i,2k+1} = -\frac{R^{\mu_i+1}}{2h^2\mu_i^3}\left[-6h\mu_i \sin(2hk\mu_i) - 2\cos(2h(k+1)\mu_i) + \right.$$
$$\left. + 2\cos(2h(k-1)\mu_i) - h\mu_i \sin(2h(k+1)\mu_i) - h\mu_i\right],\ k = 1, ..., N-1, \tag{A.13}$$

Similarly,

$$F_1 = \frac{R\alpha^2\pi^2}{120N^3}, \tag{A.14}$$

$$F_{2k} = \frac{R\alpha^2\pi^2}{30N^3}\left[10k(k-1) + 10N(1-2k) + 3\right],\ k = 2, 3, ..., N, \tag{A.15}$$

$$F_{2k+1} = \frac{R\alpha^2\pi^2}{60N^3}\left[10k^2 - 20kN - 1\right],\ k = 1, 2, ..., N-1, \tag{A.16}$$

$$F_{2N+1} = \frac{R\alpha^2\pi^2}{120N^3}\left[10N^2+1\right]. \tag{A.17}$$

Cubic basis functions

For cubic basis functions we have for $i = 1, 2, ..., N_\alpha$,

$$K_{i,1} = -\frac{R^{\mu_i+1}}{3h^3\mu_i^4}\left[(\mu_i^2h^2-3)\sin(3h\mu_i) + 3\mu_i h\cos(3h\mu_i) + 6h\mu_i - 3h^3\mu_i^3\right], \tag{A.18}$$

$$K_{i,3k+2} = -\frac{R^{\mu_i+1}}{2h^3\mu_i^4}\left[-8h\mu_i\cos(3h(k+1)\mu_i) + (6-3h^2\mu_i^2)\sin(3h(k+1)\mu_i) - \right.$$
$$\left. -10h\mu_i\cos(3hk\mu_i) + (6h^2\mu_i^2-6)\sin(3hk\mu_i)\right],\ \ k = 0, 1, ..., N-1, \tag{A.19}$$

$$K_{i,3k+3} = \frac{R^{\mu_i+1}}{2h^3\mu_i^4}\left[-10h\mu_i\cos(3h(k+1)\mu_i) + (6-6h^2\mu_i^2)\sin(3h(k+1)\mu_i) - \right.$$
$$\left. -8h\mu_i\cos(3hk\mu_i) + (3h^2\mu_i^2-6)\sin(3hk\mu_i)\right],\ \ k = 0, 1, ..., N-1, \tag{A.20}$$

$$K_{i,3k+4} = \frac{R^{\mu_i+1}}{3h^3\mu_i^4}\left[(11h^2\mu_i^2-6)\sin(3h(k+1)\mu_i) + \right.$$
$$+(3-h^2\mu_i^2)\sin(3hk\mu_i) - 3h\mu_i\cos(3hk\mu_i) - 3h\mu_i\cos(3h(k+2)\mu_i) +$$
$$\left. +(3-h^2\mu_i^2)\sin(3h(k+2)\mu_i)\right],\ \ k = 0, 1, ..., N-2, \tag{A.21}$$

$$K_{i,3N+1} = \frac{R^{\mu_i+1}}{6h^3\mu_i^4}\left[(12h\mu_i - 6h^3\mu_i^3)\cos(3hN\mu_i) + (11h^2\mu_i^2-6)\sin(3hN\mu_i) + \right.$$
$$\left. +6h\mu_i\cos(3h(N-1)\mu_i) + (6-2h^2\mu_i^2)\sin(3h(N-1)\mu_i)\right]. \tag{A.22}$$

Similarly,

$$F_1 = \frac{R\alpha^2\pi^2}{240N^3}(4N-1), \tag{A.23}$$

$$F_{3k+2} = \frac{3R\alpha^2\pi^2}{80N^3}(10kN - 5k^2 + 2N - 2k),\ k = 0, 1, ..., N-1, \tag{A.24}$$

$$F_{3k+3} = \frac{3R\alpha^2\pi^2}{80N^3}(8N - 8k - 3 + 10kN - 5k^2),\ k = 0, 1, ..., N-1, \tag{A.25}$$

$$F_{3k+4} = \frac{R\alpha^2\pi^2}{120N^3}(30N - 30k + 30kN - 15k^2 - 16),\ k = 0, 1, ..., N-2, \tag{A.26}$$

$$F_{3N+1} = \frac{R\alpha^2\pi^2}{240N^3}(15N^2-1). \tag{A.27}$$

Appendix B

In this appendix we show that the functions $\widehat{W}_j^{\ell}$ given by (5.9), satisfy the three-dimensional Laplace equation and the boundary conditions on S_1 and S_2, described by (5.1)–(5.2) in Chapter 5. In particular, we set

$$S_N(r,\theta,z) = r^{\mu_n} f_n(\theta) \left[\alpha_n(z) + \sum_{i=1}^{N} \frac{\partial^{2i}}{\partial z^{2i}} (\alpha_n(z)) \frac{r^{2i} (-1/4)^i}{\prod_{n=1}^{i} j (\mu_n + j)} \right], \tag{B.1}$$

and show that the residual of $\nabla^2 S_N(r,\theta,z)$ tends to 0, as N tends to ∞. We have

$$\nabla^2 S_N(r,\theta,z) = \frac{\partial^2 S_N}{\partial r^2} + \frac{1}{r}\frac{\partial S_N}{\partial r} + \frac{1}{r^2}\frac{\partial^2 S_N}{\partial \theta^2} =$$

$$= \mu_n(\mu_n-1) r^{\mu_n-2} f_n(\theta)\alpha_n(z) + \sum_{i=1}^{N} (\mu_n+2i)(\mu_n+2i-1) r^{\mu_n+2i-2} f_n(\theta) \frac{\partial^{2i}}{\partial z^{2i}} (\alpha_n(z)) \frac{(-1/4)^i}{\prod_{j=1}^{i} j (\mu_n + j)}$$

$$+\mu_n r^{\mu_n-2} f_n(\theta)\alpha_n(z) + \sum_{i=1}^{N} (\mu_n + 2i) r^{\mu_n+2i-2} f_n(\theta) \frac{\partial^{2i}}{\partial z^{2i}} (\alpha_n(z)) \frac{(-1/4)^i}{\prod_{j=1}^{i} j (\mu_n + j)}$$

$$+r^{\mu_n-2} f_n(\theta)\alpha_n(z) + \sum_{i=1}^{N} r^{\mu_n+2i-2} f_n''(\theta) \frac{\partial^{2i}}{\partial z^{2i}} (\alpha_n(z)) \frac{(-1/4)^i}{\prod_{j=1}^{i} j (\mu_n + j)}$$

$$+r^{\mu_n} f_n(\theta)\alpha_n''(z) + \sum_{i=2}^{N+1} r^{\mu_n+2i-2} f_n(\theta) \frac{\partial^{2i}}{\partial z^{2i}} (\alpha_n(z)) \frac{(-1/4)^{i-1}}{\prod_{j=1}^{i-1} j (\mu_n + j)}. \tag{B.2}$$

There holds $f_n''(\theta) = -\mu_n^2 f_n(\theta)$, hence the coefficient of $r^{\mu_n-2} f_n(\theta)\alpha_n(z)$ in (B.2) is

$$\mu_n(\mu_n - 1) + \mu_n - \mu_n^2 = 0. \tag{B.3}$$

Similarly, the coefficient of $r^{\mu_n} f_n(\theta)\alpha_n''(z)$ in (B.2) is

$$\left[(\mu_n+2)(\mu_n+1)+(\mu_n+2)-\mu_n^2\right]\frac{(-1/4)}{(\mu_n+1)}+1=0,$$

and finally, the coefficient of $r^{\mu_n+2i-2} f_n(\theta)\frac{\partial^{2i}}{\partial z^{2i}}(\alpha_n(z))$ for $i=2,3,\ldots,N$ in (B.2) is

$$\begin{aligned}
&\left[(\mu_n+2i)(\mu_n+2i-1)+(\mu_n+2i)-\mu_n^2\right]\frac{(-1/4)^i}{\prod_{j=1}^{i} j\,(\mu_n+j)}+\frac{(-1/4)^{i-1}}{\prod_{j=1}^{i-1} j\,(\mu_n+j)}\\
&=\left[(\mu_n+2i)(\mu_n+2i-1)+(\mu_n+2i)-\mu_n^2-4i(\mu_n+i)\right]\frac{(-1/4)^i}{\prod_{j=1}^{i} j\,(\mu_n+j)}\\
&=\left[(\mu_n+2i)^2-\mu_n^2-4i(\mu_n+i)\right]\frac{(-1/4)^i}{\prod_{j=1}^{i} j\,(\mu_n+j)}=0.
\end{aligned}$$

Therefore, the residual is

$$r^{\mu_n+2N} f_n(\theta)\frac{\partial^{2N+2}}{\partial z^{2N+2}}(\alpha_n(z))\frac{(-1/4)^N}{\prod_{j=1}^{N} j\,(\mu_n+j)}, \tag{B.4}$$

and we have

$$\begin{aligned}
&\lim_{N\to\infty}\left|r^{\mu_n+2N} f_n(\theta)\frac{\partial^{2N+2}}{\partial z^{2N+2}}(\alpha_n(z))\frac{(-1/4)^N}{\prod_{j=1}^{N} j\,(\mu_n+j)}\right|\leq\\
&\leq\ |r^{\mu_n} f_n(\theta)|\lim_{N\to\infty}\left|r^{2N}\frac{\partial^{2N+2}}{\partial z^{2N+2}}(\alpha_n(z))\frac{1}{4^N N^2}\right|\leq C(n)\lim_{N\to\infty}\left|r^{2N}\frac{1}{4^N N^2}\right|=0,
\end{aligned} \tag{B.5}$$

since $\alpha_n\in C^\infty$ and with $C(n)$ some bounded function of n. This establishes that $\widehat{W}_n:=\lim_{n\to\infty} S_n$ satisfies Laplaces equation in three-dimensions. To show that the boundary conditions are also satisfied, we note that $f_n(\theta)$ (as an eigenfunction of the 2D problem) satisfies

$$f_n(0)=f_n'(\alpha\pi)=0. \tag{B.6}$$

Therefore,

$$\widehat{W}_n|_{S_1}=\frac{\partial\widehat{W}_n}{\partial\theta}|_{S_2}=0. \tag{B.7}$$

Appendix C

Consider solving the BVP

$$\begin{cases} L(u) = 0 \text{ in } \Omega \subset \mathbb{R}^3 \\ \\ u = g \text{ on } \partial\Omega \end{cases} \tag{C.1}$$

where g is a given function and the differential operator L is given by

$$L = \sum_{i=1}^{3} \sum_{j=1}^{3} \kappa_{ij} \partial_i \partial_j \tag{C.2}$$

with $\kappa_{ij} = \kappa_{ji} \in \mathbb{R}$ and $\partial_\ell = \frac{\partial}{\partial x^\ell}$, $\ell = 1, 2, 3$. For example, if

$$\begin{aligned} \kappa_{11} = \kappa_{22} = \kappa_{33} = 1 \\ \kappa_{12} = \kappa_{13} = \kappa_{23} = 0 \end{aligned} \tag{C.3}$$

then

$$L = \nabla^2 \tag{C.4}$$

We split the operator as

$$L = M_0(\partial_1, \partial_2) + M_1(\partial_1, \partial_2)\partial_3 + M_2\partial_3^2 \tag{C.5}$$

where

M_0: second order differential operator in x_1, x_2

M_1: first order differential operator in x_1, x_2

M_2: constant.

Then the solution u has the expansion

$$u \sum_{j\geq 0} \partial_3^j A(x_3)\Phi_j(x_1,x_2) \tag{C.6}$$

where $A(x_3)$ is the EFIF. The functions Φ_j satisfy

$$\begin{aligned} M_0\Phi_0 &= 0 \\ M_0\Phi_1 &= -M_1\Phi_0 \\ M_0\Phi_j &= -M_1\Phi_{j-1} - M_2\Phi_{j-2} \end{aligned} \tag{C.7}$$

We are interested in operators for which

$$\begin{aligned} M_0 &= \kappa_{11}\partial_1^2 + 2\kappa_{12}\partial_1\partial_2 + \kappa_{22}\partial_2\partial_2 \\ M_1 &= 0 \\ M_2 &= 1 \end{aligned} \tag{C.8}$$

Suppose the domain Ω has an angle α and set

$$\omega = \arctan\left(\frac{\sqrt{\kappa_{11}\kappa_{22}-\kappa_{12}^2}\sin\alpha}{\kappa_{22}\cos\alpha - \kappa_{12}\sin\alpha}\right) \tag{C.9}$$

$$\mu_i = \frac{\pi}{\omega}i,\ i = 1,2,\dots \tag{C.10}$$

Solving $M_0\Phi_0 = 0$ we find

$$\Phi_0^{(i)}(r,\theta) = r^{\mu_i}\phi_0^{(i)}(\theta) \tag{C.11}$$

where

$$\phi_0^{(i)}(\theta) = \left(\frac{\kappa_{22}\cos^2\theta - \kappa_{12}\sin(2\theta)}{\kappa_{11}\kappa_{22}-\kappa_{12}^2}\right)^{\frac{\mu_i}{2}} \cdot \sin\left(\mu_i \arctan\left(\frac{\sqrt{\kappa_{11}\kappa_{22}-\kappa_{12}^2}\sin\theta}{\kappa_{22}\cos\theta - \kappa_{12}\sin\theta}\right)\right) \tag{C.12}$$

Once Φ_0 is known we proceed with finding Φ_1 by solving

$$M_0\Phi_1 = 0 \tag{C.13}$$

and once this is achieved we continue with Φ_2 which satisfies

$$M_0\Phi_2^{(i)} = -M_2\Phi_0^{(i)} \tag{C.14}$$

etc.

Appendix D

In this appendix we provide the elements of the matrices K and L and of the vectors B and C defined in (5.16), (5.17) and (5.18), for constant and linear approximations of the Lagrange multiplier function λ and the EFIFs $\alpha_j(z)$ defined by (5.15) and (5.10) respectively.

Locally constant approximations of $\alpha_j(z)$ ***and*** λ

Let h be the mesh width in z and $z_k = -1 + (k-1)h$ for $k = 1, 2, \ldots, M+1$.

We use:

$$\phi_k(z) = \begin{cases} 1 \text{ if } z_k < z \leq z_{k+1} \\ \\ 0 \text{ otherwise,} \end{cases} \tag{D.1}$$

for $k = 1, 2, \ldots, M$

The Lagrange multiplier function λ is also approximated by constant basis functions. The 2D domain $[0, \alpha\pi] \times [-1, 1]$ is subdivided into $N_\lambda = N_\theta \times M$ elements. Let h_θ be the mesh width in θ and $\theta_\ell = (\ell - 1)h_\theta$ for $\ell = 1, 2, \ldots, N_\theta + 1$. Therefore the basis functions are given by:

$$\Psi_{(k-1)N_\theta+\ell}(\theta, z) = \begin{cases} 1 \text{ if } \quad z_k < z \leq z_{k+1} \quad \text{and } \theta_\ell < \theta \leq \theta_{\ell+1} \\ \\ 0 \text{ otherwise} \end{cases} \tag{D.2}$$

where, $(k-1)N_\theta + \ell$ is the element number and is calculated with $k = 1, 2, \ldots, M$ and $\ell = 1, 2, \ldots, N_\theta$. The sub-matrices K, L and the vectors B, C in (5.18) are given by:

$$K_{i,j} = \begin{cases} -\mu_i \frac{\alpha\pi}{2} h \text{ if } i = j \\ \\ 0 \text{ otherwise,} \end{cases} \tag{D.3}$$

where $i, j = 1, 2, \ldots, NM$.

$$L_{(m-1)M+k,(k-1)N_\theta+\ell} = -\frac{h}{\mu_m}\left[\cos\left(\mu_m\theta_{\ell+1}\right) - \cos\left(\mu_m\theta_\ell\right)\right] \tag{D.4}$$

for $m = 1, 2, \ldots, N$, $k = 1, 2, \ldots, M$ and $\ell = 1, 2, \ldots, N_\theta$ ($L_{i,j} = 0$ otherwise).

$$C_{(k-1)N_\theta+\ell} = -\sum_{i=1}^{J}\left[\left(\alpha_{i1} - \frac{\alpha_{i1}}{2(\mu_i+1)}\right)z + \frac{\alpha_{i2}z^2}{2} + \frac{\alpha_{i3}z^3}{3}\right]_{z_k}^{z_{k+1}}\left[\frac{\cos\mu_i\theta}{\mu_i}\right]_{\theta_\ell}^{\theta_{\ell+1}} \tag{D.5}$$

for $k = 1, 2, \ldots, M$ and $\ell = 1, 2, \ldots, N_\theta$, $J = 3$ for Test Problem 2 and $J = 100$ for Test Problem 1 as shown in (5.25).

$$B_{(j-1)M+k}(\theta, z) = \begin{cases} \frac{(\alpha_{j2}-2\alpha_{j3})\alpha\pi}{4(\mu_j+1)}, j \le \min\{N, J\}, k = 1 \\ -\frac{(\alpha_{j2}+2\alpha_{j3})\alpha\pi}{4(\mu_j+1)}, j \le \min\{N, J\}, k = M \\ 0 \text{ otherwise,} \end{cases} \tag{D.6}$$

where, $j = 1, 2, \ldots, N$.

Locally linear approximations of $\alpha_j(z)$ ***and*** λ

Let h be the mesh width in z and $z_k = -1 + (k-1)h$ for $k = 1, 2, \ldots, M+1$. This time:

$$\phi_k(z) = \begin{cases} \frac{1}{h}\left(z - z_{k-1}\right) \text{ if } z_{k-1} < z \le z_k \\ -\frac{1}{h}\left(z - z_k\right) \text{ if } z_k < z \le z_{k+1} \\ 0 \text{ otherwise,} \end{cases} \tag{D.7}$$

for $k = 2, 3, \ldots, M$,

$$\phi_1(z) = \begin{cases} -\frac{1}{h}\left(z - z_2\right) \text{ if } z_1 < z \le z_2 \\ 0 \text{ otherwise,} \end{cases} \tag{D.8}$$

and

$$\phi_{M+1}(z) = \begin{cases} \frac{1}{h}\left(z - z_M\right) \text{ if } z_M < z \le z_{M+1} \\ 0 \text{ otherwise,} \end{cases} \tag{D.9}$$

The Lagrange multiplier function λ is now approximated by bilinear basis functions. The 2D domain $[0, \alpha\pi] \times [-1, 1]$ is again subdivided into $N_\lambda = N_\theta \times M$ elements. Let h_θ be the mesh

width in θ and $\theta_\ell = (\ell-1)h_\theta$ for $\ell = 1, 2, \ldots, N_\theta + 1$. The basis functions are given by:

$$\Psi_{(k-1)(N_\theta+1)+\ell}(\theta, z) = \begin{cases} \frac{(z-z_{k-1})(\theta-\theta_\ell)}{hh_\theta} \text{ if } z_{k-1} < z \leq z_k \text{ and } \theta_{\ell-1} < \theta \leq \theta_\ell \\ -\frac{(z-z_{k-1})(\theta-\theta_{\ell+1})}{hh_\theta} \text{ if } z_{k-1} < z \leq z_k \text{ and } \theta_\ell < \theta \leq \theta_{\ell+1} \\ -\frac{(z-z_{k+1})(\theta-\theta_{\ell-1})}{hh_\theta} \text{ if } z_k < z \leq z_{k+1} \text{ and } \theta_{\ell-1} < \theta \leq \theta_\ell \\ \frac{(z-z_{k+1})(\theta-\theta_{\ell+1})}{hh_\theta} \text{ if } z_k < z \leq z_{k+1} \text{ and } \theta_\ell < \theta \leq \theta_{\ell+1} \\ 0 \text{ otherwise} \end{cases} \tag{D.10}$$

for $k = 2, 3, \ldots, M$ and $\ell = 2, 3, \ldots, N_\theta$.

$$\Psi_{(k-1)(N_\theta+1)+1}(\theta, z) = \begin{cases} -\frac{(z-z_{k-1})(\theta-\theta_1)}{hh_\theta} \text{ if } z_{k-1} < z \leq z_k \text{ and } \theta_1 < \theta \leq \theta_2 \\ \frac{(z-z_{k+1})(\theta-\theta_1)}{hh_\theta} \text{ if } z_k < z \leq z_{k+1} \text{ and } \theta_1 < \theta \leq \theta_2 \\ 0 \text{ otherwise} \end{cases} \tag{D.11}$$

for $k = 2, 3, \ldots, M$.

$$\Psi_{k(N_\theta+1)}(\theta, z) = \begin{cases} \frac{(z-z_{k-1})(\theta-\theta_{N_\theta})}{hh_\theta} \text{ if } z_{k-1} < z \leq z_k \text{ and } \theta_{N_\theta} < \theta \leq \theta_{N_\theta+1} \\ -\frac{(z-z_{k+1})(\theta-\theta_{N_\theta})}{hh_\theta} \text{ if } z_k < z \leq z_{k+1} \text{ and } \theta_{N_\theta} < \theta \leq \theta_{N_\theta+1} \\ 0 \text{ otherwise} \end{cases} \tag{D.12}$$

for $k = 2, 3, \ldots, M$.

$$\Psi_\ell(\theta, z) = \begin{cases} -\frac{(z-z_2)(\theta-\theta_{\ell-1})}{hh_\theta} \text{ if } z_1 < z \leq z_2 \text{ and } \theta_{\ell-1} < \theta \leq \theta_\ell \\ \frac{(z-z_2)(\theta-\theta_{\ell+1})}{hh_\theta} \text{ if } z_1 < z \leq z_2 \text{ and } \theta_\ell < \theta \leq \theta_{\ell+1} \\ 0 \text{ otherwise} \end{cases} \tag{D.13}$$

for $\ell = 2, 3, \ldots, N_\theta$.

$$\Psi_{M(N_\theta+1)+\ell}(\theta, z) = \begin{cases} \frac{(z-z_M)(\theta-\theta_{\ell-1})}{hh_\theta} \text{ if } z_M < z \leq z_{M+1} \text{ and } \theta_{\ell-1} < \theta \leq \theta_\ell \\ -\frac{(z-z_M)(\theta-\theta_{\ell+1})}{hh_\theta} \text{ if } z_M < z \leq z_{M+1} \text{ and } \theta_\ell < \theta \leq \theta_{\ell+1} \\ 0 \text{ otherwise} \end{cases} \tag{D.14}$$

for $\ell = 2, 3, \ldots, N_\theta$.

$$\Psi_1(\theta,z)=\begin{cases}\frac{(z-z_2)(\theta-\theta_2)}{hh_\theta} \text{ if } \quad z_1<z\le z_2 \text{ and } \theta_1<\theta\le\theta_2\\ \\ 0 \text{ otherwise}\end{cases} \tag{D.15}$$

$$\Psi_{N_\theta+1}(\theta,z)=\begin{cases}-\frac{(z-z_2)(\theta-\theta_{N_\theta})}{hh_\theta} \text{ if } \quad z_1<z\le z_2 \text{ and } \theta_{N_\theta}<\theta\le\theta_{N_\theta+1}\\ \\ 0 \text{ otherwise}\end{cases} \tag{D.16}$$

$$\Psi_{M(N_\theta+1)+1}(\theta,z)=\begin{cases}-\frac{(z-z_M)(\theta-\theta_2)}{hh_\theta} \text{ if } z_M<z\le z_{M+1} \text{ and } \theta_1<\theta\le\theta_2\\ \\ 0 \text{ otherwise}\end{cases} \tag{D.17}$$

$$\Psi_{(M+1)(N_\theta+1)}(\theta,z)=\begin{cases}\frac{(z-z_M)(\theta-\theta_{N_\theta})}{hh_\theta} \text{ if } z_M<z\le z_{M+1} \text{ and } \theta_{N_\theta}<\theta\le\theta_{N_\theta+1}\\ \\ 0 \text{ otherwise}\end{cases} \tag{D.18}$$

The sub-matrices K, L and the vectors B, C in (5.18) are given by:

$$K_{(j-1)(M+1)+1,(j-1)(M+1)+1}=-\frac{\alpha\pi}{2}\left(\frac{1}{2h(\mu_j+1)}+\frac{\mu_j h}{3}\right),\quad j=1,2,\ldots,N. \tag{D.19}$$

$$K_{j(M+1),j(M+1)}=\frac{\alpha\pi}{2}\left(\frac{1}{2h(\mu_j+1)}-\frac{\mu_j h}{3}\right),\quad j=1,2,\ldots,N. \tag{D.20}$$

$$K_{(j-1)(M+1)+2,(j-1)(M+1)+1}=\frac{\alpha\pi}{2}\left(\frac{1}{2h(\mu_j+1)}-\frac{\mu_j h}{6}\right),\quad j=1,2,\ldots,N. \tag{D.21}$$

$$K_{(j-1)(M+1)+M,j(M+1)}=\frac{\alpha\pi}{2}\left(\frac{1}{2h(\mu_j+1)}-\frac{\mu_j h}{6}\right),\quad j=1,2,\ldots,N. \tag{D.22}$$

$$K_{(j-1)(M+1)+k,(j-1)(M+1)+k-1}=-\mu_j\frac{\alpha\pi}{2}\frac{h}{6},\quad j=1,2,\ldots,N,\quad k=3,4,\ldots,M+1 \tag{D.23}$$

$$K_{(j-1)(M+1)+k,(j-1)(M+1)+k}=-\mu_j\frac{\alpha\pi}{2}\frac{2h}{3},\quad j=1,2,\ldots,N,\quad k=2,4,\ldots,M \tag{D.24}$$

$$K_{(j-1)(M+1)+k,(j-1)(M+1)+k+1}=-\mu_j\frac{\alpha\pi}{2}\frac{h}{6},\quad j=1,2,\ldots,N,\quad k=2,4,\ldots,M-1. \tag{D.25}$$

Any entries of K not described by (D.19)-(D.25), are zero.

$$B_{(j-1)M+k}(\theta,z)=\begin{cases}\frac{(\alpha_{j2}-2\alpha_{j3})\alpha\pi}{4(\mu_j+1)}, j\le\min\{N,J\}, k=1\\ \\ -\frac{(\alpha_{j2}+2\alpha_{j3})\alpha\pi}{4(\mu_j+1)}, j\le\min\{N,J\}, k=M+1\\ \\ 0 \text{ otherwise,}\end{cases} \tag{D.26}$$

where, $j=1,2,\ldots,N$.

Let $\beta_i = \alpha_{i1} - \frac{\alpha_{i3}}{2(\mu_i+1)}$ for $i = 1, 2, \ldots, J$

$$C_{(k-1)(N_\theta+1)+\ell} = +\frac{1}{hh_\theta}\sum_{i=1}^{J}\left\{\left[-\beta_i z_{k-1}z + (\beta_i - \alpha_{i2}z_{k-1})\frac{z^2}{2} + (\alpha_{i2} - \alpha_{i3}z_{k-1})\frac{z^3}{3} + \alpha_{i3}\frac{z^4}{4}\right]_{z_{k-1}}^{z_k}\cdot\right.$$
$$\left.\cdot\left[\frac{(\theta_{\ell-1}-\theta)\cos\mu_i\theta}{\mu_i} + \frac{\sin\mu_i\theta}{\mu_i^2}\right]_{\theta_{\ell-1}}^{\theta_\ell}\right\} -$$
$$-\frac{1}{hh_\theta}\sum_{i=1}^{J}\left\{\left[-\beta_i z_{k-1}z + (\beta_i - \alpha_{i2}z_{k-1})\frac{z^2}{2} + (\alpha_{i2} - \alpha_{i3}z_{k-1})\frac{z^3}{3} + \alpha_{i3}\frac{z^4}{4}\right]_{z_{k-1}}^{z_k}\cdot\right.$$
$$\left.\cdot\left[\frac{(\theta_{\ell+1}-\theta)\cos\mu_i\theta}{\mu_i} + \frac{\sin\mu_i\theta}{\mu_i^2}\right]_{\theta_\ell}^{\theta_{\ell+1}}\right\} -$$
$$-\frac{1}{hh_\theta}\sum_{i=1}^{J}\left\{\left[-\beta_i z_{k+1}z + (\beta_i - \alpha_{i2}z_{k+1})\frac{z^2}{2} + (\alpha_{i2} - \alpha_{i3}z_{k+1})\frac{z^3}{3} + \alpha_{i3}\frac{z^4}{4}\right]_{z_k}^{z_{k+1}}\cdot\right.$$
$$\left.\cdot\left[\frac{(\theta_{\ell-1}-\theta)\cos\mu_i\theta}{\mu_i} + \frac{\sin\mu_i\theta}{\mu_i^2}\right]_{\theta_{\ell-1}}^{\theta_\ell}\right\} +$$
$$+\frac{1}{hh_\theta}\sum_{i=1}^{J}\left\{\left[-\beta_i z_{k+1}z + (\beta_i - \alpha_{i2}z_{k+1})\frac{z^2}{2} + (\alpha_{i2} - \alpha_{i3}z_{k+1})\frac{z^3}{3} + \alpha_{i3}\frac{z^4}{4}\right]_{z_k}^{z_{k+1}}\cdot\right.$$
$$\left.\cdot\left[\frac{(\theta_{\ell+1}-\theta)\cos\mu_i\theta}{\mu_i} + \frac{\sin\mu_i\theta}{\mu_i^2}\right]_{\theta_\ell}^{\theta_{\ell+1}}\right\}, \tag{D.27}$$

for $\ell = 2, 3, \ldots, N_\theta$ and $k = 2, 3, \ldots, M$.

$$C_{(k-1)(N_\theta+1)+1} = -\frac{1}{hh_\theta}\sum_{i=1}^{J}\left\{\left[-\beta_i z_{k-1}z + (\beta_i - \alpha_{i2}z_{k-1})\frac{z^2}{2} + (\alpha_{i2} - \alpha_{i3}z_{k-1})\frac{z^3}{3} + \alpha_{i3}\frac{z^4}{4}\right]_{z_{k-1}}^{z_k}\cdot\right.$$
$$\left.\cdot\left[\frac{(\theta_2-\theta)\cos\mu_i\theta}{\mu_i} + \frac{\sin\mu_i\theta}{\mu_i^2}\right]_{\theta_1}^{\theta_2}\right\} +$$
$$+\frac{1}{hh_\theta}\sum_{i=1}^{J}\left\{\left[-\beta_i z_{k+1}z + (\beta_i - \alpha_{i2}z_{k+1})\frac{z^2}{2} + (\alpha_{i2} - \alpha_{i3}z_{k+1})\frac{z^3}{3} + \alpha_{i3}\frac{z^4}{4}\right]_{z_k}^{z_{k+1}}\cdot\right.$$
$$\left.\cdot\left[\frac{(\theta_2-\theta)\cos\mu_i\theta}{\mu_i} + \frac{\sin\mu_i\theta}{\mu_i^2}\right]_{\theta_1}^{\theta_2}\right\}, \tag{D.28}$$

for $k = 2, 3, \ldots, M$.

$$C_{k(N_\theta+1)} = +\frac{1}{hh_\theta}\sum_{i=1}^{J}\left\{\left[-\beta_i z_{k-1}z + (\beta_i - \alpha_{i2}z_{k-1})\frac{z^2}{2} + (\alpha_{i2} - \alpha_{i3}z_{k-1})\frac{z^3}{3} + \alpha_{i3}\frac{z^4}{4}\right]_{z_{k-1}}^{z_k}\cdot\right.$$

$$\cdot \left[\frac{(\theta_{N_\theta} - \theta)\cos\mu_i\theta}{\mu_i} + \frac{\sin\mu_i\theta}{\mu_i^2} \right]_{\theta_{N_\theta}}^{\theta_{N_\theta+1}} \Bigg\} -$$

$$-\frac{1}{hh_\theta}\sum_{i=1}^{J}\Bigg\{ \left[-\beta_i z_{k+1} z + (\beta_i - \alpha_{i2} z_{k+1})\frac{z^2}{2} + (\alpha_{i2} - \alpha_{i3} z_{k+1})\frac{z^3}{3} + \alpha_{i3}\frac{z^4}{4} \right]_{z_k}^{z_{k+1}} \cdot$$

$$\cdot \left[\frac{(\theta_{N_\theta} - \theta)\cos\mu_i\theta}{\mu_i} + \frac{\sin\mu_i\theta}{\mu_i^2} \right]_{\theta_{N_\theta}}^{\theta_{N_\theta+1}} \Bigg\}, \tag{D.29}$$

for $k = 2, 3, \ldots, M$.

$$C_\ell = -\frac{1}{hh_\theta}\sum_{i=1}^{J}\Bigg\{ \left[-\beta_i z_2 z + (\beta_i - \alpha_{i2} z_2)\frac{z^2}{2} + (\alpha_{i2} - \alpha_{i3} z_2)\frac{z^3}{3} + \alpha_{i3}\frac{z^4}{4} \right]_{z_1}^{z_2} \cdot$$

$$\cdot \left[\frac{(\theta_{\ell-1} - \theta)\cos\mu_i\theta}{\mu_i} + \frac{\sin\mu_i\theta}{\mu_i^2} \right]_{\theta_{\ell-1}}^{\theta_\ell} \Bigg\} +$$

$$+\frac{1}{hh_\theta}\sum_{i=1}^{J}\Bigg\{ \left[-\beta_i z_2 z + (\beta_i - \alpha_{i2} z_2)\frac{z^2}{2} + (\alpha_{i2} - \alpha_{i3} z_2)\frac{z^3}{3} + \alpha_{i3}\frac{z^4}{4} \right]_{z_1}^{z_2} \cdot$$

$$\cdot \left[\frac{(\theta_{\ell+1} - \theta)\cos\mu_i\theta}{\mu_i} + \frac{\sin\mu_i\theta}{\mu_i^2} \right]_{\theta_\ell}^{\theta_{\ell+1}} \Bigg\}, \tag{D.30}$$

for $\ell = 2, 3, \ldots, N_\theta$.

$$C_{M(N_\theta+1)\ell} = +\frac{1}{hh_\theta}\sum_{i=1}^{J}\Bigg\{ \left[-\beta_i z_M z + (\beta_i - \alpha_{i2} z_M)\frac{z^2}{2} + (\alpha_{i2} - \alpha_{i3} z_M)\frac{z^3}{3} + \alpha_{i3}\frac{z^4}{4} \right]_{z_M}^{z_{M+1}} \cdot$$

$$\cdot \left[\frac{(\theta_{\ell-1} - \theta)\cos\mu_i\theta}{\mu_i} + \frac{\sin\mu_i\theta}{\mu_i^2} \right]_{\theta_{\ell-1}}^{\theta_\ell} \Bigg\} -$$

$$-\frac{1}{hh_\theta}\sum_{i=1}^{J}\Bigg\{ \left[-\beta_i z_M z + (\beta_i - \alpha_{i2} z_M)\frac{z^2}{2} + (\alpha_{i2} - \alpha_{i3} z_M)\frac{z^3}{3} + \alpha_{i3}\frac{z^4}{4} \right]_{z_M}^{z_{M+1}} \cdot$$

$$\cdot \left[\frac{(\theta_{\ell+1} - \theta)\cos\mu_i\theta}{\mu_i} + \frac{\sin\mu_i\theta}{\mu_i^2} \right]_{\theta_\ell}^{\theta_{\ell+1}} \Bigg\}, \tag{D.31}$$

for $\ell = 2, 3, \ldots, N_\theta$.

$$C_1 = \frac{1}{hh_\theta}\sum_{i=1}^{J}\Bigg\{ \left[-\beta_i z_2 z + (\beta_i - \alpha_{i2} z_2)\frac{z^2}{2} + (\alpha_{i2} - \alpha_{i3} z_2)\frac{z^3}{3} + \alpha_{i3}\frac{z^4}{4} \right]_{z_1}^{z2} \cdot$$

$$\cdot \left[\frac{(\theta_2 - \theta)\cos\mu_i\theta}{\mu_i} + \frac{\sin\mu_i\theta}{\mu_i^2} \right]_{\theta_1}^{\theta_2} \Bigg\}. \tag{D.32}$$

$$C_{N_\theta+1} = -\frac{1}{hh_\theta}\sum_{i=1}^{J}\left\{\left[-\beta_i z_2 z + (\beta_i - \alpha_{i2}z_2)\frac{z^2}{2} + (\alpha_{i2} - \alpha_{i3}z_2)\frac{z^3}{3} + \alpha_{i3}\frac{z^4}{4}\right]_{z_1}^{z2} \cdot \right.$$
$$\left. \cdot \left[\frac{(\theta_{N_\theta} - \theta)\cos\mu_i\theta}{\mu_i} + \frac{\sin\mu_i\theta}{\mu_i^2}\right]_{\theta_{N_\theta}}^{\theta_{N_\theta+1}}\right\}. \tag{D.33}$$

$$C_{M(N_\theta+1)+1} = -\frac{1}{hh_\theta}\sum_{i=1}^{J}\left\{\left[-\beta_i z_M z + (\beta_i - \alpha_{i2}z_M)\frac{z^2}{2} + (\alpha_{i2} - \alpha_{i3}z_M)\frac{z^3}{3} + \alpha_{i3}\frac{z^4}{4}\right]_{z_1}^{z2} \cdot \right.$$
$$\left. \cdot \left[\frac{(\theta_2 - \theta)\cos\mu_i\theta}{\mu_i} + \frac{\sin\mu_i\theta}{\mu_i^2}\right]_{\theta_1}^{\theta_2}\right\}. \tag{D.34}$$

$$C_{(M+1)(N_\theta+1)} = \frac{1}{hh_\theta}\sum_{i=1}^{J}\left\{\left[-\beta_i z_M z + (\beta_i - \alpha_{i2}z_M)\frac{z^2}{2} + (\alpha_{i2} - \alpha_{i3}z_M)\frac{z^3}{3} + \alpha_{i3}\frac{z^4}{4}\right]_{z_1}^{z2} \cdot \right.$$
$$\left. \cdot \left[\frac{(\theta_{N_\theta} - \theta)\cos\mu_i\theta}{\mu_i} + \frac{\sin\mu_i\theta}{\mu_i^2}\right]_{\theta_{N_\theta}}^{\theta_{N_\theta+1}}\right\}. \tag{D.35}$$

We kept L last because it is the most difficult matrix to describe. In practice, the mesh is scanned element by element and at each element eight integrations are performed.The results are added to the appropriate entries of L that starts as a zero matrix. For instance in the random element $[\theta_\ell, \theta_{\ell+1}] \times [z_k, z_{k+1}]$ we calculate the integrations:

$$I_{1a} = -\frac{1}{\mu_j h^2 h_\theta}\left\{-h_\theta\cos\mu_j\theta_\ell + \left[\frac{\sin\mu_j\theta}{\mu_j}\right]_{\theta_\ell}^{\theta_{\ell+1}}\right\} \cdot \left[\frac{z^3}{3} - z_{k+1}z^2 + z_{k+1}^2 z\right]_{z_k}^{z_{k+1}}, \tag{D.36}$$

$$I_{1b} = \frac{1}{\mu_j h^2 h_\theta}\left\{-h_\theta\cos\mu_j\theta_\ell + \left[\frac{\sin\mu_j\theta}{\mu_j}\right]_{\theta_\ell}^{\theta_{\ell+1}}\right\} \cdot \left[\frac{z^3}{3} - (z_k + z_{k+1})\frac{z^2}{2} + z_{k+1}z_k z\right]_{z_k}^{z_{k+1}}, \tag{D.37}$$

$$I_{2a} = \frac{1}{\mu_j h^2 h_\theta}\left\{-h_\theta\cos\mu_j\theta_{\ell+1} + \left[\frac{\sin\mu_j\theta}{\mu_j}\right]_{\theta_\ell}^{\theta_{\ell+1}}\right\} \cdot \left[\frac{z^3}{3} - z_{k+1}z^2 + z_{k+1}^2 z\right]_{z_k}^{z_{k+1}}, \tag{D.38}$$

$$I_{2b} = -\frac{1}{\mu_j h^2 h_\theta}\left\{-h_\theta\cos\mu_j\theta_{\ell+1} + \left[\frac{\sin\mu_j\theta}{\mu_j}\right]_{\theta_\ell}^{\theta_{\ell+1}}\right\} \cdot \left[\frac{z^3}{3} - (z_k + z_{k+1})\frac{z^2}{2} + z_{k+1}z_k z\right]_{z_k}^{z_{k+1}}, \tag{D.39}$$

$$I_{3a} = \frac{1}{\mu_j h^2 h_\theta} \left\{ -h_\theta \cos \mu_j \theta_\ell + \left[\frac{\sin \mu_j \theta}{\mu_j} \right]_{\theta_\ell}^{\theta_{\ell+1}} \right\} \cdot \left[\frac{z^3}{3} - (z_k + z_{k+1}) \frac{z^2}{2} + z_{k+1} z_k z \right]_{z_k}^{z_{k+1}}, \quad \text{(D.40)}$$

$$I_{3b} = -\frac{1}{\mu_j h^2 h_\theta} \left\{ -h_\theta \cos \mu_j \theta_\ell + \left[\frac{\sin \mu_j \theta}{\mu_j} \right]_{\theta_\ell}^{\theta_{\ell+1}} \right\} \cdot \left[\frac{z^3}{3} - z_k z^2 + z_k^2 z \right]_{z_k}^{z_{k+1}}, \quad \text{(D.41)}$$

$$I_{4a} = -\frac{1}{\mu_j h^2 h_\theta} \left\{ -h_\theta \cos \mu_j \theta_{\ell+1} + \left[\frac{\sin \mu_j \theta}{\mu_j} \right]_{\theta_\ell}^{\theta_{\ell+1}} \right\} \cdot \left[\frac{z^3}{3} - (z_k + z_{k+1}) \frac{z^2}{2} + z_{k+1} z_k z \right]_{z_k}^{z_{k+1}}, \quad \text{(D.42)}$$

and

$$I_{4b} = +\frac{1}{\mu_j h^2 h_\theta} \left\{ -h_\theta \cos \mu_j \theta_{\ell+1} + \left[\frac{\sin \mu_j \theta}{\mu_j} \right]_{\theta_\ell}^{\theta_{\ell+1}} \right\} \cdot \left[\frac{z^3}{3} - z_k z^2 + z_k^2 z \right]_{z_k}^{z_{k+1}}. \quad \text{(D.43)}$$

Then, I_{1a} is added to$L_{(j-1)(M+1)+k,(k-1)(N_\theta+1)+\ell}$, i.e.:

$$L_{(j-1)(M+1)+k,(k-1)(N_\theta+1)+\ell} = L_{(j-1)(M+1)+k,(k-1)(N_\theta+1)+\ell} + I_{1a}. \quad \text{(D.44)}$$

Similarly,

$$L_{(j-1)(M+1)+k+1,(k-1)(N_\theta+1)+\ell} = L_{(j-1)(M+1)+k+1,(k-1)(N_\theta+1)+\ell} + I_{1b}, \quad \text{(D.45)}$$

$$L_{(j-1)(M+1)+k,(k-1)(N_\theta+1)+\ell+1} = L_{(j-1)(M+1)+k,(k-1)(N_\theta+1)+\ell+1} + I_{2a}, \quad \text{(D.46)}$$

$$L_{(j-1)(M+1)+k+1,(k-1)(N_\theta+1)+\ell+1} = L_{(j-1)(M+1)+k+1,(k-1)(N_\theta+1)+\ell+1} + I_{2b}, \quad \text{(D.47)}$$

$$L_{(j-1)(M+1)+k,k(N_\theta+1)+\ell} = L_{(j-1)(M+1)+k,k(N_\theta+1)+\ell} + I_{3a}, \quad \text{(D.48)}$$

$$L_{(j-1)(M+1)+k+1,k(N_\theta+1)+\ell} = L_{(j-1)(M+1)+k+1,k(N_\theta+1)+\ell} + I_{3b}, \quad \text{(D.49)}$$

$$L_{(j-1)(M+1)+k,k(N_\theta+1)+\ell+1} = L_{(j-1)(M+1)+k,k(N_\theta+1)+\ell+1} + I_{4a}, \quad \text{(D.50)}$$

and

$$L_{(j-1)(M+1)+k+1,k(N_\theta+1)+\ell+1} = L_{(j-1)(M+1)+k+1,k(N_\theta+1)+\ell+1} + I_{4b}. \quad \text{(D.51)}$$

This is done for every $j = 1, 2, \ldots, N$, $k = 1, 2, \ldots, M$ and $\ell = 1, 2, \ldots, N_\theta$.

Appendix E

One future direction for the expansion of the SFBIM is the theoretical convergence analysis for the three-dimensional Laplace problem of Chapter 5. In this appendix the preliminary steps of such an analysis are carried out. Let us recall the problem, which for convenience we restate here: Find u such that

$$\nabla^2 u = 0 \text{ in } \Omega = [0,1] \times [0, \alpha\pi] \times [-1,1]\,, \tag{E.1}$$

with

$$\left.\begin{array}{c} u = 0 \text{ on } S_1 \\ \frac{\partial u}{\partial \theta} = 0 \text{ on } S_2 \\ u = g(\theta, z) \text{ on } S_3 \\ \frac{\partial u}{\partial z} = q_1(r,\theta) \text{ on } S_4 \\ \frac{\partial u}{\partial z} = q_2(r,\theta) \text{ on } S_5 \end{array}\right\}, \tag{E.2}$$

where n denotes the outward unit normal pointing outside $\partial\Omega = \bigcup_{i=1}^{5} S_i$ (see also Fig. 5.1). Let us multiply (E.1) by a test function v (to be specified shortly) and integrate over Ω:

$$\iiint_{\Omega} v \nabla^2 u = 0.$$

By Green's Theorem, we have

$$-\iiint_{\Omega} \nabla v \cdot \nabla u + \iint_{S_1 \cup S_3} v \frac{\partial u}{\partial n} + \iint_{S_4} v q_1 + \iint_{S_5} v q_2 = 0, \tag{E.3}$$

where the boundary conditions (E.2) were used. Suppose, now, that v is chosen to satisfy

$$\nabla^2 v = 0 \text{ in } \Omega,\ v = 0 \text{ on } S_1,\ \frac{\partial v}{\partial \theta} = 0 \text{ on } S_2. \tag{E.4}$$

Then (E.3) becomes

$$-\iiint_{\Omega} \nabla v \cdot \nabla u + \iint_{S_3} v \frac{\partial u}{\partial n} = -\iint_{S_4} v q_1 - \iint_{S_5} v q_2. \tag{E.5}$$

Now, since $u = g$ on S_3 we have

$$-\iint_{S_3} \frac{\partial v}{\partial n}(u - g) = 0,$$

so adding this to (E.5), we get (using (E.4))

$$\iiint_{\Omega} \nabla v \cdot \nabla u - \iint_{S_3} u \frac{\partial v}{\partial n} - \iint_{S_3} v \frac{\partial u}{\partial n} = -\iint_{S_3} \frac{\partial v}{\partial n} g + \iint_{S_4} v q_1 + \iint_{S_5} v q_2. \tag{E.6}$$

Letting

$$\lambda = \left.\frac{\partial u}{\partial n}\right|_{S_3},\ \mu = \left.\frac{\partial v}{\partial n}\right|_{S_3}, \tag{E.7}$$

equation (E.6) becomes

$$\iiint_{\Omega} \nabla v \cdot \nabla u - \iint_{S_3} u\mu - \iint_{S_3} v\lambda = -\iint_{S_3} \mu g + \iint_{S_4} v q_1 + \iint_{S_5} v q_2.$$

So we arrive at the following *variational problem* to be solved: Find $(u, \lambda) \in H^1_{\#}(\Omega) \times H^{-1/2}(S_3)$ such that

$$B(u, v) + b(u, v; \lambda, \mu) = F(v, \mu) \quad \forall\ (v, \mu) \in H^1_{\#}(\Omega) \times H^{-1/2}(S_3), \tag{E.8}$$

where

$$B(u, v) = \iiint_{\Omega} \nabla v \cdot \nabla u, \tag{E.9}$$

$$b(u, v; \lambda, \mu) = -\iint_{S_3} u\mu - \iint_{S_3} v\lambda, \tag{E.10}$$

$$F(v, \mu) = -\iint_{S_3} \mu g + \iint_{S_4} v q_1 + \iint_{S_5} v q_2. \tag{E.11}$$

The space $H^1_{\#}(\Omega)$ appearing in (E.8) is defined as

$$H^1_{\#}(\Omega) = \left\{ w \in H^1(\Omega) : w|_{S_1} = 0 \right\}, \tag{E.12}$$

and $H^{-1/2}$ is the usual dual of the space of trace functions $H^{1/2}$. The discrete problem corresponding to (E.8), then, reads: Find $(u_N, \lambda_h) \in \left[V_1^N \times V_2^h\right] \subset \left[H^1_{\#} \times H^{-1/2}(S_3)\right]$ such that

$$B(u_N, v) + b(u_N, v; \lambda_h, \mu) = F(v, \mu) \ \ \forall \ (v, \mu) \in V_1^N \times V_2^h, \tag{E.13}$$

with $B(u,v), b(u,v;\lambda,\mu)$ and $F(v,\mu)$ given by (E.9)–(E.11), and with V_1^N, V_2^h finite dimensional spaces to be selected.

The above problem is equivalent to the formulation used in the SFBIM and presented in the Chapter 5. To see this we first state the discrete problem (E.13) in *mixed* form: find $(u_N, \lambda) \in V_1^N \times V_2^h$ such that

$$\left.\begin{array}{c} \iiint\limits_{\Omega} \nabla v \cdot \nabla u_N - \iint\limits_{S_3} v\lambda = \iint\limits_{S_4} q_1 v + \iint\limits_{S_5} q_2 v \ \forall \ v \in V_1^N \\ \iint\limits_{S_3} (u_N - g)\,\mu = 0 \ \forall \ v \in V_2^h \end{array}\right\}. \tag{E.14}$$

Now, from Green's theorem and the boundary conditions that v satisfies (cf. (5.5)) we have

$$\begin{aligned} \iiint\limits_{\Omega} \nabla v \cdot \nabla u_N &= \iint\limits_{\partial\Omega} \frac{\partial v}{\partial n} u_N - \iint\limits_{\partial\Omega} u_N \nabla^2 v = \iint\limits_{\partial\Omega} \frac{\partial v}{\partial n} u_N \\ &= \iint\limits_{S_3 \cup S_4 \cup S_5} \frac{\partial v}{\partial n} u_N, \end{aligned}$$

and (E.14) becomes

$$\left.\begin{array}{c} \iint\limits_{S_3 \cup S_4 \cup S_5} \frac{\partial v}{\partial n} u_N - \iint\limits_{S_3} v\lambda = \iint\limits_{S_4} q_1 v \iint\limits_{S_5} q_2 v \ \forall \ v \in V_1^N \\ \iint\limits_{S_3} (u_N - g)\,\mu = 0 \ \forall \ v \in V_2^h \end{array}\right\}. \tag{E.15}$$

It is then easily seen that if u_N satisfies (E.15) then it also satisfies (E.14) and in turn (E.8), and vice versa.

Next, upon selecting the finite dimensional spaces V_1^N, V_2^h, one would like to establish a best approximation result analogous to (2.20) that will ultimately lead to the rate of convergence of the method.

Another issue we wish to address is the choice of singular functions (cf. (5.13)). It turns out that the function

$$\widehat{W}_j^{\ell}(r,\theta,z) = r^{\mu_j} f_j(\theta) \left[\beta_j^{\ell}(z) + \sum_{i=1}^{\infty} \frac{\partial^{2i}}{\partial z^{2i}} \left(\beta_j^{\ell}(z) \right) \frac{r^{2i} \left(-\frac{1}{4} \right)^i}{\prod_{n=1}^{i} n \left(\mu_j + n \right)} \right], \tag{E.16}$$

with $\beta_j^{\ell}(z) \in C^{\infty}(AB)$ arbitrary, also satisfies the three-dimensional Laplace equation and the boundary conditions on S_1, S_2 (as is shown in Appendix B). Hence, any function of the form (E.16) may be used as a singular function, especially if $\beta_j^{\ell}(z)$ are chosen as polynomials (so that the inner sum terminates after a finite number of terms). In fact, the singular functions used in the previous chapter are a special case of (E.16) with $\beta_j^{\ell}(z)$ being (piecewise) constant/linear polynomials. What remains is the selection of the finite dimensional spaces V_1^N, V_2^h and the corresponding norms.

Appendix F

In this appendix we discuss the application of the SFBIM for solving a Stokes flow problem within a circular sector assuming that the circular boundary is rotating at a constant speed.

Moffatt eddies

Moffatt (1964) analyzed the two-dimensional Stokes flow in an infinite wedge of angle 2α with a far-field disturbance. He came to the conclusion that there exist a critical half angle (α crit) under which eddies are formed and that for these cases there can be constructed a series solution in which the eigenvalues are complex. The eigenfunctions are known as Moffatt eddy functions.

Consider the two-dimensional creeping incompressible flows in polar coordinates. By eliminating the pressure from the $r-$ and $\theta-$ components of the Navier-Stokes equations, we obtain the biharmonic equation for ψ:

$$\nabla^4\psi = \nabla^2(\nabla^2\psi) = 0. \tag{F.1}$$

The stream function ψ is expanded in a series of the form:

$$\psi(r,\theta) = \sum_{k=1}^{\infty} \alpha_{\lambda_k} r^{\lambda_k+1} f_k(\theta), \tag{F.2}$$

where,

$$f_k(\theta) = A_{\lambda_k}\cos(\lambda_k+1)\theta + B_{\lambda_k}\sin(\lambda_k+1)\theta + C_{\lambda_k}\cos(\lambda_k-1)\theta + D_{\lambda_k}\sin(\lambda_k-1)\theta, \tag{F.3}$$

with the exception of the cases $\lambda_k = 0, 1, 2$, where $f_k(\theta)$ degenerates to

$$f_k(\theta) = A_{\lambda_k} + B_{\lambda_k}\theta + C_{\lambda_k}\theta^2 + D_{\lambda_k}\theta^3, \tag{F.4}$$

$$f_k(\theta) = A_{\lambda_k}\cos\theta + B_{\lambda_k}\sin\theta + C_{\lambda_k}\theta\cos\theta + D_{\lambda_k}\theta\sin\theta, \tag{F.5}$$

$$f_k(\theta) = A_{\lambda_k}\cos 2\theta + B_{\lambda_k}\sin 2\theta + C_{\lambda_k}\theta + D_{\lambda_k}, \tag{F.6}$$

respectively.

Flow near a corner

We consider the flow problem that was solved by Hills (2001 b). The fluid is maintained

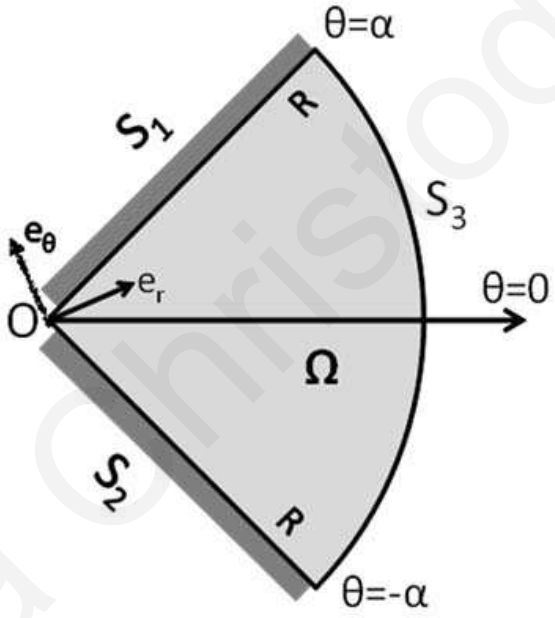

Figure F.1: Problem domain for a Stokes flow within a circular sector where the circular boundary is rotating at a constant speed.

in two-dimensional steady motion, contained in the region formed by a finite wedge of side $R = 1$ and internal angle 2α, as depicted in Fig. F.1, where :

$$\left.\begin{array}{c} \nabla^4 u = 0, \quad \text{in } \Omega \\ \frac{\partial u}{\partial r} = \frac{\partial u}{\partial \theta} = 0, \quad \text{on } S_1 \cup S_2 \\ \frac{\partial u}{\partial r} = 1 \quad \text{and} \quad \frac{\partial u}{\partial \theta} = 0, \quad \text{on } S_3 \end{array}\right\}. \tag{F.7}$$

A boundary singularity occurs at the origin O which is due to the geometry. The motion is caused by the rotation of the curved boundary S_3 about an axis through O. As indicated by Hills (2001 b), the boundary condition $\partial u/\partial r = 0$ on $S_1 \cup S_2$, is equivalent to the condition $u = 0$, from the continuity of the steamfunction.

As pointed out by Dean and Montagnon (1949), a disturbance far from the corner can generate either an antisymmetric or a symmetric flow pattern near the corner, and the corresponding stream function is an even or odd function of θ, respectively.

If the flow is symmetric near the corner then $f_\mu(\theta)$ is odd ($A_\mu = C_\mu = 0$) and

$$f_\mu(\theta) = B_\mu \sin(\mu+1)\theta + D_\mu \sin(\mu-1)\theta, \tag{F.8}$$

where the eigenvalues satisfy the equation $\sin 2\mu\alpha = \mu \sin 2\alpha$.

If the flow is antisymmetric near the corner then $f_\lambda(\theta)$ is even ($B_\lambda = D_\lambda = 0$) and

$$f_\lambda(\theta) = A_\lambda \cos(\lambda+1)\theta + C_\lambda \cos(\lambda-1)\theta, \tag{F.9}$$

where the eigenvalues satisfy the equation $\sin 2\lambda\alpha = -\lambda \sin 2\alpha$.

The computed eigenvalues for symmetric and antisymmetric flow for $\alpha = 45°$ are ploted in Fig. F.2.

As shown by Moffatt (1964) the eigenvalues are all complex for α sufficiently small (less than 73.2°). Moreover if λ is an eigenvalue then so are the conjugates of λ and $-\lambda$.

The asymptotic expansion for u in the neighborhood of the singular point O can be expressed in terms of an eigenfunction expansion of the form:

$$u(r,\theta) = \sum_{j=1}^{\infty} \left(c_j W_1^j + d_j W_2^j \right), \tag{F.10}$$

where the even eigenfunctions W_1^j are:

$$W_1^j(r,\theta) = r^{\lambda_j+1} \left[\frac{\cos(\lambda_j+1)\theta}{\cos(\lambda_j+1)\alpha} - \frac{\cos(\lambda_j-1)\theta}{\cos(\lambda_j-1)\alpha} \right], \tag{F.11}$$

and the odd eigenfunctions W_2^j are:

$$W_2^j(r,\theta) = r^{\mu_j+1} \left[\frac{\sin(\mu_j+1)\theta}{\sin(\mu_j+1)\alpha} - \frac{\sin(\mu_j-1)\theta}{\sin(\mu_j-1)\alpha} \right]. \tag{F.12}$$

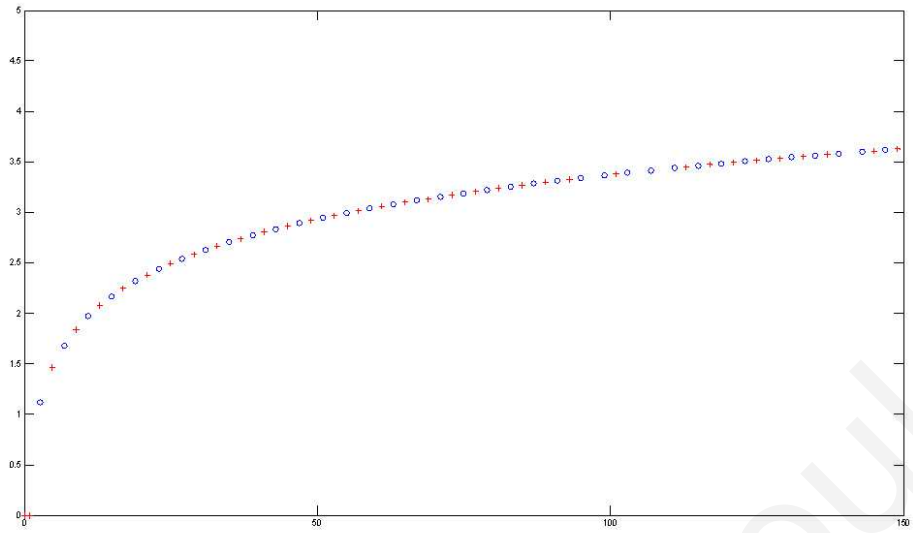

Figure F.2: Computed eigenvalues for symmetric (o) and antisymmetric (+) flow for $\alpha = 45°$.

It turns out that for this problem the eigenvalues are complex and they are chosen so that $0 < Re(\lambda_1) < Re(\lambda_2) < \ldots$ and $0 < Re(\mu_1) < Re(\mu_2) < \ldots$.

Hills (2001 b) solved the problem using a collocation scheme for determining the physical streamfunction ψ:

$$\psi(\theta) = Re\left\{\sum_{k=1}^{N} A_k \lambda^k \left(\frac{\cos(\mu_k + 1)\theta}{\cos(\mu_k + 1)\alpha} - \frac{\cos(\mu_k - 1)\theta}{\cos(\mu_k - 1)\alpha}\right)\right\}. \tag{F.13}$$

Since the coefficients A_k are complex, they each require two constrains that are obtained by satisfying the conditions on ψ at discrete collocation points on S_3. A total number of N collocation points are needed where the required components of velocity are strictly enforced. The collocation points are chosen in the positive range . Since ψ is even in θ the boundary conditions are satisfied on $2N - 1$ (if $\theta = 0$ is a collocation point) or on $2N$ boundary points on the whole arc.

Preliminary formulation of the SFBIM

As always, the first step in the method is to approximate the solution by the leading N_α even

terms of the asymptotic expansion

$$\bar{u}(r,\theta) = \sum_{j=1}^{N_\alpha} \bar{c}_j W_1^j. \tag{F.14}$$

Next, the problem is discretized by applying Galerkins principle. The governing equation is weighted by the singular functions yielding the following set of equations

$$\int_\Omega \nabla^4 \bar{u} W_1^i dV = 0, i = 1, 2, \dots N_\alpha. \tag{F.15}$$

The discretized equations are then turn into boundary integrals by double application of Greens theorem. Taking into account that the singular functions satisfy the governing equation we obtain these equations:

$$\int_{\partial\Omega} \left[\frac{\partial \bar{u}}{\partial n} \nabla^2 W_1^i - \bar{u} \frac{\partial (\nabla^2 W_1^i)}{\partial n} \right] dS + \int_{\partial\Omega} \left[\frac{\partial (\nabla^2 \bar{u})}{\partial n} W_1^i - \nabla^2 \bar{u} \frac{\partial (W_1^i)}{\partial n} \right] dS = 0, \quad i = 1, 2, \dots, N_\alpha. \tag{F.16}$$

Taking into account the boundary condition we have this system:

$$\int_{-\alpha}^{\alpha} \left[\frac{\partial (\nabla^2 \bar{u})}{\partial r} W_1^i - \nabla^2 \bar{u} \frac{\partial (W_1^i)}{\partial r} \right] d\theta = - \int_{-\alpha}^{\alpha} \nabla^2 W_1^i d\theta, \quad i = 1, 2, \dots, N_\alpha. \tag{F.17}$$

Therefore we only have to integrate along S_3, away from the singular point. The Dirichlet condition $u = 0$ along S_3 is imposed by means of a Lagrange multiplier function ξ, which replaces the normal derivative of the Laplacian of u. The function ξ is expanded in terms of standard, polynomial basis functions M^j of order p:

$$\xi = \frac{\partial \nabla^2 \bar{u}}{\partial n} = \sum_{\ell=1}^{N_\xi} \xi_\ell M^\ell, \tag{F.18}$$

where N_ξ represents the total number of the unknown discrete Lagrange multipliers ξ_j along S_3. The basis functions M^j are used to weight the Dirichlet condition along the corresponding boundary segment S_3. The following symmetric system of $N_\alpha + N_\xi$ discretized equations is thus obtained:

$$\int_{-\alpha}^{\alpha} \left[\xi W_1^i - \nabla^2 \bar{u} \frac{\partial (W_1^i)}{\partial r} \right] d\theta = - \int_{-\alpha}^{\alpha} \nabla^2 W_1^i d\theta, \quad i = 1, 2, \ldots, N_\alpha, \tag{F.19}$$

$$\int_{-\alpha}^{\alpha} \bar{u} M^\ell d\theta = 0, \quad \ell = 1, 2, \ldots, N_\xi. \tag{F.20}$$

Bibliography

[1] M. Arad, Z. Yosibash, G. Ben-Dor, and A. Yakhot, Comparing the flux intensity factors by a boundary element method for elliptic equations with singularities, *Commun. Numer. Meth. Eng.* **14** (1998) 657–670.

[2] I. Babuška, A. Miller, The post-processing approach in the finite element method Part 2: The calculation of stress intensity factors, *Int J Numer Meth Engng* **20** (1984) 1111–1129.

[3] A. Beagles, and A.-M. Sändig, Singularities of rotationally symmetric solutions of boundary value problems for the Lamé equations, *ZAMMM Z. Angew. Math. Mech.* **71** (1991) 423–431.

[4] A.E. Beagles and J.R. Whiteman, General conical singularities in three-dimensional Poisson problems, *Math. Methods Appl. Sci.* **11**(1989) 215–235 .

[5] F. Bernal, G. Gutierrez and M. Kindelan, Use of singularity capturing functions in the solution of problems with discontinuous boundary conditions, *Eng. Anal. Bound. Elem.* **33** (2009) 200–208.

[6] F. Bernal and M. Kindelan, Radial basis function solution of the Motz problem, *Eng. Comp.* **27** (2010) 606–620.

[7] E. Christodoulou, C. Xenophontos, and G. Georgiou, The singular function boundary integral method for elliptic problems with boundary singularities, *Recent Advances in*

Boundary Element Methods: A Volume to honor Prof. D. Beskos, G. Manolis and D. Polyzos (Eds), Springer Science+Business B.V., 43–56 (2009).

[8] E. Christodoulou, C. Xenophontos, G. Georgiou, The Singular Function Boundary Integral Method for singular Laplacian problems over circular sections, *Appl. Math. Comp.* **217** (2010) 2773–2787.

[9] E. Christodoulou, M. Elliotis, C. Xenophontos and G. Georgiou, Analysis of the singular function boundary integral method for a biharmonic problem with one boundary singularity, in press in Numer. Meth. PDEs, (2011).

[10] M. Costabel, and M. Dauge, General edge asymptotics of solution of second order elliptic boundary value problems I II, *Proceedings of the royal Society of Edinburgh* **123A** (1993) 109–184.

[11] M. Costabel, M. Dauge, and Y. Lafranche, Fast semi-analytic computation of elastic edge singularities, *Compt. Methods Appl. Mech. Engrg.* **190** (2001) 2111–2134.

[12] M. Costabel, M. Dauge, and Z. Yosibash, A Quasi-Dual Function Method for Extracting Edge Stress Intensity Functions, *SIAM J. Math. Anal.* **35** (2004) 1177–1202.

[13] M. Costabel, M. Dauge and S. Nicaise, *Corner singularities and analytic regularity of linear elliptic systems*, in preparation (2011).

[14] W.R. Dean and P.E. Montagnon, On the steady motion of viscous liquid in a corner,*Proc. Camb. Phil. Soc.* **45**(1949) 389–394.

[15] A.A. Dosiyev and S.C. Buranay, On solving the cracked-beam problem by block method, *Comm. Num. Meth. Eng.* **24** (2008) 1277–1289.

[16] M. Elliotis, G. Georgiou, and C. Xenophontos, The solution of a Laplacian problem over an L-shaped domain with a singular function boundary integral method, *Comm. Numer. Methods Eng.* **18** (2002) 213–222.

[17] M. Elliotis, G. Georgiou, and C. Xenophontos, Solving Laplacian problems with boundary singularities: A comparison of a singular function boundary integral method with the p/hp version of the finite element method, *Appl. Math. Comp.* **169** (2005a) 485–499.

[18] M. Elliotis, G. Georgiou, and C. Xenophontos, Solution of the planar Newtonian stick-slip problem with the singular function boundary integral method, *Int. J. Numer. Meth. Fluids* **48** (2005b) 1000–1021.

[19] M. Elliotis, G. Georgiou, and C. Xenophontos, The singular function boundary integral method for a two-dimensional fracture problem, *Eng. Anal. Bound. Elem.* **30** (2006) 100–106.

[20] M. Elliotis, G. Georgiou, and C. Xenophontos, The singular function boundary integral method for biharmonic problems with crack singularities, *Eng. Anal. Bound. Elem.* **31** (2007) 209–215.

[21] G. Georgiou, L.G. Olson, and Y. Smyrlis, A singular function boundary integral method for the Laplace equation, *Commun. Numer. Meth. Eng.* **12** (1996) 127–134.

[22] G. Georgiou, A. Boudouvis, and A. Poullikkas,Comparison of two methods for the computation of singular solutions in elliptic problems, *J. Comput. Appl. Math.* **79** (1997) 277–290.

[23] P. Grisvard, *Singularities in boundary value problems*, RMA 22, Masson, France, (1992).

[24] P. Grisvard, *Elliptic Problems in Nonsmooth Domains*, Pitman Publishers, London, 1995.

[25] C. P. Hills, Eddies induced in cylindrical containers by a rotating end-wall, *Phys. Fluids* **8**(2001) 2279–2286.

[26] C. P. Hills, Eddy structures induced within a wedge by a honing circular arc, *Theoret. Comput. Fluid Dynamics* **15** (2001) 1–10.

[27] O. Huber, J. Nickel, and G. Kuhn, On the decomposition of the J-integral for 3-D crack problems, *Int. J. Fracture* **64** (1993) 339–348.

[28] C. Johnson, Solution of Partial Differential Equations by the Finite Element Method, Cambridge University Press (1987).

[29] V. A. Kondratiev, Boundary value problems for elliptic equations in domains with conical or angular points, *Trans. Moscow Math. Soc.* **16** (1967) 227–313.

[30] Z.C. Li, R. Mathon, P. Sermer, Boundary methods for solving elliptic problems with singularities and interfaces, *SIAM J. Numer. Anal.* **24** (1987) 487-498.

[31] Z.C. Li, Penalty combinations of Ritz-Galerkin and finite-difference methods for singularity problems, *J. Comput. Appl. Math* **81** (1997) 1-17.

[32] Z.C. Li, *Combined methods for elliptic equations with singularities, interfaces and infinities*, Kluwer Academic Publishers (1998).

[33] Z.C. Li, T.T. Lu, and H.Y. Hu, The collocation Trefftz method for biharmonic Eqs. with crack singularities, *Eng. Anal. Bound. Elem.* **28** (2004) 79–96.

[34] Z.C. Li, T.T. Lu, H.T. Huang and A. Cheng, Trefftz, Collocation, and Other Boundary Methods – A Comparison, *Num. Meth. PDEs* **23** (2007) 93–144.

[35] Z.C. Li,Y.L. Chen, G. Georgiou, C. Xenophontos, Special boundary approximation methods for Laplace equation problems with boundary singularities, *Comp. and Math. Appl.*. **51** (2006) 115–142.

[36] Z.C. Li, T.T. Lu, and H.Y. Hu, *AHD Cheng, Trefftz and Collocation Methods,* WIT Press,Southampton, Boston, (2008).

[37] JL. Lions, E. Magenes, -homogeneous boundary value problems and applications, Vol. I. Springer-Verlang (1972).

[38] T.T. Lu, C.M. Chang, H.T. Huang, Z.C. Li, Stability analysis of Trefftz methods for the stick slip problem, *Eng. Anal. Bound. Elem.* **33** (2009) 474-484.

[39] G. Meda, T. W. Messner, G. B. Sinclair and J. S. Solecki, Path-independent H integrals for three-dimensional fracture mechanics , *Int. J. Fracture* **94** (1998) 217–234.

[40] D.H. Michael, The separation of a viscous fluid, *Mathematica* **5** (1958) 82-84.

[41] H.K. Moffatt,Viscous and resistive eddies near a sharp corner, *J. Fluid Mech.* **18** (1964) 1-18.

[42] L.G. Olson, G. Georgiou, W.W. Schultz, An efficient finite element method for treating singularities in Laplace's equation, *J. Comp. Physics* **96** (1991) 391–410.

[43] N. Omer, Z. Yosibash, M. Costabel, M. Dauge, Edge flux intensity functions in polyhedral domains and their extraction by a quasidual function method, . J. Fracture, **129** (2004) 97–130.

[44] T. Papanastasiou, G. Georgiou, A. Alexandrou, *Viscous Fluid Flow,* CRC Press, Boca Raton. (1999).

[45] S Richardson,A stick-slip problem related to the motion of a free jet at low Reynolds number, *Proceedings of the Cambridge Philosophical Society.* **67** (1970) 477-489.

[46] A. Rössle, Corner singularities and regularity of weak solutions for the two-dimensional Lamé equations on domains with angular corners, *J. Elasticity* **60** (2000) 57–75.

[47] B.D. Schiff, D. Fishelov, and J.R. Whiteman, *Determination of a stress intensity factor using local mesh refinement*, in: J.R. Whiteman (Ed.), *The mathematics in finite elements and applications III*, Academic Press, London, 1979, pp. 55–64.

[48] H. Schmitz, K. Volk, W. Wendland, Three-dimensional singularities of elastic fields near vertices, *Numer. Meth. PDEs* **9** (1993) 323–337.

[49] E. Stephan and J. R. Whiteman, Singularities of the Laplacian at corners and edges of three-dimensional domains and their treatment with finite element methods, *Math. Methods Appl. Sci.* **10** (1988) 339–350 .

[50] B. Szabó and I. Babuška, *Finite Element Analysis*, John Wiley and Sons, New York, (1991).

[51] B. Szabó, Z. Yosibash, Numerical analysis of singularities in two dimensions. Part 2: Computation of generalized flux/stress intensity factors, *Int. J. Numer. Meth. Engng.*. **39** (1996) 409-434.

[52] J. Wloka, Partial Differential Equations, *Cambridge University Press*; (1987).

[53] C. Xenophontos, M. Elliotis, and G. Georgiou, The singular function boundary integral method for elliptic problems with singularities, *SIAM J. Sc. Comp.* **28** (2006) 517–532.

[54] Z. Yosibash, R. Actis, and B. Szabó, Extracting edge flux intensity factors for the Laplacian, *Int. J. Numer. Methods Engin.* **53** (2002) 225–242.

[55] Z. Yosibash, N. Omer, M. Costabel and M. Dauge, Edge stress intensity functions in polyhedral domains and their extraction by a quasidual function method, *Int. J. of Fracture*, **129** (2004) 97–1303.

[56] Z. Yosibash, N. Omer, Numerical methods for extracting edge stress intensity functions in anisotropic three-dimensional domains, *Comp. Meth. Appl. Mech. Engg.* **196** (2007) 3624–3649.

[57] T. Zaltzman, and Z. Yosibash, Vertex singularities associated with conical points for the 3D Laplace equation, *Numer. Methods PDEs* **27** (2011) 662–679.